Student thesis series INES nr 415

Tracing mangrove forest dynamics of Bangladesh using historical Landsat data

Md. Monirul Islam

2017
Department of
Physical Geography and Ecosystem Science
Lund University
Sölvegatan 12
S-223 62 Lund
Sweden

Md. Monirul Islam (2017).
Tracing mangrove forest dynamics of Bangladesh using historical Landsat data

Master degree thesis, 30 credits in *Master of Physical Geography and Ecosystem Analysis*
Department of Physical Geography and Ecosystem Science, Lund University

Level: Master of Science (MSc)

Course duration: *January* 2016 until *June* 2017

Disclaimer

Tracing mangrove forest dynamics of Bangladesh using historical Landsat data

Md. Monirul Islam

Master Thesis, 30 credits, in Physical Geography and Ecosystem Analysis

Supervisor
Dr. Helena Borgqvist
Lecturer, Department of Physical Geography and Ecosystem Science

Co-Supervisor
Dr. Lars Eklundh
Professor, Department of Physical Geography and Ecosystem Science

Exam committee:
Dr. Jonas Ardö, Department of Physical Geography and Ecosystem Science

Dr. Jonathan Seaquist, Department of Physical Geography and Ecosystem Science

Abstract

Present, accurate, and reliable estimation of mangrove forests in Bangladesh is limited. Former estimation of mangroves extent and density has been more or less restricted to the Sundarbans and do not represent the whole country. In this study, a time series analysis was performed using Landsat images from four epochs, namely: 1976 (Landsat MSS), 1989 (Landsat TM), 2000 (Landsat ETM+) and 2015 (Landsat L8 OLI) to accurately quantify mangroves extent and density change/variation in the study area. An atmospheric correction using the Dark Object Subtraction method and a radiometric normalization using pseudo-invariant features was performed to reduce haze and sedimentation effects of the images. A standard approach to study changes in forest characteristics is to perform a time series analysis using images that have undergone a supervised classification. Results are indicating a gradual increase of forest area in most parts of the study area. Overall, the areal coverage increased by 3.10% (58140 ha) from 1976 to 2015, where 1.79% (33587 ha) of this increase took place from 2000 to 2015. The Sundarbans area turned out to be an exception. There, the mangrove forest area remained almost unchanged, although a little change (decrease by 1.03%) was found between 2000 and 2015. The study also claimed that one of the oldest mangrove forests in Bangladesh (Chakaria Sundarbans) had lost 4135 ha (32%) of forest area between 1976 and 1989. Similarly, a vegetation index (NDVI) analysis suggested that not only the area but also the density of the mangroves has changed over the years. The forests seem to have been denser in 1976 than in 1989. In 2000 the density appeared to have increased again, while decreased again in 2015. The study also found a substantial increase between 1989 and 2000 while a considerable density decreases in the Sundarbans region between 2000 and 2015. However, Mangroves area change was not significant in the context of classification uncertainty. A little error source was found due to the similar spectral reflectance between mangroves and non-mangrove vegetation, for example, in Patuakhali-Bhola. An accuracy assessment was performed using confusion matrices, showed maximum likelihood algorithm produce a better result for mangrove classes than other Land use/ Land cover classes. The overall accuracy of Landsat 8 OLI, ETM+, TM, and the MSS classified images (five classes) were found to be 97%, 87%, 80%, and 80% respectively, with Kappa values of 0.96, 0.82, 0.73, 0.74. Several possible factors such as cyclones, sedimentation and erosion, deforestation, shrimp and salt farming, and mangrove plantation were identified, which might be responsible for mangroves variations/changes in Bangladesh.

Key Words: Mangroves, Landsat, Time Series, Change Detection, Bangladesh, NDVI, Supervised Classification

Dedicated to My Parents...

Acknowledgements

All the time, all praises go to Allah, for giving me the patience to complete the research.

This research has been done in my scholarship period at Lund University. As a Swedish Institute (SI) fellow, I want to thank Swedish Institute for giving me an opportunity to study in the world's prestigious University. I want to thank Department of Physical Geography and Ecosystem Science, to grant my proposal for the research.

I want to acknowledge my supervisor Dr. Helena Borgqvist for her continuous motivational support from the first to the end. I also want to thank especially Professor Lars Eklundh to accept my proposal and for select exceptional supervisor for this research. I would like to thank Dr. Jonathan Seaquist, Dan Metcalfe, and Dr. Jonas Ardö for their valuable feedbacks to draw the present form of the report. I also want to thank Martin Berggren for his cooperation during the thesis time. I would like to thank Ricardo Guillen for his consistent support in the research lab.

I would like to thank United State Geological Survey (USGS), NASA Landsat Science for providing Landsat Scene through the website used in the study. I want to thank United Nations Environment program, World Conservation Monitoring Centre (UNEP-WCMC) for providing Global Mangrove Distribution data through the website used in the study. Also, thanks to Forest Department of Bangladesh to get some information for the study.

I would like to thank virtual friend James Varghese and Eric Ariel for providing useful information to manage the problem in the research. Also like to acknowledge research gate, Twitter, Youtube and Google to find helpful information about the research.

I want to express gratitude to Abdalla Eltayeb, Harun ar-Rashid, Mostarin Ara, Sakib Bin Redhwan, Sabbir Ahmed Khan, Stefanos Georganos and Lund University friends for their inspirational support by the different way. I am grateful to Swedish people for their friendly behavior in my everyday life in Lund.

Finally, my gratitude and thanks go to my family members for their emotional support in my foreign study time.

Contents

List of Acronyms

CEGIS : Center for Environmental and Geographic Information Services
DN : Digital Number
DOS : Dark Object Subtraction
ETM+ : Enhanced Thematic Mapper Plus
FAO : Food and Agricultural Organization
L8OLI : Landsat 8 Operational Land Imager
LTS : Landsat Time Series
LU/LC : Land use/ Landover
MSS : Multispectral Scanner
MOEF : Ministry of Environment and Forestry
NASA : National Aeronautics and Space Administration
NDVI : Normalized Difference Vegetation Index
PIFs : Pseudo Invariant Features
RMA : Reduced Major Axis Regression
TM : Thematic Mapper
TOARef : Top of Atmospheric Reflectance
UNEP : United Nations Environment Program
USGS : United States Geological Survey
WCMC : World Conservation Monitoring Centre

Units

ha : Hectares
m : Metres

Chapter One-
Introduction

1.1 Context

Mangrove forests are salt-tolerant woody plants that form intertidal and fragile ecosystems between sea and land (Alongi, D.M., 2002). Globally, Mangrove ecosystems are distributed along coasts within the tropical and lower latitudes of the subtropical climate zones, at latitudes from the equator to about 32° N and 38° S (Spalding *et al.*, 1997). However, most Mangrove forests are found within latitudes between 5° N and 5° S (Giri *et al.*, 2010).

The Mangroves are known to provide various ecosystem services, both in an ecological and economic perspective. They have a role as protectors for damage from tsunamis and cyclones (Forbes *et al.*, 2007), they are critical breeding zones for shrimp and fish (Roy *et al.*, 2015), they provide a source of fuelwood and timber (Uddin *et al.*, 2013), they offer an environment suitable for medicinal plants to grow, and they attract tourists (Kuenzer *et al.*, 2011; Pham & Yoshino 2015, Uddin *et al.*, 2013). Furthermore, they contribute to a terrestrial carbon source and act as distributors of dissolved organic Carbon (C) to the oceans (Dittmar *et al.*, 2006).

Recent estimates of the extent of Mangrove forests claim that globally we lost about 36% of the total mangrove area in the last two decades, due to human-induced actions such as forest reduction for aquaculture, agriculture, infrastructure, tourism and dam constructions on rivers; but also due to catastrophic natural disasters, such as cyclones and typhoons (FAO 2007). A study performed by Giri *et al.*, (2007) found that Asia lost 12% of the Mangrove forests between 1975 and 2005. On the country level, the mangrove forest area is estimated to have declined about 9% (1989-2001) in Vietnam and 1.2% (1973-2000) in India-Bangladesh, while increased 1.5% (Indus Delta, Pakistan) between 1973 and 2010 (Pham & Yoshino 2015; Giri *et al.*, 2015). Regarding the Sundarbans of Bangladesh-India, the study performed by Giri *et al.* (2007) claim a slow increase of forest area by 1.4% from the 1970s to 1990s and gradual decrease by 2.5% from 1990s to 2000s, due to deforestation, coastal erosion, and aggradation. Another study, Islam, M.T. (2014) came to the conclusion that land area of Sundarbans (Bangladesh-India) decreased by 5.1% from 1975 to 1989 and by 4.5% from 1989 to 2000 (due to erosion, and several tropical cyclones between 1977 and 1988). These threats and mangrove losses are leading to the increasing demand of extracting up-to-date and reliable information on mangrove forest. This information is essential for mangrove mapping and monitoring, for change detection, estimating carbon stock and for sustainable

management (Giri *et al.,* 2007; Green *et. al.,* 2000; Jones *et. al.,* 2016; Heumann, W. B., 2011).

The Sundarbans, largest continuous mangrove forests in the earth covering about one million hectares extended between Bangladesh and India (between 21°27 and 22°30 N, and 89°02 and 89°55 E). However, more than 60% of the Sundarbans ecosystems are within Bangladesh, which is approximately 600,386 ha (MoEF 2011). The total carbon stock of the Sundarbans Reserve Forest of Bangladesh is estimated to be 55.8 Megatons (excluding C storage in soils) using biomass estimation method by measuring aboveground biomass and belowground pools (MoEF 2011).

The Landsat program offers collected earth observation data continuously from the last 44 years. The images have a spatial resolution of (30x30) m and a temporal resolution of 16 days. It also provides continuous land surface records and modification over time (Roy *et al.,* 2014). Landsat 8 was launched recently in 2013 which has cirrus cloud detection and two thermal infrared bands. The Landsat images are free of charge, making it possible for projects with limited financial budgets to perform sophisticated analyses still.

Satellite remote sensing has been widely used for purposes aiming to estimate the extensions and dynamics of the Mangrove ecosystems, as well as for change detection purposes (Sulaiman *et al.,* 2013). Globally, numerous studies have tried to detect mangrove forest change using the Landsat time series data, for instance, Shapiro *et al.,* 2015 in Zambezi Delta, Long & Giri, 2011 in Philippine, global mangrove forest status, and distribution by Giri *et al.,* 2010. However, using remote sensing techniques, previous mangrove ecosystems studies conducted mostly in Indian and Bangladesh Sundarbans part together, for example, Islam, M.T. (2014), Chandra Giri *et al.* (2015), but a few studies have restricted their work to the Sundarbans of Bangladesh, for example (Akhter, 2006; Diyan, M.A., 2011; Salam *et al.,* 2007; Emch *et. al.* 2006). Furthermore, National level mangrove study in Bangladesh is limited except a few study (but not up-to-date) such as Rahman *et. al.* 2013. So, there are knowledge gaps about current and details information of mangrove changes in the country.

Over the last two decades, Vegetation indices (Vis) have been used for estimating the density of the Mangrove forests where Normalized Difference Vegetation Index (NDVI) is common Vis. Besides, Supervised and unsupervised classification and support vector machine (SVM)

techniques are widely used in mangrove change detection (Kanniah *et al.,* 2015; Long & Giri 2011). Using classification and Vegetation indices approach has the potential to quantify mangrove extent and density within the area in temporal and spatial scale.

1.2 Knowledge Gap and Problem Statement

Existing mangroves extent maps/information of Bangladesh have little details such as the absence of local mangroves change. However, most of the remote sensing estimation of mangrove forest were up to 2000 (Rahman *et. al*., 2013; FAO 2005), and have not represented the mangrove extent of the whole country (such as Sundarbans studies by Emch *et. al.,* 2006; Giri *et. al.,* 2007; Islam, M. T., 2015; Chakaria Sundarbans study by Rahman *et al.*, 2015;). Furthermore, available mangrove estimations among studies vary. For time-series forest change detection purposes, image pre-processing is a crucial part. It may involve some more or less complicated steps, such as image co-registration and ortho-rectification, radiometric correction, topographic correction, geometric correction, atmospheric adjustment to surface reflectance and radiometric normalization (Banskota *et al.,* 2014; Schott *et al.,* 1988; Zhong *et al.,* 2016). Previous studies looking at change detections of the Mangrove forests in Bangladesh have used rather simplified pre-processing methods (Giri *et al.,* 2007; Salam *et al.,* 2007). In this study, however, the images went through a radiometric normalization including an atmospheric correction and a relative radiometric normalization. Another difference between this study and many of the former studies is to investigate both the areal coverage (using land use/ land cover classification) and the forest density (using a vegetation index obtained from the satellite images). Also, the present study offers an accuracy assessment using confusion metrics to evaluate the reliability of mangrove estimation using land use/land cover classification in the study area. The research problem can be outlined as- *there is a substantial knowledge gap related to mangrove extent and density changes from local to regional scale in Bangladesh using satellite remote sensing data.*

1.3 Aim and Objectives of the Study

To fill the research mentioned above gap, the aim of this study was to detect changes in the mangrove dynamics (changes in mangrove extent and density over time) within the whole country of Bangladesh, covering a substantially larger area. Specifically, the objective is

1. **To accurately quantify and mapping mangrove areal extent, and how the mangrove vegetation density changes in the study area in the past four epochs.**

To conduct this study four types of Landsat data (MSS, TM, ETM+, L8OLI) in four epochs (1976, 1989, 2000 and 2015) is used, summing up to twenty-eight images in total.

Based on literature review, expected the outcome of the study is that mangrove forests have been increasing in the last four epochs especially after 2000 and density have to vary in temporal and spatial scale. Deposition of the sediment in the open sea could be one of the main reason why mangrove has increased in the study area. Variation also expected in different epochs and different regions due to various factors such as erosion and deposition of landform, cyclone, deforestation, mangrove plantation, shrimp and salt culture.

Chapter Two-
Background of the Study

2.1 What is the Mangrove Ecosystems?

In general, mangrove ecosystems (Figure 1a and 1b) are cluster groups of plants, shrubs, palms, and ferns which have aerating roots, formed mainly in the coastal areas where fresh water and saline water meet.

1a 1b

Figure.1: *A typical example of mangrove ecosystem characteristics. The photograph was taken by the author in 2011 at Satkhira Sundarbans part.*

2.2 Global distribution of mangroves

Globally, mangroves are extended between 32° N and 38° S and 110 different species are found in tropics and subtropics (Spalding *et al.,* 1997; Kathiresan & Bingham, 2001; Rosati *et al.,* 2010;) These mangrove ecosystems cover about **138,000 km^2** spread in 118 countries, where only 15 countries have 75% of the global mangroves (Giri *et al.,* 2010). Table.1 shows mangroves area and percentages at a continent scale, and Figure 2 shows the global distribution of the Mangroves.

Mangrove ecosystems are found in Ganges-Brahmaputra delta, Andaman-Nicobar Islands, and Sumatra coast in Indonesia, west coast of Florida, estuaries in Queensland, west, and east Africa, Borneo and Papua New Guinea (Islam, M.S. 2001). However, in South Asia, they cover 1,187476 ha which is about 7% of the total extent (Giri *et al.,* 2015). Figure 3 shows South Asian mangrove distribution.

Table.1: *Global percentage of mangroves by region (based on top 15 mangrove richest countries; after Giri et al. 2010 remote sensing study); S. N. means Serial Number*

S. N.	Region	Area (ha)	Global Percentage
1	Asia	5,180,942	37.7
2	Africa	1,589,250	11.5
3	North & Central America	1,163,455	8.5
4	Oceania	977,975	7.1
5	South America	741,917	7

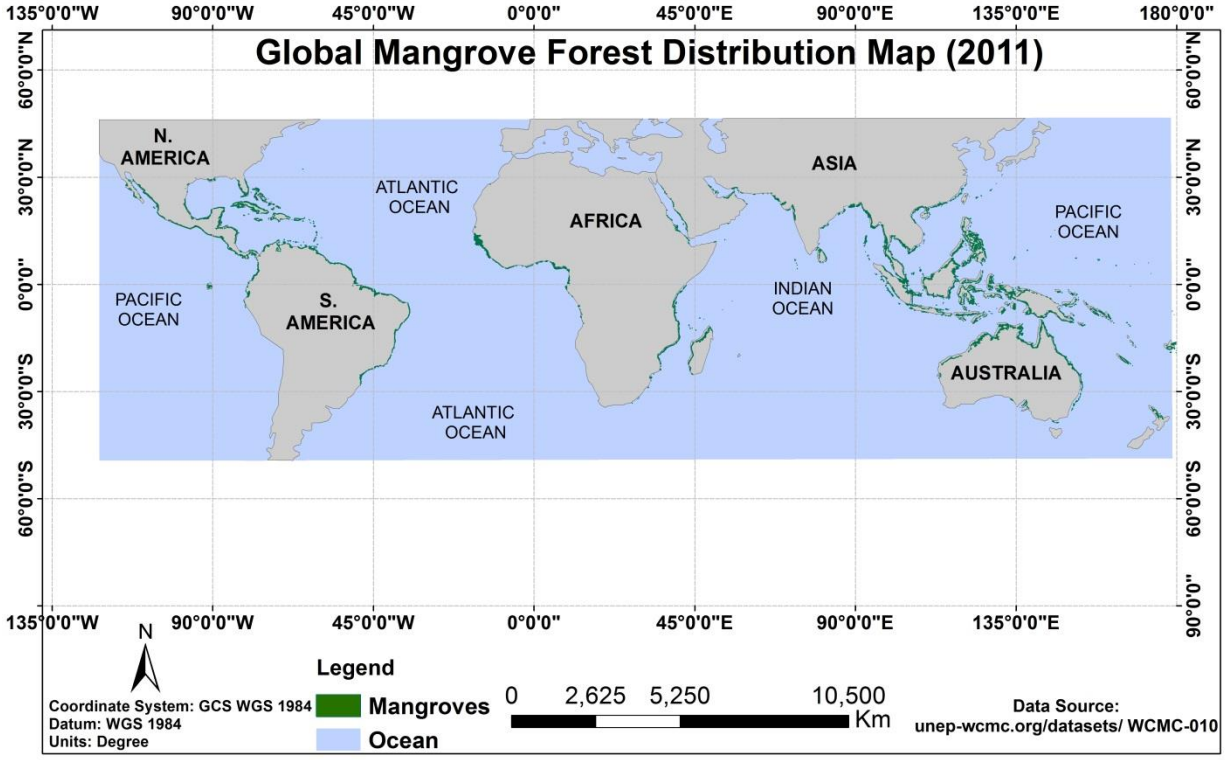

Figure.2: *Global mangrove forest distribution, (data source: unep-wcmc.org)*

2.3 Global Importance of Mangrove Forests

Globally, in tropics and subtropics, about 10 millions of people depend on mangrove forests (Rosati *et al.*, 2010). Mangrove forests have contributed to protecting coastal areas in dike systems from tsunamis and cyclones, shrimp and fish breeding zones, the source of fuel and medicinal plants and attracting place for tourist (Kuenzer *et al.*, 2011). Furthermore, it's not also terrestrial carbon source but also dissolved organic carbon source to the oceans (Dittmar *et al.*, 2006).

Tsunami hazards have lowered the consistent areas behind the mangrove forests (Fobes & Jeremy 2007). However, Bhowmik & Cabral (2013) found that 45% of Sundarbans affected by Cyclone SIDR in 2007. Fortunately, the forests reduced the intensity of the cyclone and protected the country from its severity. The provisioning and cultural service values of the Sundarbans in Bangladesh are estimated to US$ 744,000 and US$ 42,000 per year respectively during financial years between 2001–2002 and 2009–2010 (Uddin *et al.*, 2013). Where provisioning services include timber, fuel wood, fish, honey, thatching materials, and waxes and cultural services are mainly tourism (Uddin *et al.*, 2013).

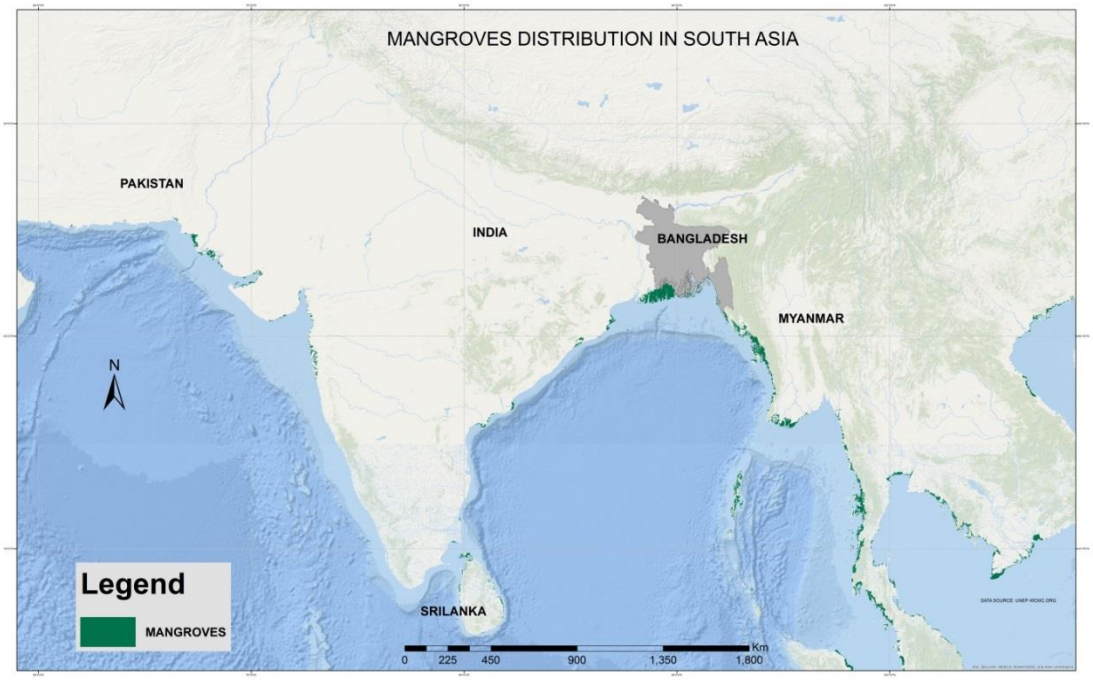

Figure.3: *Mangrove forests distribution in South Asia (data source: unep-wcmc.org, a base map from ESRI).*

2.4 Threats to Mangrove Ecosystems

Globally, the mangroves are degraded due to natural disasters, (for example; tropical cyclone Sidr in 2007 affected 1900 Km² Sundarbans area of Bangladesh (CEGIS 2007). Top dying diseases is another natural cause. Top dying diseases of Sundari tree is defined as a decline and or death of foliage and twigs in the crown which starts at the top of the trees and ends with the death of the lower part of the tree (Rahman, M.A. 1996; Awal, M.A. 2014). Sundarbans is located approximately 2m above mean sea level and is the potential threat to sea level rise. Payo *et al*., 2016 projected changes in the Sundarbans mangrove forest area which showed Sundarbans might lose 81 km² to 1393 km² due to sea level rise of 0.46 to 1.48

m by 2100. Erosion also a threats to mangrove changes in the study area. Rahman *et al.,* 2011 claimed that due to erosion, the coast of the Sundarbans in India and Bangladesh had lost 940 ha per year between 2000 and 2010. Human disturbance is also contributed to the destruction of the mangrove forest in the study area. Land use changes due to shrimp farming are responsible for mangrove loss (for example; Chakaria Sundarbans) in the study area (Hossain & Lin 2001, Iftekhar & Islam 2004, Rahman & Hossain 2015). Rapid withdrawal of sediment-laden freshwater into the Bay of Bengal from 1975 to present through the Sundarbans from *farakka barrage* (artificial barrier across a river used for irrigation) point in India has led to a polyhaline environment in the sundarban mangrove forest in Bangladesh. This polyhaline environment has affected the growth and distribution of mangroves mainly affected by Sundari trees (*Heritiera fomes*) in the study area (Aziz *et al.,* 2015).

2.5 Literature Review

2.5.1 Remote Sensing data to mangrove mapping and Time-series Study

Optical and Radar Remote sensing data are now widely used for mangrove mapping and monitoring in the world. In the last two decades, optical remote sensing data have become a helpful tool in studies dealing with the Mangroves. Besides medium resolution images, such as Landsat (30m), high-resolution images like QUICKBIRD, and WORLDVIEW-2 have been used to detect the change on smaller scales (Heumann, W.B., 2011).

Globally, several mangrove studies have been done using remote sensing data, but only a few time-series studies have been conducted. The main time series studies of mangrove forests at a global scale are stated in Table.2.

2.5.2 Classification Techniques in Mangrove Time-Series Study

In remote sensing, various methods have been developed to detect temporal changes in the mangrove forests. In Unsupervised classification, based on spectral signatures software automatically classify the images which can use for mangrove change detection. Most of the unsupervised studies used an iterative self-organization classification algorithm (ISOCLUST) for mangrove change detection (Giri *et al.,* 2007; Jones *et al.,* 2016; Shapiro *et al.,* 2015). However, the Unsupervised Otsu method is a simple method based on threshold selection. Chen *et al.* (2013) applied these techniques for multi-decadal mangrove change detection in Honduras.

In Supervised Classification, training samples are obtained from images to classify the land cover. The Maximum likelihood supervised classification approach is widely used for mangrove time-series analysis (Chandra Giri *et al.,* 2007; Kanniah *et al.,* 2015; Pham & Yoshino, 2015; Sremongkontip *et al.,* 2000). Pseudo-Variant Features (PVFs) techniques now used in some mangrove change detection studies (Chen *et al.,* 2013). For post image classification Object-based image (OBI) techniques (Son *et al.,* 2015; Chen *et al.,* 2013) also famous for mangrove change detection.

Vegetation Indices (VI) have been used in mangrove mapping and change detection worldwide. For example, Hasmadi *et al.,* (2011) used vegetation indices (NDVI, IPVI, PVI, SAVI, NSAVI, etc.) for comparison of mangrove mapping in Peninsular Malaysia. The most common one is the Normalized Difference Vegetation Index (NDVI). This index has also been widely used to study mangrove change detection (Islam, M.T. 2014). The Landsat programs have a long record of data that is suitable for computing NDVI Worldwide. NDVI is calculated from the Red and Near Infrared spectral bands.

2.5.3 Previous Mangrove mapping and change detection studying in the study area

There have been some studies done about vegetation classification in the Sundarbans mangrove forests of Bangladesh using satellite images. For example, Diyan M. A, (2011) used Quick bird images for mangrove vegetation classification and applied pixel based, object-based image analysis techniques. Syed *et al.* (2001) used optical (Landsat TM) and radar images to detect fragmented mangrove forest in Sundarbans. However, few Landsat time-series studies have been conducted in the study area to detect mangrove changes. Among them, most of the studies performed are based on supervised classification techniques (Emch & Peterson 2006; Rahman 2012) while some studies also used the NDVI vegetation (Akhter, 2006; Bhowmik & Cabral, 2013; Islam, M.T., 2014). Landsat MSS, Thematic Mapper (TM) and the Enhanced Thematic Mapper (ETM+) are the remote sensing data that all of those researchers used. However, all of these studies only focus the world heritage site Sundarbans (Table.3). Unfortunately, the south central and southeast part of mangrove forest in Bangladesh change detection was avoided in those study. Furthermore, there is a lack of information of current estimation (increasing or decreasing) of mangrove forest in the whole country (see Table.3).

Table.2: *Review summary of the main time-series studies of mangrove ecosystems in the world (S.N. means Serial Number)*

S. N.	Region /Country	References	Satellite Data (Landsat)	Classification Techniques	Locations	Main Findings
1	118 Countries	Giri *et al.* 2010	ETM+ (1997-2000)	Hybrid supervised and unsupervised	Tropics and Subtropics	Mangrove area 137,760 Sq. Km (2000)
2	Asia	Giri *et al.* 2007	MSS, TM, ETM+ (1975-2000)	Hybrid supervised and unsupervised	Indonesia, Malaysia, Thailand, Burma (Myanmar), Bangladesh, India, and SriLanka	Mangrove lost 12% (1975-2005)
3	South Asia	Giri *et al.* 2015	ETM+ (2000-2012)	Classification and Regression Tree (CART) algorithm	Bangladesh, India, Pakistan, and Sri Lanka	areal extent 1,187,476 ha (7% globally) and 92, 135 deforested (2000-2012)
4	Mozambique	Shapiro *et al.* 2015	TM, ETM+, L8 OLI; Worldview-2	Unsupervised	Zambezi River Delta	Net increase 3723 ha over 19 years
5	Peninsular Malaysia	Kanniah *et al.* 2015	TM, ETM+, OLI (1989-2014)	Max likelihood, Support Vector Machine	The Iskandar Malaysia	lost 6740 ha of mangrove areas from 1989 to 2014
6	China	Li *et al.* (2013)	MSS, TM, ETM+ (1977-2010)	Unsupervised	Guangdong province of Southern China	Decreased sharply (1977-1991) due to deforestation, and increased (1977 to 1991) Due to afforestation
7	Indonesia	Ramdani *et al.* 2015	ETM+, L8OLI (2002-2013)	NDVI, Supervised Classification	Maros Regency, South Sulawesi Province	Decreased mangroves due to fish pond activity
8	Thailand	Sremongkontip *et al.* 2000	TM (1988-1996)	Max likelihood	Bang-Toey sub-district, Phang-Nga Province	degradation of mangrove and ecological disturbance.
9	Madagascar	Jonese *et al.* 2016	TM, ETM+ (1990-2010)	supervised and unsupervised	Ambaro-Ambanja bays, Mahajamba Bay Mahajamba Bay, Tsiribihina-Manambolo Delta	nation–wide net loss of 21% (i.e., 57,359 ha) from 1990 to 2010
10	Vietnam	Nguyen-Thanh Son (2015)	MSS,TM, ETM+ (1979-2013)	Object-based image analysis	Ca Mau province, southernmost Vietnam	Decreased 74 % from 1979 to 2013
11	Vietnam	Dat Pham *et al*. (2015)	TM, ETM+, OLI (1989-2013)	supervised	Hai Phong city,	1989 to 2001 and gain from 2001 to 2013.
12	Honduras	Chi-Farn Chen *et al.* (2013)	TM, ETM+, OLI (1985-2013)	Unsupervised Otsu's method	Choluteca and Valle department (Gulf of Fonseca)	1985 to 2013, approximately 11.9% of the mangrove forests were transformed
14	Myanmar	Chiang *et al.* (2015)	TM, ETM+, L8 OLI	Cellular Automata (CA) algorithm	Irrawaddy Delta	26.7% decreased between 1989 and 2014

Table.3: *Review summary of the main time-series study of mangrove forests in Bangladesh (S.N. means Serial Number)*

S. N.	**Country**	**References**	**Satellite Data (Landsat)**	**Classification Techniques**	**Locations**	**Main Findings**
1	Bangladesh	Emch *et al.* 2007	TM, ETM+ (1989-2000)	NDVI, Max like, Subpixel	South-west (Sundarbans)	*Deforested areas are southeastern comer and the western edge*
2		Giri *et al.* 2007	MSS, TM, ETM+ (1973-2000)	Supervised	India-Bangladesh (Sundarbans)	*Mangrove forest changed 1.2% in last 25 years*
3		Rahman, M.M. 2012	MSS, TM,ETM+ (1973-2010)	Max likelihood	South-west (Sundarbans)	*Erosion rate of Sundarbans western part is high(15mm/year) than eastern part (14mm/year)*
4		Islam, M.T. 2014	MSS, TM, ETM+ (1975-2006)	NDVI	India-Bangladesh (Sundarbans)	*19.3% forest decreased in 1989 due to cyclone in 1977 and 1988*
5		Akhter, M. 2006	TM, ETM+ (1989-2000)	NDVI	Central Sundarbans	*Mangrove changes occur due to illegal removal of trees from the forest*
6		Bhowmik *et al.* (2013)	ETM+ (2007-2010)	Unsupervised, NDVI	South-west (Sundarbans)	2500sq.km mangrove forest affected by cyclone SIDR in 2007

Chapter Three-
Methodology

3.1 Study Area

The study area is located in the southern coastal belt in Bangladesh. It extends to the southwest part called *Sundarbans*, and to the southeast coastal belt of Noakhali and Chittagong regions to the Cox's Bazar (Figure.4). The study area covers about 18785.01 km². Sundarbans covers the largest part of the mangrove forest in Bangladesh. Mangroves are also found in the southeast part of the country in Cox's Bazar, the *Chakaria Sundarbans, and Moheshkhali Island*.

The dominating tree species are Sundari (*Heritiera minor*, Figure.5) and Gewa (*Excoecaria agallocha*). Other common species are Passur (*Xylocarpus moluccensis)*, Goran (*Ceriops roxburghiana*), kankra (*Bruguiera gymnorhiza*), keora (*Sonneratia apetala*) and baen (*Avicennia officinalis*) (FAO, 1981). Tree heights vary with geographical regions in the study area. Mangrove heights variation in Sundarbans range from 0-5 m (south central, northwest), from 5-10 (southwest) and 10-15 m (north to southeast). These mangrove height variations are adopted from European Space Agency (ESA) satellite map (ESA, 2015). Tree height also varies based on species types. Sundarbans south-central is Sundari-gewa dominant; South-west is Goran-gewa dominant, Sundari and geoa dominant (CEGIS 2007). However, outside Sundarbans average, mangrove forest height varies from 0 to 12.8 m in Mirersarai at Chittagong (Uddin *et al.*, 2014).

The study area lies between 89°1' 43.19" E and 21°55 ' 10.32" N and between 92° 24' 48.71" E, and 20° 32' 53.48" N. The study area is topographically flat land, and average rainfall in this coastal region is about 700 mm per year. Rainfall season in the study area starts from mid-May to late October. Figure 6 shows June-August occurred the highest rainfall varies between 430-550 mm and temperature ranges from 27-28°C from 1900 to 2012. Climate (rainfall, sufficient sunlight), mudflats and estuarine deltas, soil pattern (Unripened soil, ripening soil, Organic soil), storm and wind act as a seed spreading and pollination, nutrients, saline water, high tide and ocean current and sedimentation and freshwater flow from upstream such as mangroves of Bangladesh (Islam, M.S., 2001; Aziz *et al.*, 2015) are the general conditions for growth and development of mangrove ecosystems.

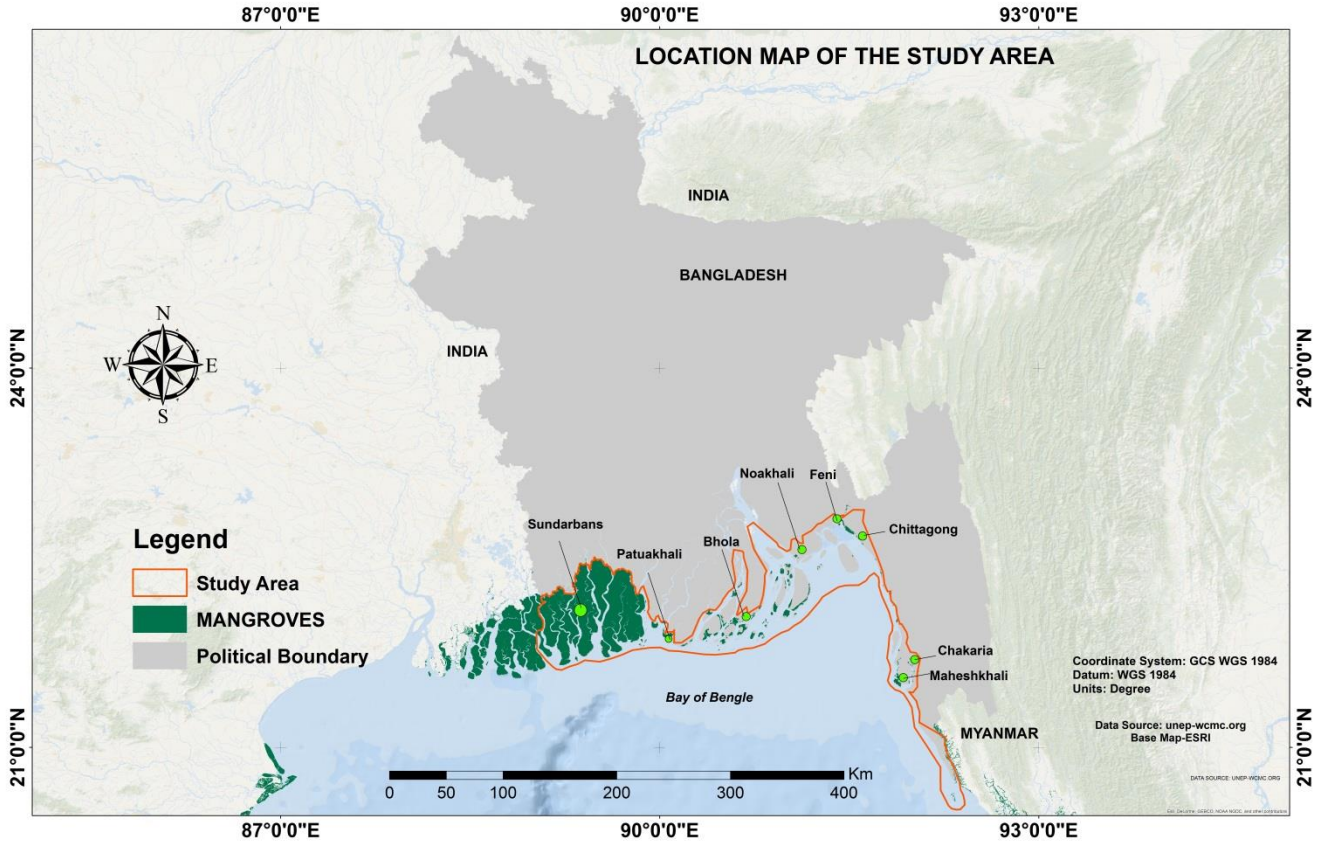

Figure.4: *Study area and distribution of Mangroves (Data Source: unep-wcmc.org, Base map from ESRI).*

5a 5b

Figure.5: *A typical example of Mangrove ecosystem characteristics in the study area (Nipa Fruticans locally called Golpata in 5a and Sundari trees root in 5b). The photograph was taken by Author in 2011 at Satkhira Sundarbans part.*

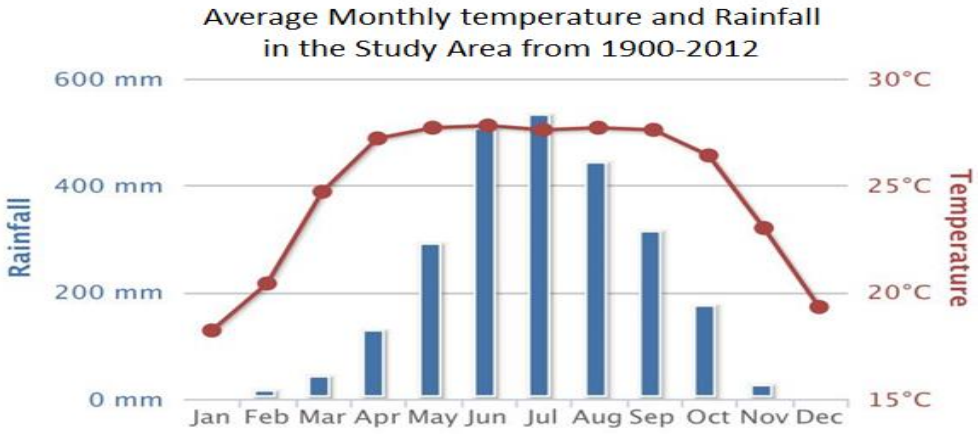

Figure.6: *Mean monthly temperature and rainfall pattern at location 21.97° N, 89.95° E in the study area (Data was collected from World Bank climate portal).*

3.2 Landsat Time Series Preparation

Figure.13 (methodological flowchart of the study) summarizes the steps of Landsat time series preparation, sample collection, classification, change detection and accuracy assessment.

3.2.1. Image collection

In this study, twenty-eight level-1 Terrain corrected (L1T) Landsat scenes (for example of Landsat scene, see Figure.8) were collected from USGS Earth observation website (USGS, 2016a). The Landsat scenes fall into two Worldwide Reference System (Figure.7). The scenes were collected from four-time epochs (1976, 1989, 2000, and 2015). Each epoch consists of seven Landsat scenes. The images were obtained mainly from the cold-dry season (November to March) and with a two years' time interval within in each epoch (Table S1 in appendix-A)). Four images (out of 28 images) were collected in leaf fall (acquired image time in November,) in Bangladesh, November-December is considered as the leaf fall season. Those images were chosen because there were rare cloud-free images found in leaf on time and maximum leaf fall started in December (no images was selected at this time). The rest of the images were collected from the leaf-on the season in Bangladesh. The cold-dry season (November-March) is selected in most of the mangrove studies (Giri *et al.*, 2007; Rahman *et al.*, 2013) in the study area. The study area's dominant mangroves are evergreen and the leaf-fall (not leaf-off like as forests such as Oaks in Northern latitudes) time is November-December. The Mangroves are mainly evergreen forest and leaves have a longer life span

that varies from one to five years (Nitta, I. and Ohsawa, M., 1997). Mangrove forest leaves are not off during the leaf-fall season. For instance, in present study area, most of the dominating tree species are evergreen such as Sundari (*Heritiera minor)*, Goran (*Ceriops roxburghiana*), kankra (*Bruguiera gymnorhiza*), keora (*Sonneratia apetala*) (Rahman *et al.* 2015). **The study assumed that there are no leaf-off effects** in the time-series analysis. Cloud-free images were only available for Landsat MSS, TM, and ETM+. There were no cloud-free images found for Landsat-8 (launched recently in 2013) in the study area. Only images having a cloud cover of less than 0.2% (Table.S1 in appendix-A) were carefully selected to be used here. The cloud found outside of the mangrove regions.

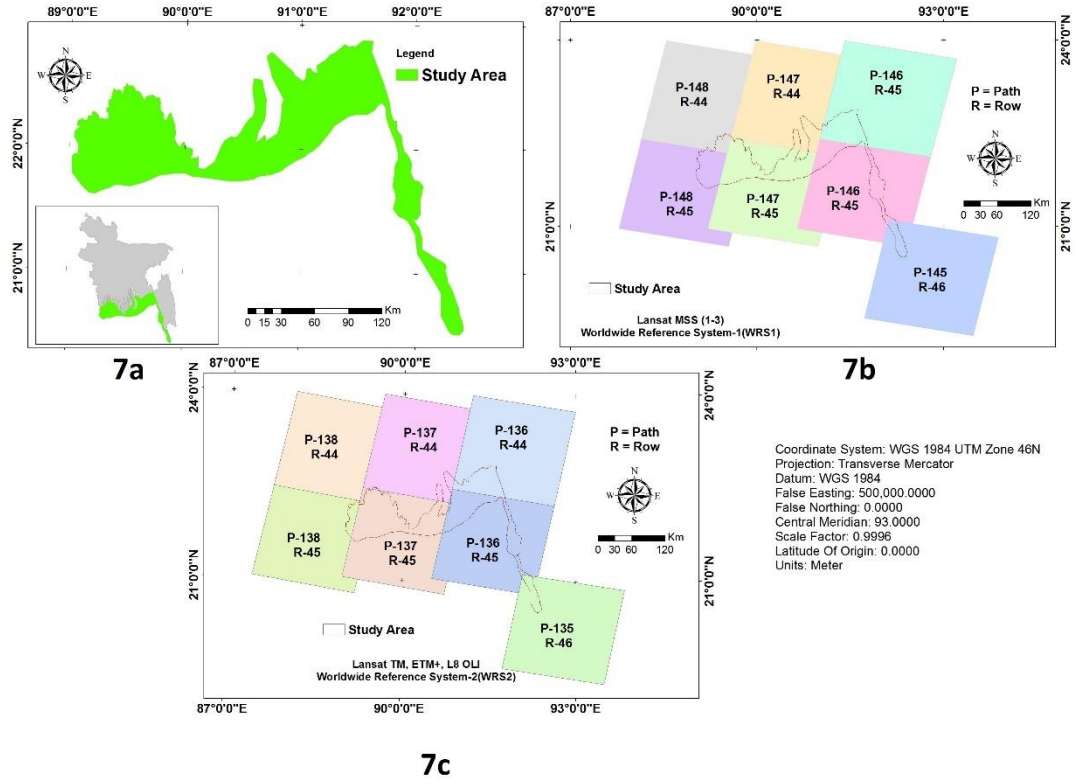

Figure.7: *Path/Row (7b and 7c) of the acquired Landsat Scenes in the study area (7a). Path/Row number is the Indexing system for locating Landsat scenes (LDEO, 1998) and Path/Row number individually identifies a scene center (Baumann, P.R., 2010).*

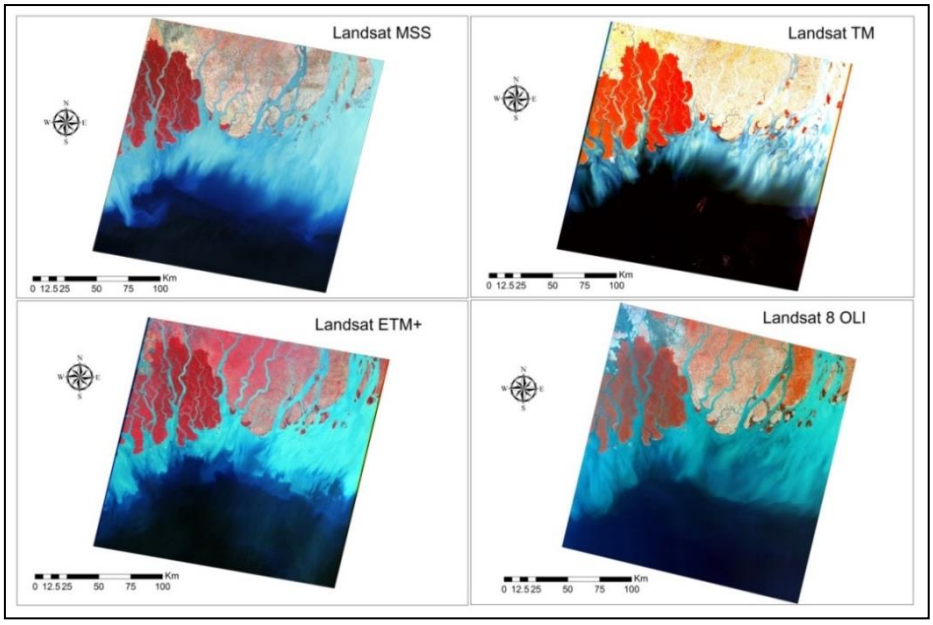

Figure.8: *An example of some scenes used in the study (MSS (1976) band 321, TM (1989) band 432, ETM+ (2000) band 432, L8 OLI (2015) band 543). For the band, explanation sees in Table S2 (in the appendix-A). Here, Red color represents Near Infrared wavelength where plant chlorophyll reflects near infrared energy. Blue color represents green and blue wavelength reflects by water bodies.*

3.2.2 Image Co-registration, Ortho-rectification, and Re-sampling

To perform image co-registration is time-consuming, but essential step in time-series studies (Gao *et al.,* 2009). Co-registration has been done based on pairs of the image. Here, Landsat 7 ETM+ of each path/row image was used as a base image and the other image was used as warp image (Figure. 9). Tie points are pairs of pixels consistent with the same locations of images overlap areas (Harris geospatial solutions, 2016). This tie point selection has been made by using Fast Fourier Transform (FFT) based algorithm in ENVI. However, for some images, some manual tie point selected first and used the automatic function for more tie point selection. At least 25 Tie points were chosen for each pair of images, resulting in an RMSE of less than 0.5 (means half of the size of pixel resolution) (Table S3 in appendix-A). Ortho-rectification is used to reduce pixel error caused by the off-nadir viewing of topography and is measured by using geoid height, earth model, co-registered image (Huang *et al.,* 2009; Gao *et al.,* 2009). Although all of the Landsat images were already Ortho-rectified, additional corrections were necessary for Landsat MSS images to improve geometric consistency (Pflugmacher et al., 2012). Only resampling techniques were applied for Landsat MSS images to convert spatial/pixel resolution from 60 m to 30 m (Pflugmacher et al., 2014). Here, the Cubic convolution method was used for resampling (Giri *et al.* 2007).

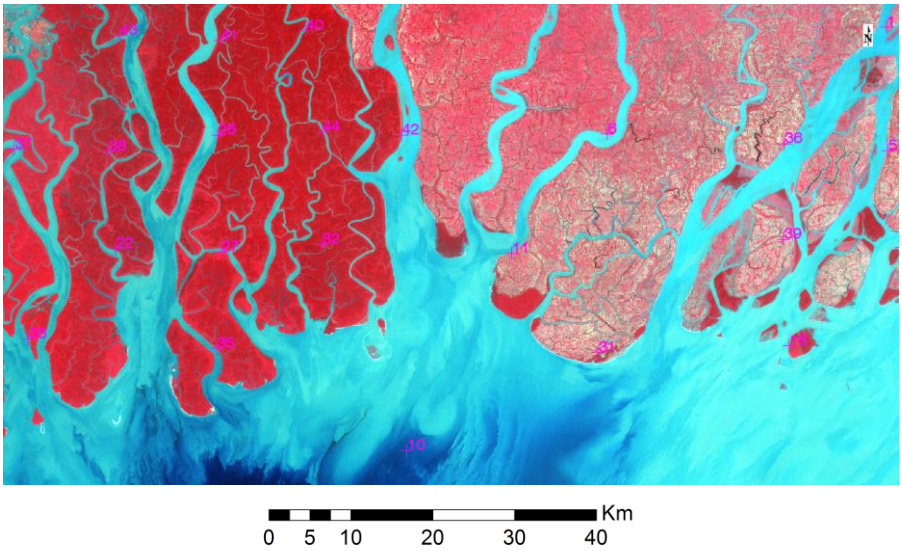

(a) *Base image (ETM+P137 R45; 2000-11-26)*

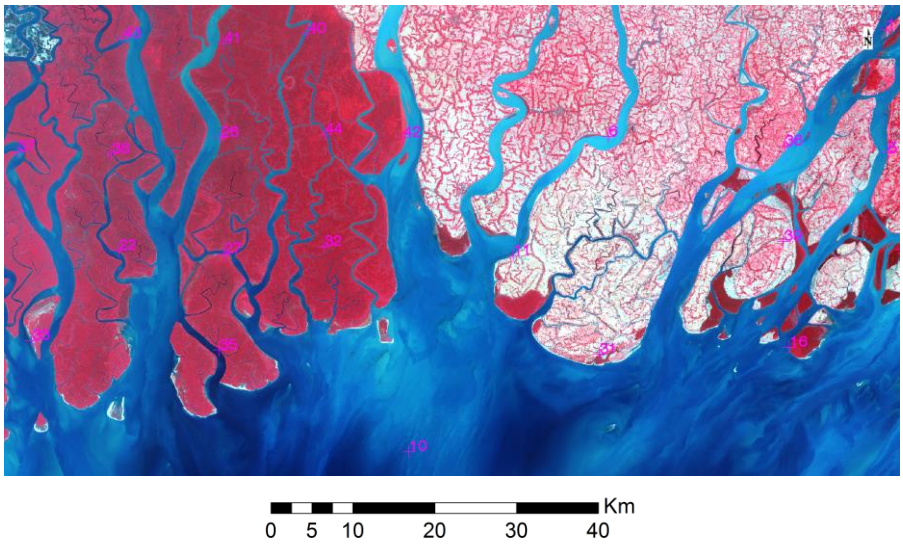

(b) *Warp image (L8 OLI P137 R45; 2015-03-17)*

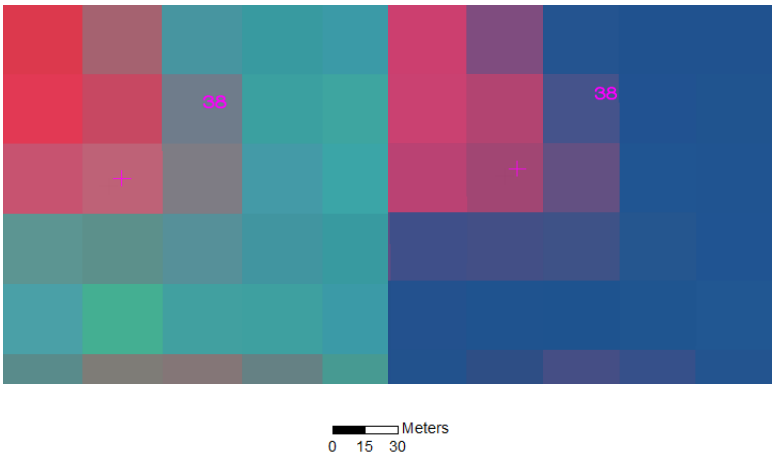

(c) *Base image (ETM+P137 R45; 2000-11-26)* (d) *Warp image (L8 OLI P137 R45; 2015-03-17)*

Figure.9: *Co-registration tie points of pair images* (a) *and* (b) *show enough tie points found;* (c) *and* (d) *show for clear view of tie point location*

This method produces a smoother image than for instance the nearest neighborhood method. It has no stair-stepped effect (break up of image features) like nearest neighboring approach (Baboo, S.S., and Devi, M.R., 2010). Cubic convolution uses the nearest sixteenth pixels weighted average to the focal cell. The first order (linear) polynomial equation was used in image Co-registration. This polynomial function is suitable for image adjustment of Landsat images rather than quadratic and cubic polynomial (Mohammed, N.Z. and Eisa Eiman, A.E., 2013).

3.2.3 Radiometric Calibration

Radiometric characterization and calibration are required to get high quality and downstream images (Chander *et al.,* 2009). Radiometric calibration is done in two step process using Markham and Barker equation (1986)-

a. **Conversion of Digital Number (DN) to Radiance:** The equation is-

$$L\lambda = Gain\lambda * DN\lambda + Bias\lambda \quad (1)$$

Where Lλ is the at-satellite radiance, Symbol λ refers to spectral band λ; gain and biases are provided in the header file.

In previous times, the spectral radiance unit of [mW/(m^2 sr μm)] was used for MSS and TM, but to maintain consistency with ETM+, and later for Landsat 8 OLI spectral radiance, units of, [W m^{-2} sr^{-1} μm^{-1}] are now used (Landsat 8 Data User Handbook, USGS, 2016b)

b. **Conversion of radiance to TOA Reflectance:** The Top of Atmospheric Reflectance of the earth is calculated by following equations-

For MSS, TM, ETM+

$$\rho\lambda = (\pi * L\lambda * d2)/(ESUN\lambda * \cos\theta s) \quad (2)$$

For OLI-

$$\rho\lambda = \rho\lambda' / \sin(\theta) = (M\rho * Qcal + A\rho)/ \sin(\theta) \quad (3)$$

Where,

ρλ= Planetary TOA reflectance [unitless]

π= Mathematical constant equal to 3.1416 [unitless]

Lλ= Spectral radiance at the sensor's aperture [W/(m2 sr μm)]

d= Earth–Solar distance (astronomical units)

ESUNλ= Mean exoatmospheric solar irradiance [W/(m2 μm)]

θs= Solar zenith angle [degrees]

ρλ' = Top-of-Atmospheric Spectral Reflectance, without correction for solar angle. (Unitless)

Mρ = Reflectance multiplicative scaling factor for the band (REFLECTANCEW_MULT_BAND_n from the metadata).

Aρ = Reflectance additive scaling factor for the band (REFLECTANCE_ADD_BAND_N from the metadata).
Qcal = Level 1 pixel value in DN
θ = Solar Elevation Angle (from the metadata, or calculated).

ENVI 5.1v Software (Exelis Visual information solutions, 2016) automatically used equation-1 to convert DN value to radiance. Then radiance was converted to Top of atmospheric reflectance (TOARef) automatically in ENVI using equation-2 and equation-3 (see chapter two). The process is often called first order normalization (Huang *et al.,* 2001).

3.2.4 Atmospheric Correction

For accurate absolute atmospheric correction in-situ, atmospheric measurements are needed to be done during satellite image capturing time. Atmospheric measurements are not possible all the time, and therefore, a radiative transfer code (RTC) is required to remove atmospheric effects (Chávez 1996). However, the radiative transfer codes are used for scan-off line and look up table for scan on-line corrections (Liang *et al.,* 2001; Chander *et al.,* 2009). It is a difficult task to estimate atmospheric parameters from the imagery (Liang *et al.,* 2001). In this case, the dark object subtraction technique (DOS), which is an image-based procedure, can be applied. This application is straight forward and requires an in-situ field measurement is not mandatory (Chávez 1996). This method assumes that some pixels of the existing features in a satellite image have zero reflectance, for example, shadow, clear and deep water; and the recorded signal from those features is due to atmospheric scattering (Chávez 1996).

In this study, a most common absolute atmospheric method called Dark Object Subtraction (DOS) method using ENVI 5.1v software was used to convert at-satellite reflectance to surface reflectance. A dark object subtraction method uses the darkest pixels (red circle in Figure.10) in the image by subtracting their values from all other pixels. This method can be used to remove atmospheric effects such as scattering effects (Figure.10) using pixels from the second image. The purpose of Dark Object Subtraction (DOS) is to eliminate atmospheric effects such as scattering from the imagery and used to get good result of vegetation indices (e.g. NDVI) to monitor vegetation dynamics. NDVI at the canopy level is always higher than at the top of the atmosphere.

Before DOS L8 (band 543) DOS (using grayscale (band 1) After DOS (band 543)

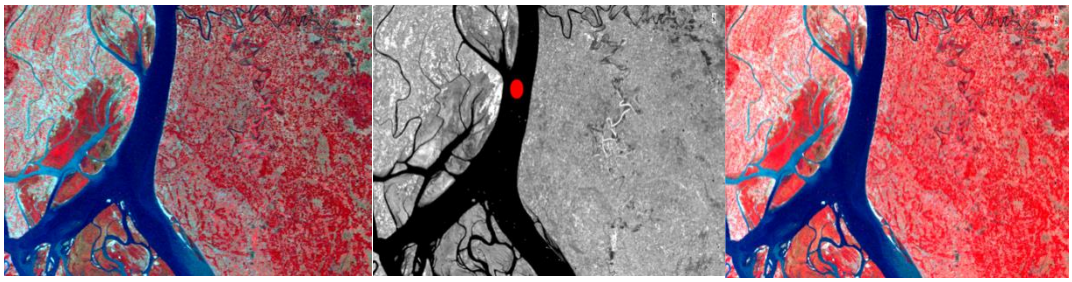

Figure.10 *shows Dark Object Subtraction method (left image show before DOS, red circle of middle image indicates dark object, right image shows noise and brightness change after atmospheric correction)*

3.2.5 Relative Radiometric Normalization

Relative radiometric normalization does not need any physical atmospheric data at the moment the satellite image was acquired. Relative normalization corrects disturbance factors such as sensor response, noise, etc. Schroeder *et al.* (2006) used this approaches for Landsat-time series analysis, and they concluded that the benefits of applying this approaches are the reliance on the more reliable relative normalization process to produce an improved temporal common scale, while afterward converting all images in a time-series to units of surface reflectance. Relative radiometric normalization using pseudo-invariant features (PIFs) are mainly developed by Schott *et al.,* (1988) and later used by manual selection e.g. Schroeder *et al.,* (2006); Wulder *et al.,* (2004) and by automatic selection using Multivariate alteration detection (MAD) transformation e.g. Schroeder *et al.,* (2006); Canty & Nielsen, (2004). Pseudo-invariant features are those features in the image where reflectance properties are the same over longer time periods, such as water, forest, lava, urban, bare ground, rock, dune, quarries, and gravel pits have uniform reflectance over time (Eckhardt *et al.,* 1990). Relative normalization produces consistent results across scenes, and it depends on the accuracy of PIFs (Pseudo-invariant Features) selection and reference image correction.

In this study, PIFs were carefully selected by hand and results gave good accuracy (Table 4). Sediment in water might affect during the dark object selection in atmospheric correction, and Relative normalization from the absolute corrected (DOS) images was performed here to reduce this effect (see Figure.S2 in appendix-A). Here, Relative normalization was performed in three steps.

- Firstly, atmospherically corrected Landsat ETM+ (2000) images were selected as a reference image. ETM+ images were selected as reference image because of their

high radiometric quality, the fact that they move relatively cloud free and the time begin in the middle of the time-series.

- Secondly, so-called "pseudo-invariant features" (PIFs) were extracted from the images. They are named invariant since the reflectance is stable (does not vary) over time, and "pseudo" because this is (naturally) not entirely true. In this method, 50 (PIFs) for each image band were selected, based on the spectral brightness, 25 dark (water, forest) and 25 Bright (coastal land, bareland, etc.) using BEAM VISAT 5.0v software. After the PIFs selection, the pixel values were extracted on a band by band basis, and total 1150 PIFS were selected from twenty- eight images (4bands*50 PIFs +6 bands*50 PIFs +6 bands*50 PIFs +7 bands*50 PIFs). Figure.11 shows an example of the PIFs collection from the ETM+ Landsat scene. All the pixel values from the selected PIFs were exported to an Excel sheet for further processing. A form of regression analyses (Table. 4) named "Reduced major axis regression" (RMA), was performed to normalize the images on a band-by-band basis. The RMA method was presented by Bohonak (2004) and was developed by Cantey *et al.* (2004) and used by Schorder *et al.*, (2006).
- Thirdly, Landsat TM, ETM+, L8 OLI images were normalized using regression coefficient.

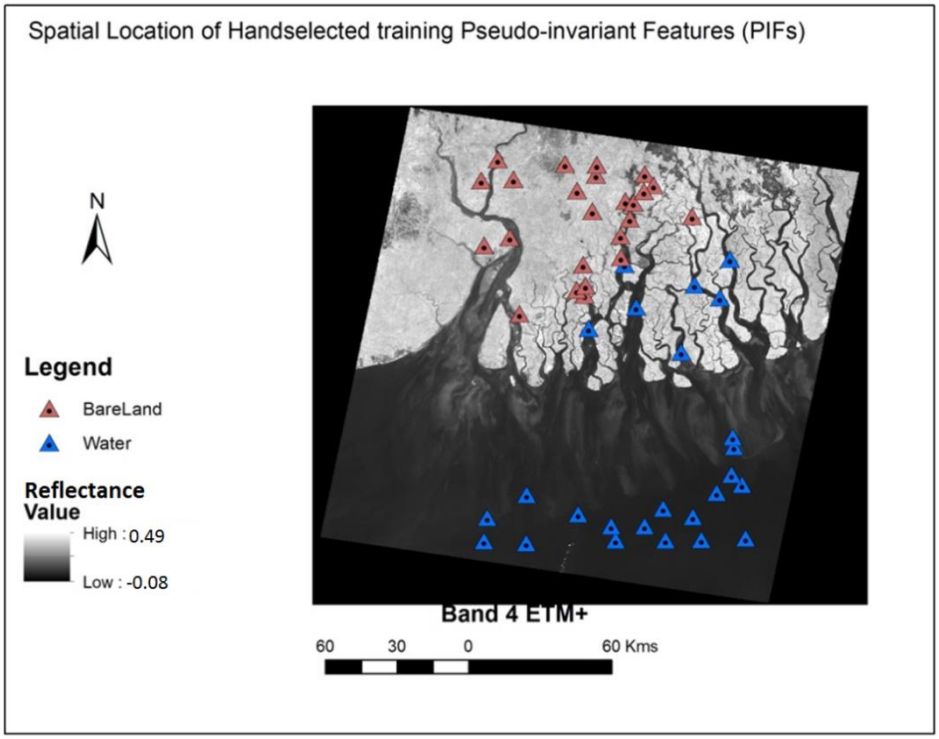

Figure.11: *Spatial location of hand selected Pseudo-invariant features (PIFs) of Landsat ETM+ (P134 R45) images*

Table.4: *Results of regression coefficient using pseudo-invariant Feature (PIFs) after Reduced Major Axis Regression (RMA). ETM+ (Path 138/Row 45) used as reference image and MSS, TM, ETM+ used to calculate RMA*

Landsat	Scene	Band	RMA Intercept	RMA Slope	R^2	St. Error RMA	St. Error Slope
MSS	Path 148 Row 45	1	-3.456e-03	1.31	0.60	4.214e-03	0.12
		2	-1.422e-03	1.60	0.65	5.099e-03	0.13
		3	8.099e-03	0.64	0.94	3.300e-03	0.02
		4	-4.818e-03	0.83	0.97	3.443-03	0.02
TM	Path 138 Row145	1	-4.205e-03	1.65	0.64	2.157e-03	0.15
		2	-6.793e-03	1.37	0.55	4.382e-03	0.13
		3	-7.684e-03	1.60	0.68	4.867e-03	0.13
		4	1.296e-03	0.74	0.96	3.074e-03	0.02
		5	-1.511e-03	1.43	0.94	4.795e-03	0.04
L8 OLI	Path 138 Row145	2	-7.491e-04	1.30	0.59	4.060e-03	0.12
		3	-9.454e-03	1.31	0.61	4.111e-03	0.11
		4	-4.305e-03	1.66	0.65	5.381e-03	0.14
		5	-5495e-03	0.49	0.83	4.156e-03	0.15
		6	-6.594e-03	1.153	0.847	5.831e-03	0.07
		7	-6.665e-03	0.9867	0.844	5.108e-03	0.06

3.2.6. Cloud Masking

Cloud is a big problem for time-series analysis of satellite images. Cloud masking was not performed for Landsat MSS, TM, and ETM+ images because these images were free from clouds. Recently launched Landsat 8 images have a quality band which is used to cloud detection and clouds remove (USGS 2016c). Cloud masking for Landsat 8 OLI images was accomplished using quality assessment band (downloaded with L8 images). Cloud shadow masking was not done because the minimum amount of clouds present, were found outside the Mangrove forest regions.

3.3 Normalized Difference Vegetation Index (NDVI) Calculation

Chlorophyll in plant leaves pigment absorbs visible light (from 0.4 to 0.7 μm) for photosynthesis, and plant leaves reflect near-infrared light (from 0.7 to 1.1 μm) due to the inner structure of the leaves.

Normalized Difference Vegetation Index (NDVI) was calculated from the NIR and Red bands using Eq. 4

$$NDVI = (NIR\ Band - Red\ Band)/ (NIR\ Band + Red\ Band) \quad (4)$$

An NDVI value varies between -1 to +1.

3.4 Mosaicking

BTM is conformal cylindrical projection, and it preserves the shape and is the most likely to be accurate for the areas close to the equator. And the fact that the study area falls into two Universal Transverse Mercator (UTM) zone 45 and 46. This could lead error in projection accuracy and can introduce bias in mangrove classification accuracy (Giri *et al.*, 2007) and to avoid this problem all images were projected to local projection (developed by Bangladesh Flood Action Plan 19) system called Bangladesh Transverse Mercator (BTM) Projection before mosaicking. Seamless mosaicking was performed to mosaic each epoch of Landsat images.

3.5 NDVI Change Detection

NDVI change detection was carried out by image differencing techniques using threshold values. In total, ten threshold values (see Figure.26) were determined to identify the minimum reflectance variation considered to represent a change in vegetation properties. In this case, more threshold values gave more spatial NDVI difference (level of details) in the study area. Maps were produced to display the change in vegetation characteristics from 1976 to 1989, from 1989 to 2000 and from 2000 to 2015 in Sundarbans.

3.6 Sample Collection

Training samples were selected from the images by careful investigation of homogeneous pixels of Land use/Land cover (LULC) class (Mangroves, Non-mangrove, Water bodies, Bare land, Shrimp & Salt Farm). Google earth was used as a reference to identify the actual LULC class**. Test samples (points) were collected manually for better classification of the images and used the simple random sampling techniques for the validation**. Validation samples (points) were used for classification accuracy. Here, sampling areas (polygon data) was not used for sampling selection because it could lead to optimistic bias in the supervised image classification (Hammond *et al.,* 1996, Friedl *et al.,* 2000, Zhen *et al.,* 2013). A total 324 of training samples (162 points for test and 162 points for validation) have been collected from the study area (Figure.12).

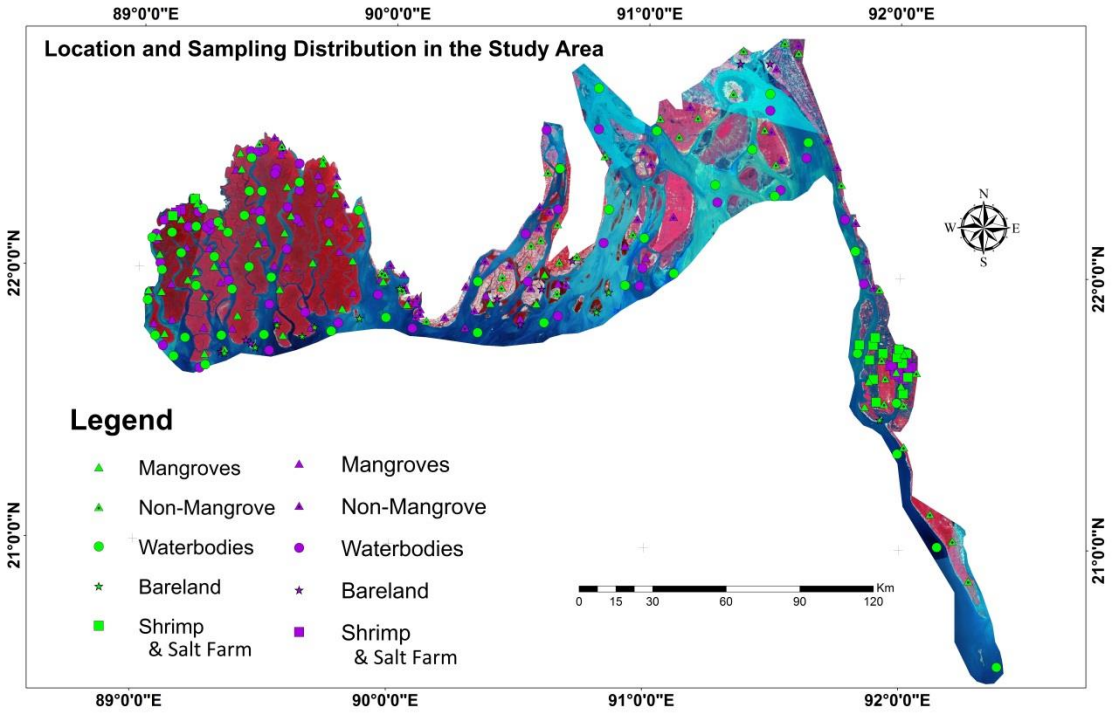

Figure.12: *Location and sampling distribution of the study area. Here, Light green color represents test samples and violet color represents validation samples respectively. The manual selection was performed to select test samples, and a simple random sampling technique was used for validation. The Image shows Landsat 8 OLI 543 (Near-Infrared, Red, and Green) band combination.*

The training samples were distributed among the land-use classes as follows: 45 samples for mangroves, 58 for water bodies, 32 for non-mangrove vegetation, 12 for bare land, and 15 for shrimp & salt farm. Test samples were used for LULC classification. An equal amount of samples was picked in each class for the validation samples. The selection of test and validation points is dependent on the variation of reflectance within the land use class. Here, a larger number of points were selected for mangroves because this is the primary focus of the study and water bodies (because the variation of water reflectance due to shrimp & salt farming) and the variation of extent is expected to change between water and mangrove, not between bare land and mangrove.

In the study area, the water body color is different in coastal regions than in the open sea, due to the sedimentation that occurs nearer to the coasts and the open sea. Another problem is that some agricultural fields, bare land areas show similar spectral properties.

3.7 Supervised Classification

In supervised classification, known classes are used to classify unknown areas/pixels in the whole images (Campbell, 2002b), and the user selects training sites where software uses these training sites to classify the images. Maximum likelihood is a traditional supervised classification method used in mangrove change detection studies *(*Kanniah *et al., 2015; Jones et al.,* 2016; Pham & Yoshino 2015; Giri *et al.,* 2007). Maximum Likelihood supervised classification was applied for the land use/land cover classification of the study area. Four land use/land cover (LULC) classification maps were made (1976, 1989, 2000 and 2015). This classification assumes the probability of a specific pixel goes to a particular class using by probability density function. This parametric method is most accurate and considers variability in the classification. For example, if an unknown pixel has brightness values within the mangrove spectral region, it has the highest probability of being mangrove forest. Other parametric rules such as maximum distance classifier (calculate pixels based on the spectral distance between candidate pixels and mean signature value of each class) do not incorporate the same signature variability.

3.8 Change Detection

Change detection can be applied by using cross-tabulation techniques (El-Hattab, M.M., 2016, Alphan, H., Doygun, H. and Unlukaplan, Y.I., 2009) or by subtraction of classified images from one to another (Erener, A. and Düzgün, H.S., 2009, Mas, J.F., 1999). Change detection was performed by subtracting (image subtraction method for mangrove study used by e.g. Giri, C. and Muhlhausen, J., 2008) the classification maps of 1976 from 1989, 1989 from 2000, and 2000 from 2015 by using raster calculator in ArcGIS. Two Areas of Interest (AOI) called Kalir Char, and Feni-Chittagong were selected for Change detection analysis.

3.9 Accuracy Assessment

Accuracy assessment was done using confusion matrix (by overall accuracy, producer's accuracy, user's accuracy) and Kappa Coefficient (Giri *et al.,* 2007; Kanniah *et al.,* 2015, Long *et al.,* 2011). The user accuracy represents the probability that a point randomly chose on the map has the same value in the field. For instance, Users accuracy of ETM+ images showed that the probability of randomly selected point of mangrove sample on the map has 88.89% same value in the field. The producer accuracy is the contrary. It represents the probability that a point randomly selected on the field will be correctly mapped on the map.

So for instance, Producer's accuracy of ETM+ images showed that the probability of randomly chosen of mangrove sample point on the field has 86.96% correctly mapped on the map. User's and producer's accuracy measures errors of commission and errors of omission present in the classification. The overall accuracy of classification is estimated by summing the corrected classified pixels and dividing by the total number of pixels. Overall accuracy does not incorporate off-diagonal elements (omission and commission errors), but kappa coefficient indirectly includes of this element as a product of the row and column marginals (Congalton 1991). Kappa is used to determine if the values contain in confusion matrix represents the results significantly better than the random. Kappa coefficient range from 0-1, where zero (0) accounts for no agreement, and 1 accounts for a perfect agreement between reality and or the classified images. In that case, this study has 0.7-0.96 kappa value which means classification results close to perfect agreement between reality and or the classified images.

The following equation (5) from Congalton (1991) was used for kappa coefficient calculation.

$$K\hat{} = \frac{\sum_{i=1}^{r} xii - \sum_{i=1}^{r}(xi+ * x+i)}{N^2 - \sum_{i=1}^{r}(xi+ * x+i)} \quad (5)$$

Here,

$K\hat{}$ = Kappa Coefficient
r = Number of Rows in the Matrix
xii = Number of rows in row i and column i
xi+ and x+i =Marginal totals of row i and column i
N = Total Number of observations

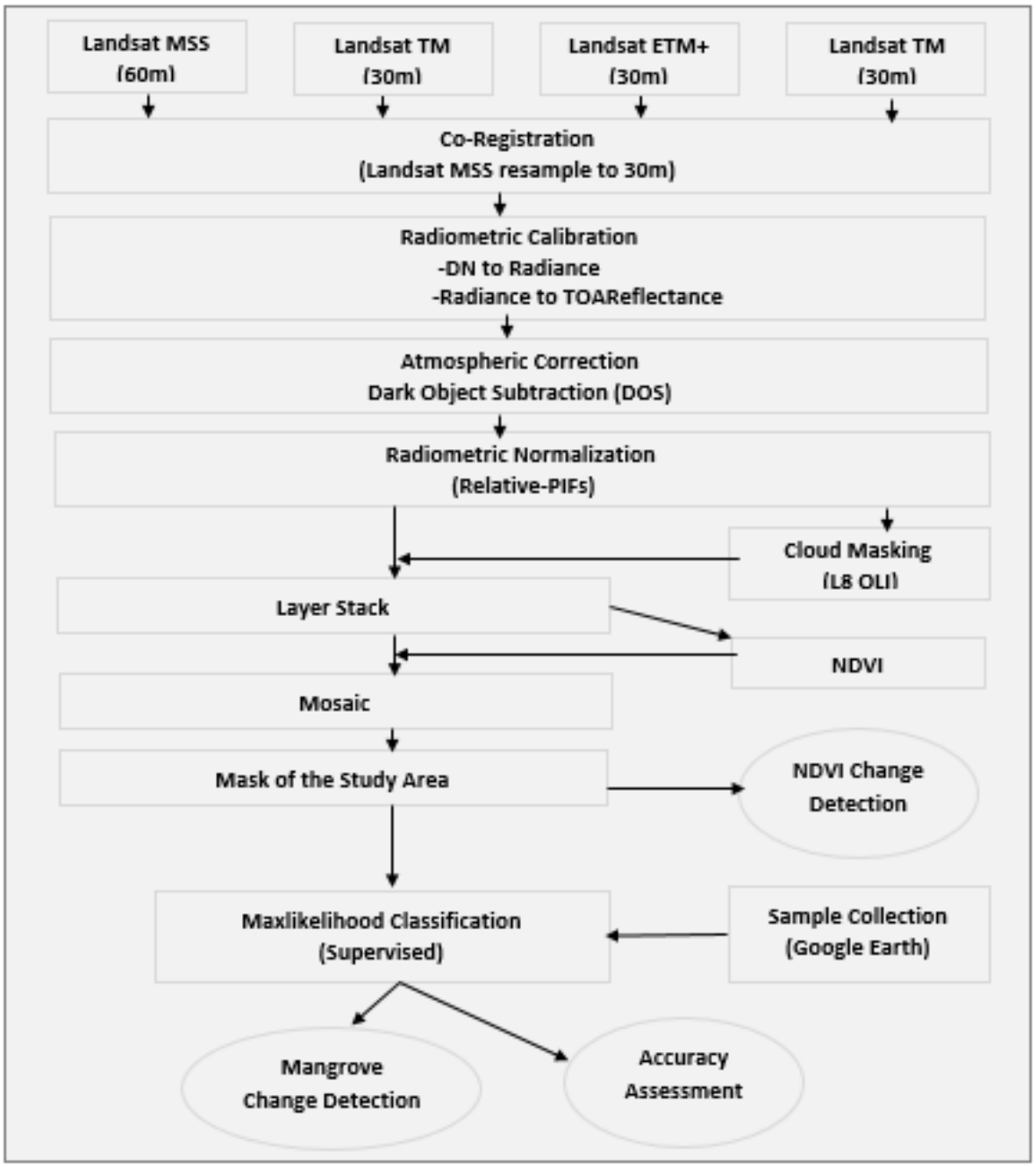

Figure.13: *A Methodological flowchart of the study*

Chapter Four -
Results

This classification was used to determine the extent of the Mangrove forests, and how this extent has varied in relation to the other land use classes within the studied time periods. Further, a vegetation index (NDVI) was computed, aiming to achieve an estimate on how the density of the forests may have varied within the studied time periods.

4.1 Accuracy Assessment

Tables (5-8) depicts producers' and user's accuracy. Mangroves, waterbodies, non-mangroves and shrimp & salt farms produced higher user and producer accuracies. Mangroves produced 100%, 88.89%, 91.11%, 86.67% producer's accuracy and 97.83%, 86.96%, 89.13%, 90.70% user accuracy for 2015, 2000, 1989, and 1976 epoch. This result indicates that mangroves were well classified. However, Bareland producers and users accuracy are lower than the other classes due to some bareland spectrally similar to non-mangrove vegetation.

The overall accuracy of Landsat 8 OLI, ETM+, TM,MSS classified images were found 97%,87%, 80%, 80% respectively. The kappa Coefficient of these images were 0.96, 0.82, 0.73, 0.74.

Table.5: *Confusion Matrix of L8 OLI (2015) images represents classification accuracy of Supervised classification. The values represent points. The columns represent the actual values, and the rows represent the classified values.*

Class / Class	Mangroves	Water-bodies	Non-Mangrove	Bare-land	Shrimp & Salt Farm	Row Total	Producer's Accuracy (%)	User's Accuracy (%)
Mangroves	45	0	0	1	0	46	100	97.83
Water bodies	0	57	0	1	0	58	98.28	98.28
Non-Mangrove	0	0	30	0	0	30	93.75	100
Bare land	0	1	2	10	0	13	83.33	76.92
Shrimp & salt Farm	0	0	0	0	15	15	100	100
Column Total	45	58	32	12	15	162		
Overall Accuracy = 96.91%					Overall Kappa = 0.96			

Table.6: *Confusion Matrix of ETM + (2000) images represents classification accuracy of Supervised classification. The values represent points. The columns represent the actual values, and the rows represent the classified values.*

Class / Class	Mangroves	Water-bodies	Non-Mangrove	Bare-land	Shrimp & Salt Farm	Row Total	Producer's Accuracy (%)	User's Accuracy (%)
Mangroves	40	0	5	1	0	46	88.89	86.96
Water bodies	0	55	0	3	0	58	94.82	94.82
Non-Mangrove	1	2	27	0	0	30	84.38	90.00
Bare land	0	0	0	8	5	13	66.67	61.53
Shrimp & salt Farm	4	1	0	0	10	15	66.67	66.67
Column Total	45	58	32	12	15	162		
Overall Accuracy = 87%					Overall Kappa = 0.82			

Table.7: *Confusion Matrix of TM (1989) images represents classification accuracy of Supervised classification. The values represent points. The columns represent the actual values, and the rows represent the classified values.*

Class / Class	Mangroves	Water-bodies	Non-Mangrove	Bare-land	Shrimp & Salt Farm	Row Total	Producer's Accuracy (%)	User's Accuracy (%)
Mangroves	41	2	3	0	0	46	91.11	89.13
Water bodies	3	50	0	5	0	58	86.20	86.20
Non-Mangrove	0	5	22	3	0	30	68.75	73.33
Bare land	0	0	7	4	2	13	33.33	30.77
Shrimp & salt Farm	4	1	0	0	13	15	86.67	86.67
Column Total	45	58	32	12	15	162		
Overall Accuracy = 80.24%					Overall Kappa = 0.73			

Table.8: *Confusion Matrix of MSS (1976) images represents classification accuracy of Supervised classification. The values represent points. The columns represent the actual values, and the rows represent the classified values.*

Class / Class	Mangroves	Water-bodies	Non-Mangrove	Bare-land	Shrimp & Salt Farm	Row Total	Producer's Accuracy (%)	User's Accuracy (%)
Mangroves	39	0	4	0	0	43	86.67	90.70
Water bodies	2	48	0	0	0	50	82.76	96
Non-Mangrove	4	4	21	2	0	31	65.62	67.74
Bare land	0	6	7	9	2	24	75	37.5
Shrimp & salt Farm	0	0	0	1	13	14	86.67	92.86
Column Total	45	58	32	12	15	162		
Overall Accuracy = 80%					Overall Kappa = 0.74			

4.2 A general perspective regarding variations of the extent and density of the Mangrove forests

The maps present the extent of Mangrove forests (after normalization and classification into the different land use classes) in 1976, 1989, 2000, and 2015 (Figure.15-18). The Mangroves area was increased gradually from 1976 to 2015 in Bangladesh (Figure.14). The mangroves in the Sundarbans area remain almost unchanged (400212 ha to 408912 ha) from 1976 to 2015, while a gradual increase is found in the central part of the study area such as Patuakhali-Bhola, Noakhali, Feni-Chittagong coast. Moreover, the extent of shrimp & salt farms has also increased in Chakaria in this period. Looking at the variations between the individual time steps, Patuakhali-Bhola has gained mangroves from 1976 to 1989 (Figure.15-16), while the extent of waterbodies have decreased (1125358 ha to 1039373 ha) and land areas increased (Table 9).

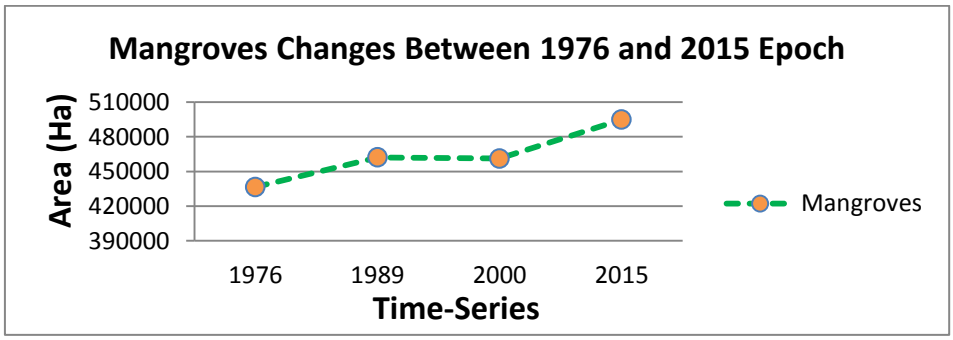

Figure.14: *Increases of the Mangrove forest over the last forty years from 1976 to 2015*

The highest density of mangroves was estimated from the NDVI measurements recorded in the Sundarbans area in 1976 (Figure.19), but a decrease in density was discovered in central Sundarbans in 1989 (Figure.20). An increase in density 2000 (Figure.21) while finally another decrease in 2015, indicates fluctuations of density within the Sundarbans. However, there has been a high vegetation density (mangroves and non-mangroves) observed in Noakhali-Feni-Chittagong coast in 2015 (Figure.22). A medium density of mangroves was revealed in Chakaria in 1976, following a notable change (negative) from 1989 to 2015. These indicate that the mangrove forests decreased in this area after 1976. Figure.19-22 are represented these fluctuations.

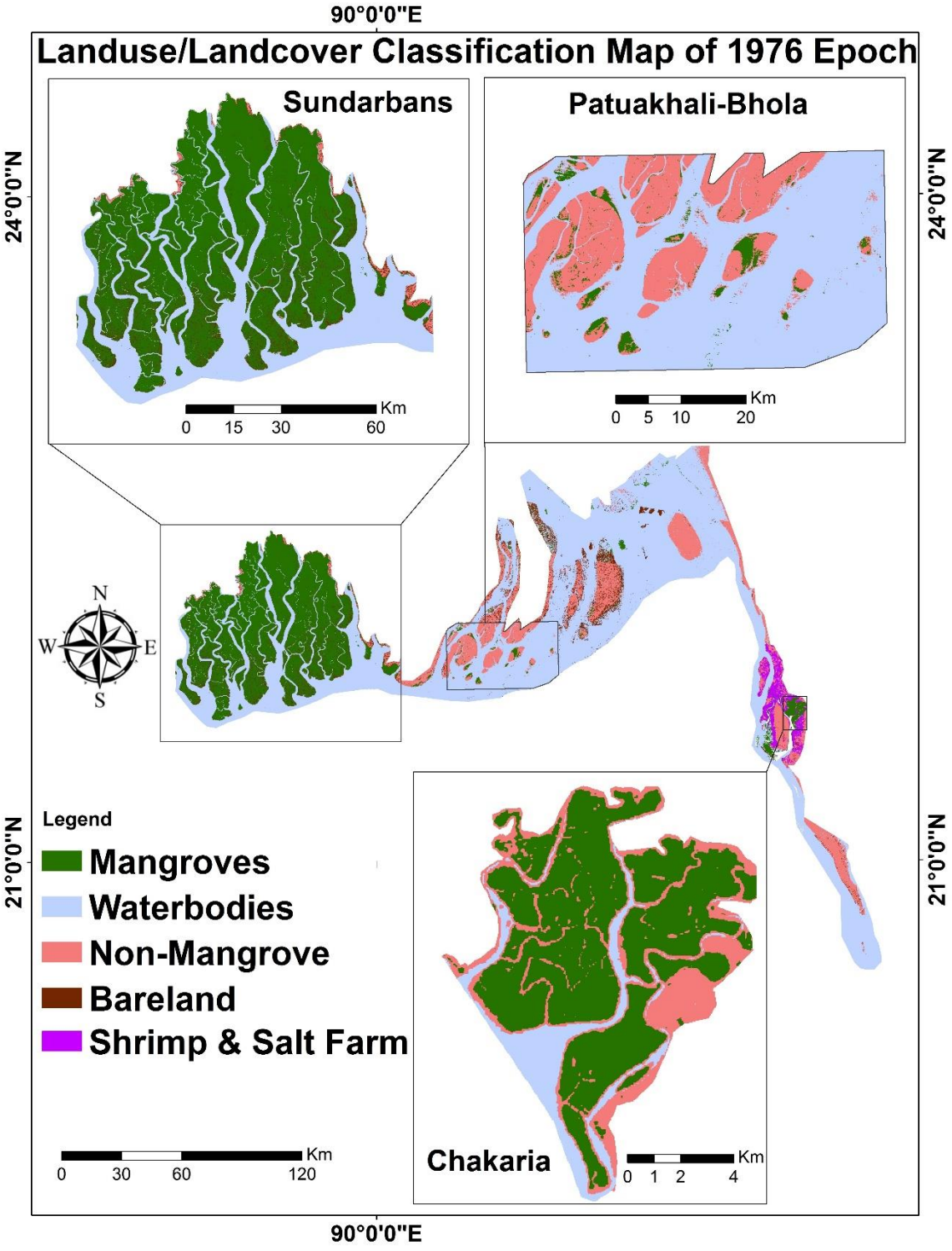

Figure.15: Supervised Landuse/Landcover Classification map of the study area obtained from Landsat MSS images: Sundarbans mangrove dominant region, a little mangrove seen in Patuakhali-Bhola, and a major proportion of mangrove seen in Chakaria in 1976.

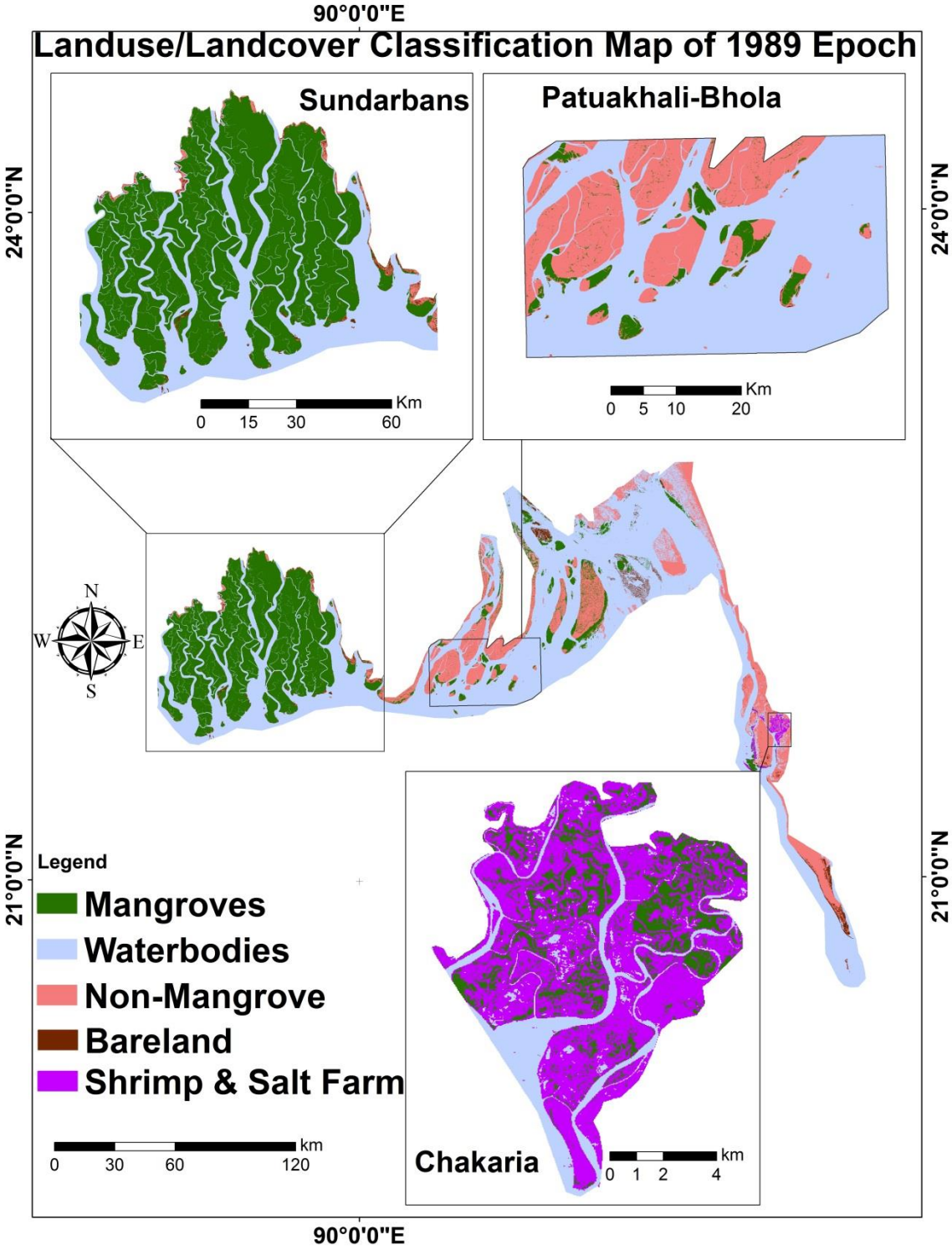

Figure.16: Supervised Landuse/Landcover Classification map of the study area obtained from Landsat TM images: Sundarbans mangrove dominant region, a remarkable amount of mangroves seen in Patuakhali-Bhola, and a major proportion of shrimp & salt farm and a small proportion of mangroves (mainly found in the northwest) seen in Chakaria in 1989.

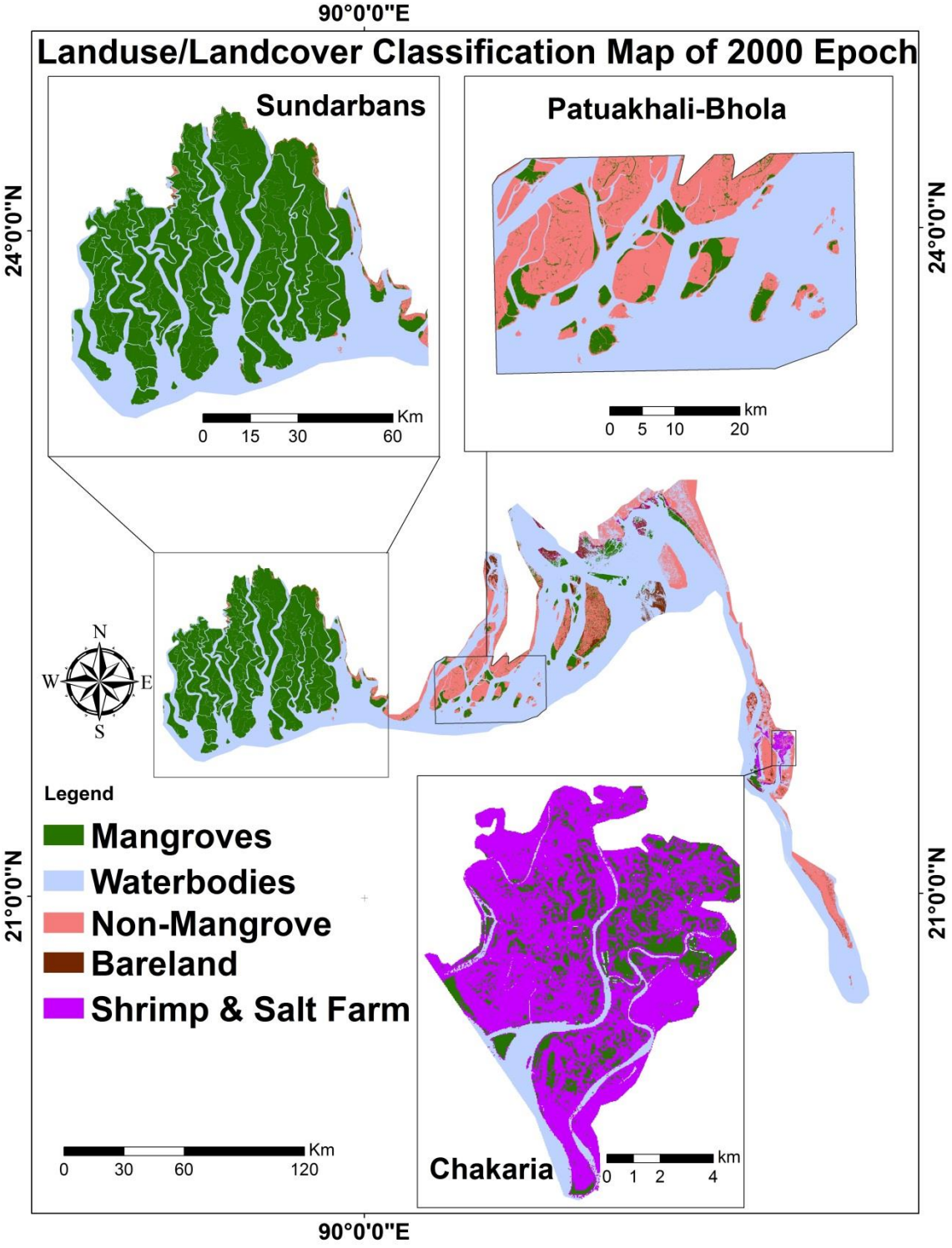

Figure.17: Supervised Landuse/Landcover Classification map of the study area obtained from Landsat TM images: Sundarbans mangrove dominant region, a remarkable amount of mangroves seen in Patuakhali-Bhola, and c) a major proportion of shrimp & salt farm and little proportion of mangroves (mainly found in the north-west, and the coast) seen in Chakaria in 2000.

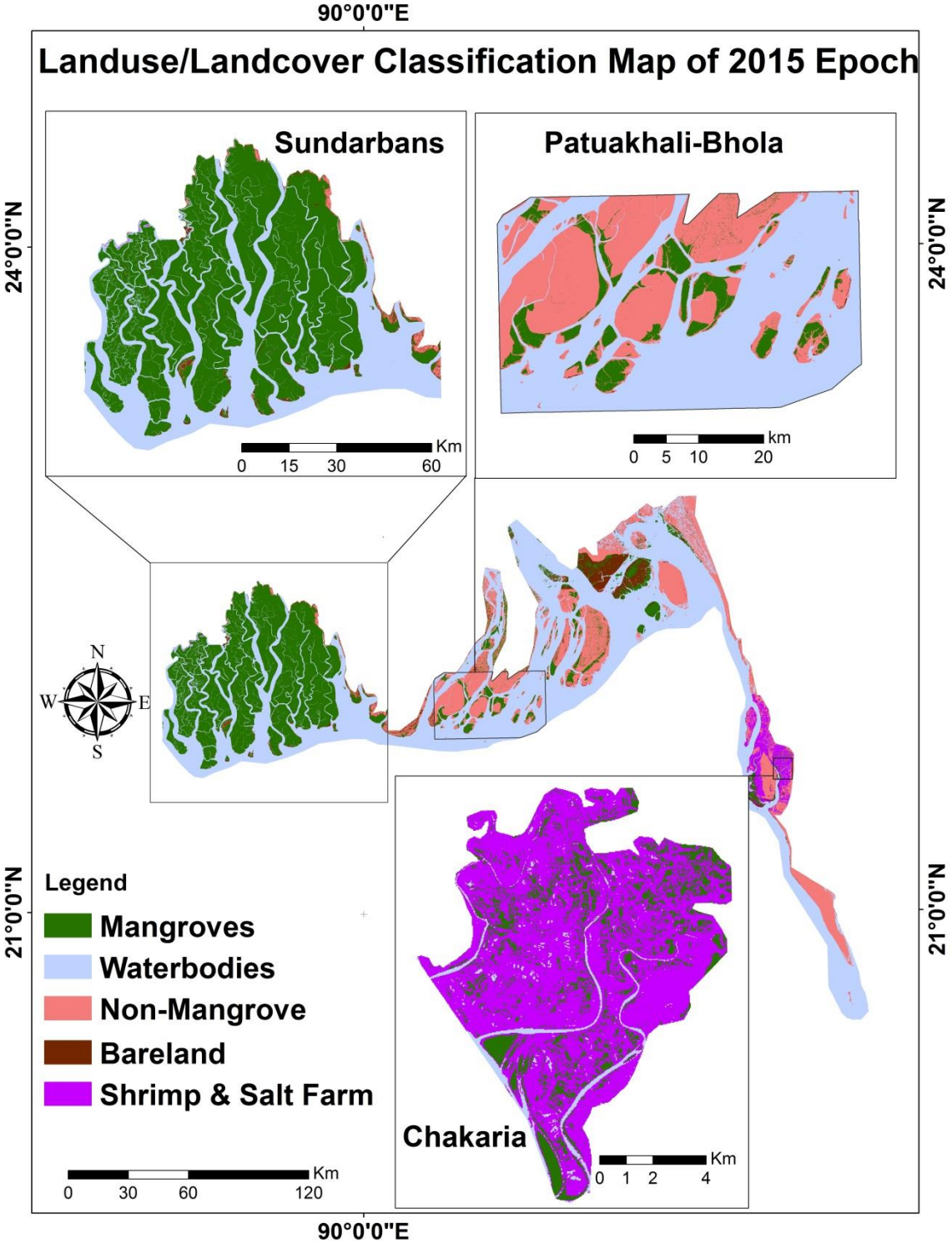

Figure.18: Supervised Landuse/Landcover Classification map of the study area obtained from Landsat TM images: Sundarbans mangrove dominant region, a remarkable amount of mangroves seen in Patuakhali-Bhola, and a major proportion of shrimp & salt farm and a tiny proportion of mangroves (mainly found on the coast) seen in Chakaria in 2015.

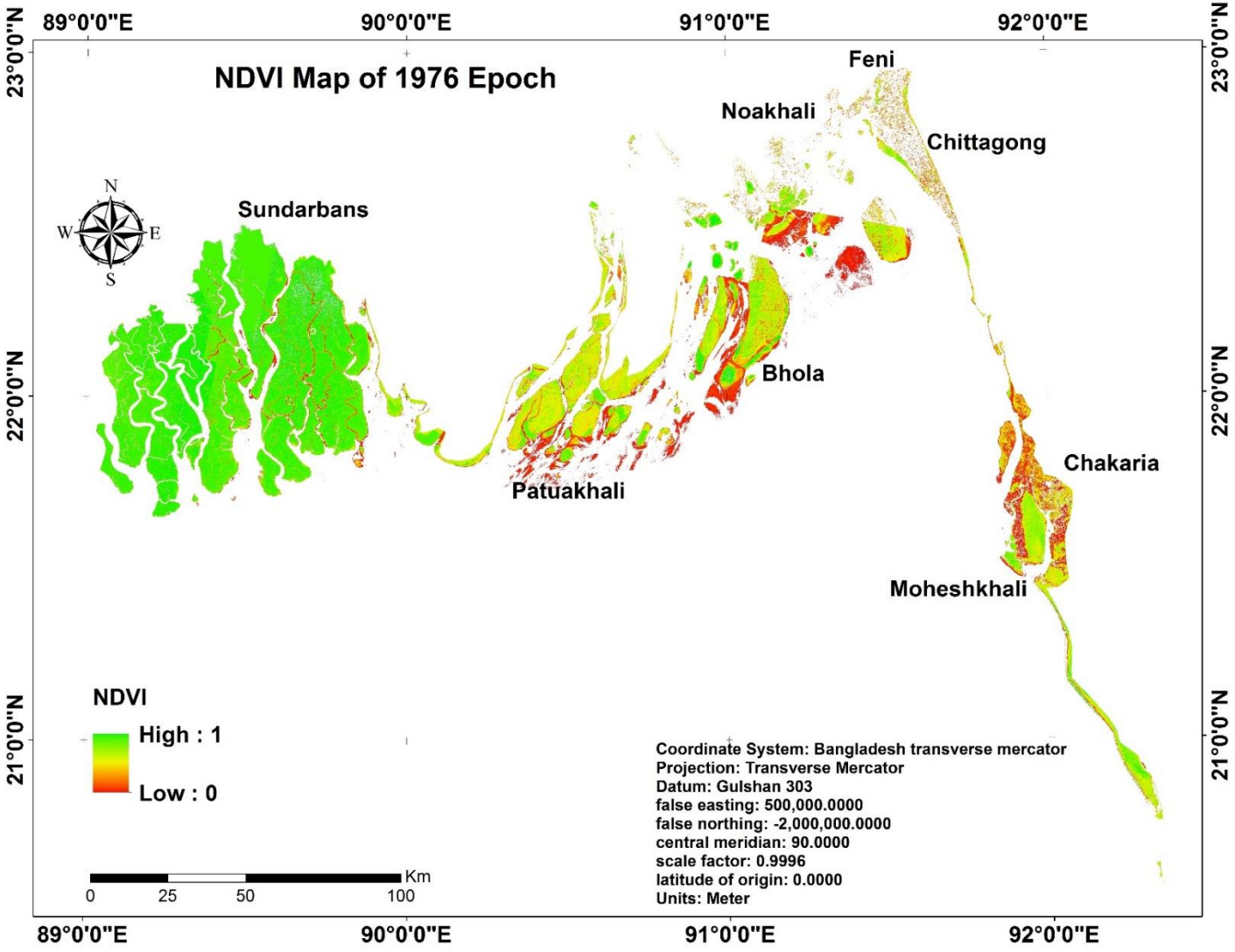

Figure.19: *NDVI map in 1976 shows high vegetation (mangrove) density in Sundarbans, medium density in Chakaria*

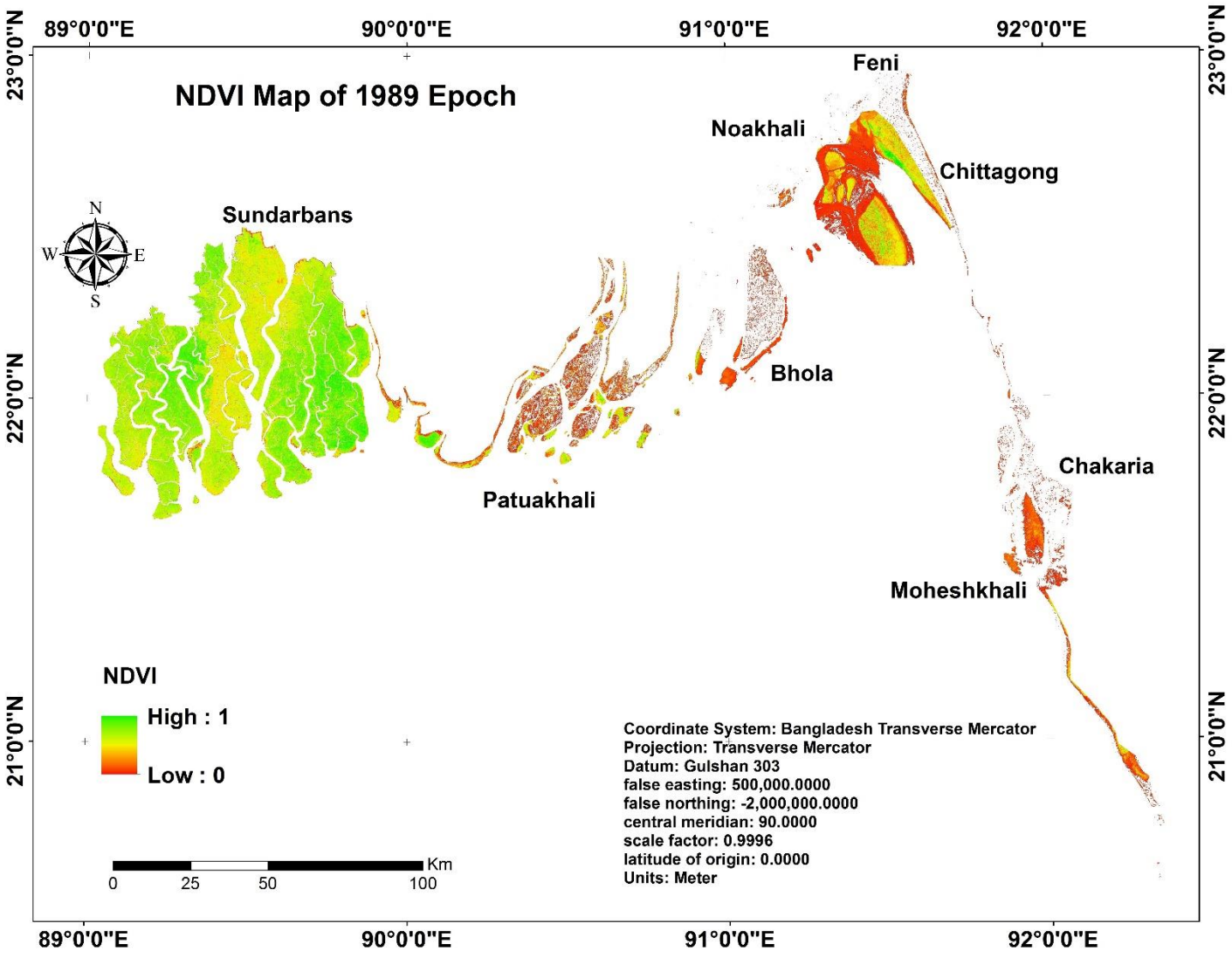

Figure.20: *NDVI map in 1989 shows decrease of vegetation (mangrove) density in central Sundarbans, low density in Chakaria*

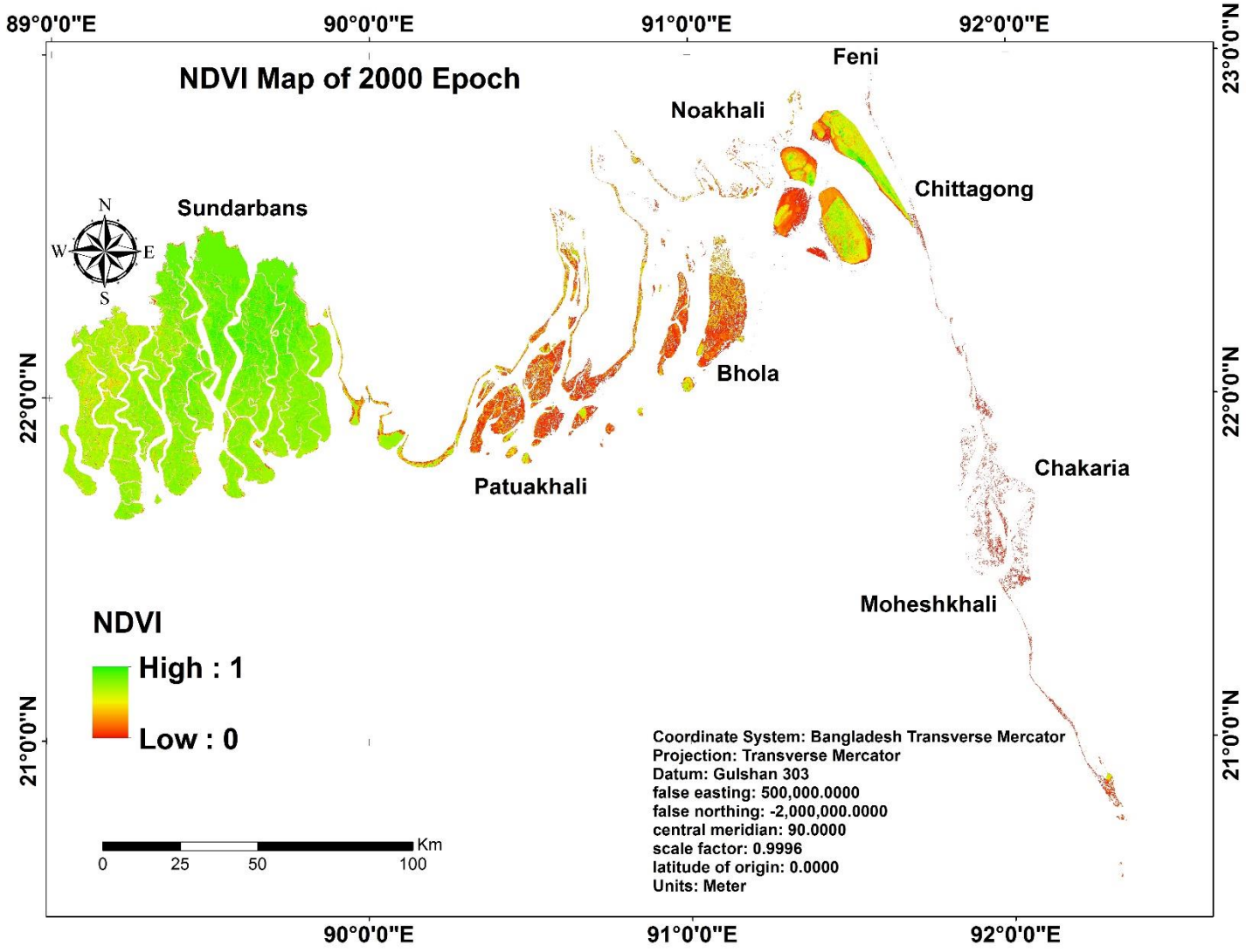

Figure.21: *NDVI map in 2000 shows moderate vegetation (mangrove) density in Sundarbans, low density in Chakaria*

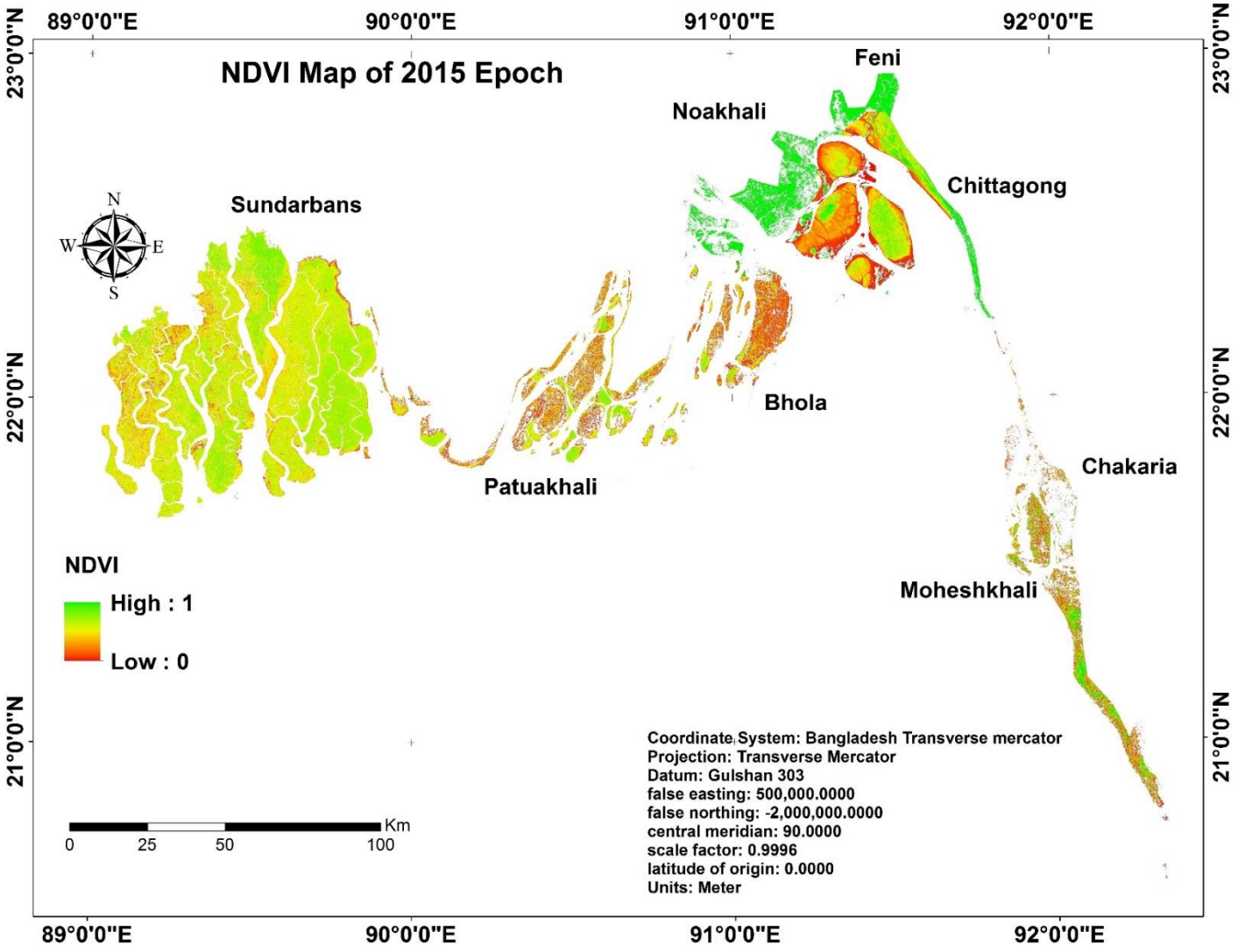

Figure.22: *NDVImap in 2015 shows decrease of vegetation (mangrove) density in Sundarbans, high density in Feni-Chittagong*

4.3. Variations of the extent of the mangrove forests

4.3.1 *Variations in land use/ land cover (classification)*

Figure.15-18 shows five land use class in the study area between 1976 and 2015. Table.9 reveals that over the last forty years (from 1976 to 2015), Bangladesh gained 58140 hectares of mangrove forests. If we assume equal yearly increase, this would mean an increase of 2240 ha per year between 2000 and 2015. Regarding proportions, mangroves have been found statistically significant increased 1.36%, decreased 0.05%, and increased 1.79% between 1976 and 1989, 1989 and 2000, and from 2000 to 2015, respectively (Table.9). Shrimp & salt farms, however, decreased by 14675 ha from 1976 to 1989, while increased by 60220 ha from 1989 to 2000, following a decline of 27987 ha from 2000 to 2015. Areas of waterbody displayed a remarkable decrease by 85985 ha from 1976 to 1989, while a slight increase between 1989 and 2000 was noticed, following a decline of 68729 ha from 2000 to 2015 (Table.10).

Table.9: *The extent of land use/land cover in the study area classified using the 'Maximum likelihood' algorithm on the satellite images (1976, 1989, 2000 and 2015), in hectares (ha) and as a percentage of all land use/land cover classes.*

Land use/land cover class-satellite image	1976		1989		2000		2015	
	(ha)	(%)	(ha)	(%)	(ha)	(%)	(ha)	(%)
Mangroves	**436617**	23.24	462182	24.60	**461170**	24.55	**494757**	26.34
Water bodies	1125358	59.90	1039373	55.32	1054153	56.11	985424	52.46
Non-Mangrove	249837	13.30	267678	14.25	263213	14.01	290542	15.47
Bare land	41201	2.20	98455	5.25	28932	1.55	64732	3.44
Shrimp & salt farm	25488	1.36	10813	0.58	71033	3.78	43046	2.29
Total Area	1878501	100	1878501	100	1878501	100	1878501	100

Mangrove Changes in Sundarbans

The Mangrove forests in Sundarbans has remained almost unchanged over the time (Table.10, Figure.15-18).There has been approximately 15000 ha mangrove increase between 1976 and 1989. While between 1989 and 2000, no more changes occurred in Sundarbans. However, mangrove forests were decreased from 415910 ha to 408912 ha between 2000 and 2015. The Non-mangrove changes were followed the same trend as mangrove changes. Shrimp & salt farm covered 398 ha in 2015, but no shrimp & salt farm was found in other three images (1976, 1989, and 2000).

Table.10: *Maximum likelihood Land use/ Land cover (LULC) classification results (in hectares (ha) and as a percentage of all land use classes)in Sundarban mangrove forest between 1976 and 2015.*

LULC	1976		1989		2000		2015	
	(ha)	(%)	(ha)	(%)	(ha)	(%)	(ha)	(%)
Mangroves	**400212**	59.22	415830	61.54	**415910**	61.55	**408912**	60.52
Waterbodies	229200	33.92	239975	35.52	247045	36.56	248895	36.84
Non-Mangrove	8776	1.30	10493	1.55	10178	1.51	9589	1.41
Barren land	37587	5.56	9377	1.39	2542	0.38	7881	1.17
Shrimp & salt farm	0	0	0	0	0	0	398	0.06
Total	675775	100	675675	100	675675	100	675675	100

Mangrove Changes in Patuakhail-Bhola Coastal region

According to the classification analysis, the Mangrove forests have increased by 6042 ha to 16419 ha from 1976 to 2015. Non-mangrove (agriculture, grassland, etc.) vegetation increased during the same time (Table.11). There has been a gradual decrease of waterbodies from 123796 ha to 102468 ha from 1976 to 2015 (Table.11, Figure.15-18). This area is also a highly sedimented zone.

Table.11: *Maximum likelihood Landuse/ Landcover classification results in Patuakhail-Bhola Coastal region between 1976 and 2015 epoch*

LULC	1976(ha)	1989(ha)	2000(ha)	2015(ha)
Mangroves	6082	9365	12652	16419
Non-Mangrove	47904	50090	51942	58752
Bareland	21	83	0	164
Waterbodies	123796	118265	113209	102468
Total	177803	177803	177803	177803

Mangrove Forests Changes in Chakaria Sundarbans

Supervised classification (Table.12) shows that this area was covered by mangrove forests of 60% (6097 ha) in 1976. In 1989, there has been a rapid decrease of the mangroves to only 20% (1962 ha). The mangrove forests were replaced by shrimp & salt farms between 1976 and 1989. Non-Mangrove (e.g. agriculture) land also transformed to shrimp and salt farms during this period.

Table.12: *Maximum likelihood Land use/ Land cover classification results in part of Chakaria Sundarbans between 1976 and 2015. Here, non-mangrove forest includes agricultural areas, forest, and grassland.*

LULC	1976 (ha)	1989 (ha)	2000 (ha)	2015 (ha)
Mangroves	6097	1962	1959	1761
Shrimp & Salt farm	0	5925	6623	7276
Water bodies	1764	1674	979	524
Non-Mangrove	1700	0	0	0
Total	9561	9561	9561	9561

The mangroves cover between 1989 and 2000 (Figure.15-18) has remained mainly the same except for a little increase in the coast of a southern part in Chawkaria Sundarbans. A small change was observed in south and southwest and a middle part between 2000 and 2015 (Figure.17-18).

Change detection through subtraction

A change detection analysis was performed on two areas of interest: Kalir char in the Sundarbans and Feni-Chittagong coastal zone in the north-eastern part of the study area. These areas of interest were chosen to know how much mangrove change has occurred in the Sundarbans and outside the Sundarbans in the study area. In this study, to identify any change, the classified maps of 1976 was subtracted from 1989, 1989 from 2000, and 2000 from 2015.

Kalir Char Area's Mangrove Change

Kalir char area is one of the changing landforms in the study area (Figure.23). This area consists of 9797 Ha. About 43% of the mangrove area has remained unchanged between 1976 and 1989, 1989-2000 and 2000-2015 (Table.13). About 3% of water bodies has changed into mangrove forest in between 1976 and 1989. 11% of mangrove forests has transformed to bareland and waterbodies, respectively, during this period. Between 1989 to 2000, 6.9% bareland turned into mangroves while a distinguishable proportion (13%) of mangroves transformed into bareland between 2000 and 2015.

Table 13. *Mangrove Changes in hectares and percentages between 1976 and 1989, 1989-2000, and 2000-2015 in Kalir Char Area. Note: WB- Waterbodies, M-Mangroves, BL-Bareland, and WB to WB means no change of waterbodies.*

Mangrove Changes	1976-1989 (ha)	%(change)	1989-2000 (ha)	%(change)	2000-2015 (ha)	%(change)
WB to M	295	3	147.15	1.5	196.2	2
BL to M	0	0	676.17	6.9	0	0
M to BL	795.3	8	0	0	1320.15	13
M to WB	298.41	3	167.85	1.7	226.26	2.3
M (No Change)	4211.46	43	4243.17	43	4199.72	43
WB to WB	4196.84	43	3981.96	41	3684.92	38
BL to WB	0	0	580.71	5.9	0	0
WB to BL	0	0	0	0	169.76	1.7
Total	9797.01	100	9797.01	100	9797.01	100

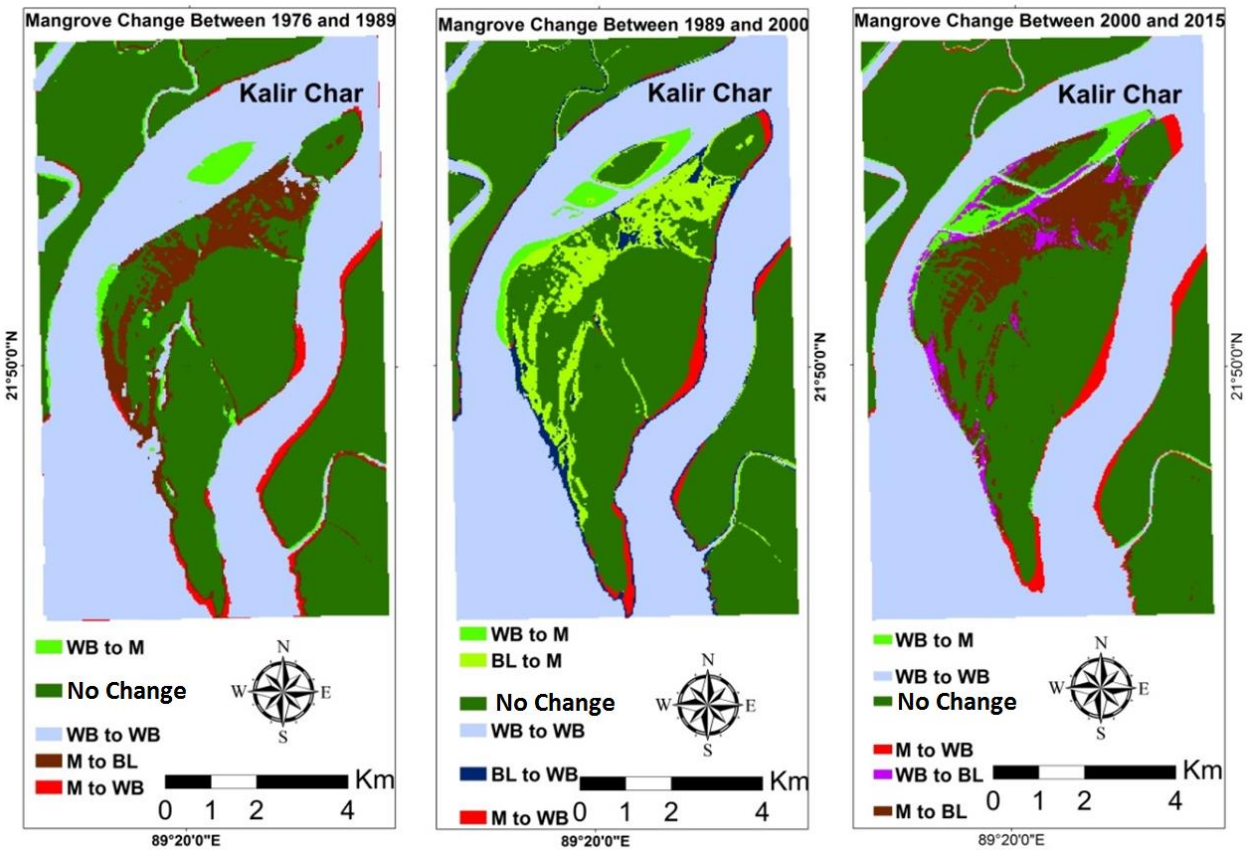

Figure 23. *Mangrove Changes in Kalir Char Area between 1976 and 1989, 1989-2000, and 2000-2015. Note: WB- Waterbodies, M-Mangroves, BL-Bareland*

Feni-Chittagong Mangrove Change: This area covers 12940 hectares located in the north-east of the study area. 'No Change' of mangrove areas were 5.5%, 30.30%, and 23.09% respectively between 1976 and 1989, 1989-2000, and 2000-2015 (Table.14). The highest proportion of water bodies was unchanged in these time periods. Between 1976 and 1989, 17% of the mangroves was gained from the water in this region while between 1989 and 2000 a little proportion (1.64%) was gained by mangroves from water bodies (Figure.24). Again, between 2000 and 2015, mangroves was gained from water (Figure.25). However, Between 1989 and 2000, a remarkable proportion of mangroves (7.70%) was lost to waterbodies.

Mangrove forests were limited only in Chittagong coast in 1976 but gradually extended into feni coast in the north to 2015 (Figure.24-25).

Table 14. *Mangrove Changes in hectares and percentages between 1976 and 1989, 1989-2000, and 2000-2015. Note: WB- Waterbodies, M-Mangroves, BL-Bareland, and WB to WB means no change of waterbodies.*

Mangrove Change	1976 and 1989 (ha)	% change	1989 and 2000(ha)	% Change	2000 and 2015(ha)	% Change
No Change	712	5.5	3921	30.30	2988	23.09
WB to WB	8919	68.93	7179	55.48	7145	55.21
BL to BL	0	0	411	3.18	0	0
M to WB	329	2.55	997	7.70	482	3.72
WB to M	2179	16.83	213	1.64	2325	17.98
BL to WB	223	1.71	0	0	0	0
BL to M	578	4.48	0	0	0	0
WB to BL	0	0	219	1.70	0	0
Total	12940	100	12940	100	12940	100

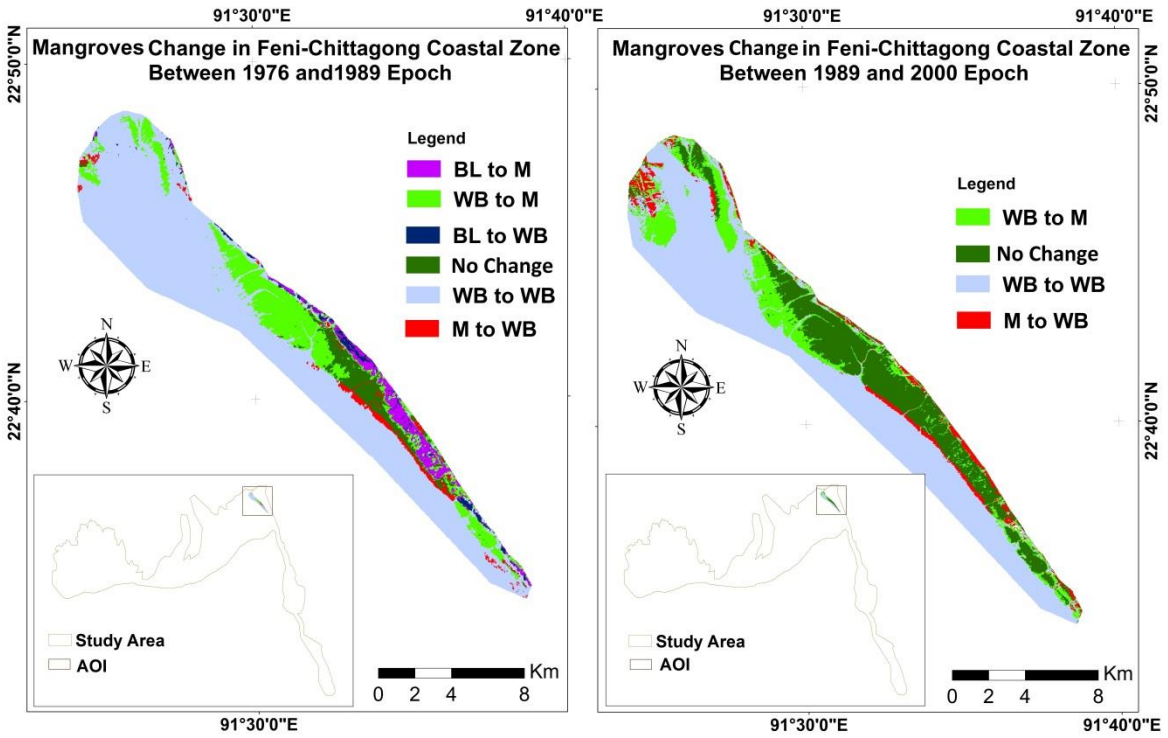

Figure 24. *Mangrove Changes in Feni-Chittagong between 1976 and 1989, 1989-2000. Note: WB- Waterbodies, M-Mangroves, BL-Bareland*

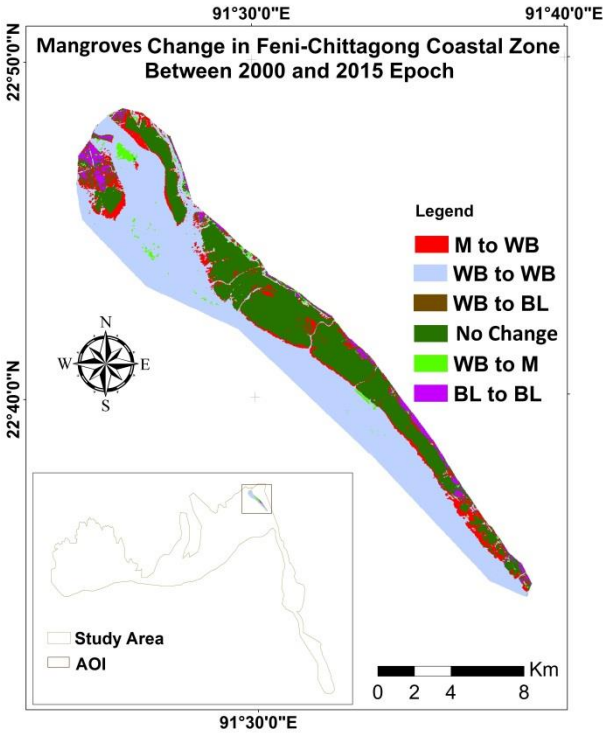

Figure 25. *Mangrove Changes in Feni-Chittagong between 2000 and 2015. Note that WB-Waterbodies, M-Mangroves, BL-Bareland.*

4.3.2. Variations in vegetation density (NDVI) for the Mangroves and Non-mangroves

The NDVI change detection analysis found that the NDVI values vary both temporally and spatially in the study area.

Variations in vegetation density (Mangroves) in Sundarbans

Mangrove forests have been presented here to trace vegetation density variation between different time intervals. The NDVI change detection map reveals that vegetation density increased in the northeastern part of the Sundarban between 1976 and 1989 epoch (Figure.26). However, density has been decreased 79% (344821ha) in the corresponding period. Vegetation density decrease rate was found in a medium range from 0.2-0.4 (50%) and 0.4-0.6(30%).

Table.15: *NDVI Differencing Results between different epoch (in Sundarbans)*

Difference in NDVI	**Change in Area 1976-1989 (ha)**	**1976-1989 (%) change**	**Changing in Area 1989-2000 (ha)**	**1989-2000 (%) Change**	**Changing in Area 20010-2015 (ha)**	**2000-2015 (%) Change**
Increased 0.8-1	74.79	0	153.36	0	320.04	0
Increased 0.6-0.8	2527.11	0	2997.45	0	4531.86	3
Increased 0.4-0.6	4511.97	0	15953.4	5	548.9	0
Increased 0.2-0.4	7578.99	0	100277.37	25	2439.54	0
Increased 0-0.2	73005.66	17	185945.58	45	3675.42	0
Decreased 0.0-0.2	226324.17	55	108456.93	25	69620.85	15
Decreased 0.2-0.4	86080.14	20	10103.58	0	218763.09	50
Decreased 0.4-0.6	20077.92	5	3346.38	0	123393.78	30
Decreased 0.6-0.8	11930.22	4	1415.07	0	8937.18	2
Decreased 0.8-1	408.6	0	92.97	0	4844.79	0
Total	444449.79	100	428742.09	100	437075.45	100

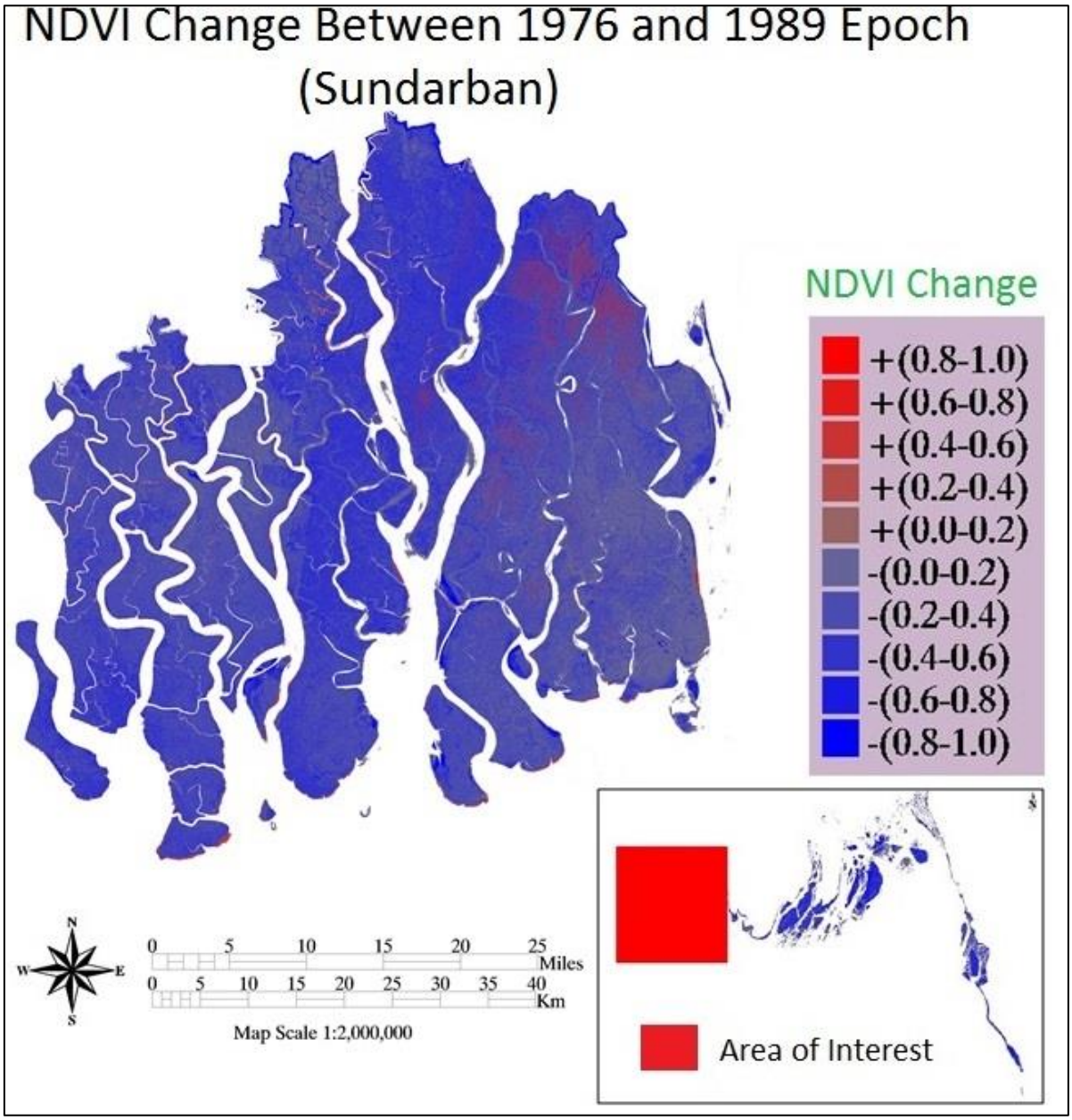

Figure.26: *NDVI Difference Map between 1976 and 1989 epoch*

On the other hand, between 1989 and 2000 epoch, The NDVI change detection map (Figure.27) reveals that mangrove density increased in the north central and central parts of the Sundarbans while the density decreased in the western and southeastern parts. Table.13shows, 70% (305327 ha of the area) NDVI increased while 28% NDVI dropped in this period. However, the NDVI increase rate mainly was found in a medium range from 0.0-0.4 (45%) and 0.2-0.4(25%).

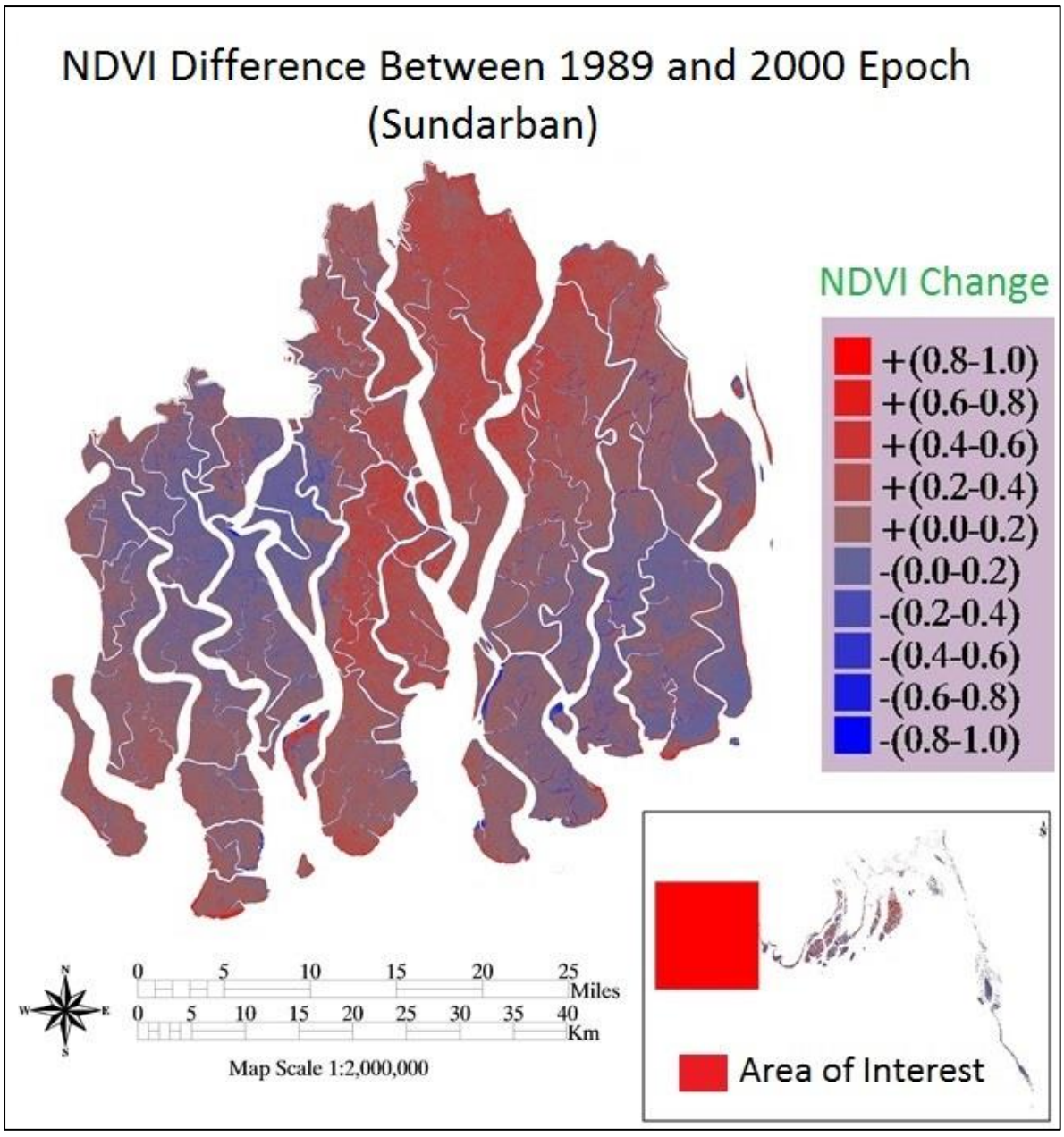

Figure.27: *NDVI Difference Map between 1989 and 2000 epoch*

Between 2000 and 2015 epoch, The NDVI change detection map (Figure.28) reveals that mangrove density displayed a massive decrease all over the Sundarbans, especially in the coast while NDVI density increased. Table.15 shows that 97% area of the Sundarbans lost mangrove density in this period. However, NDVI increased rate mainly found in the medium range from 0.0-0.4 (50%) and high 0.2-0.4(30%).

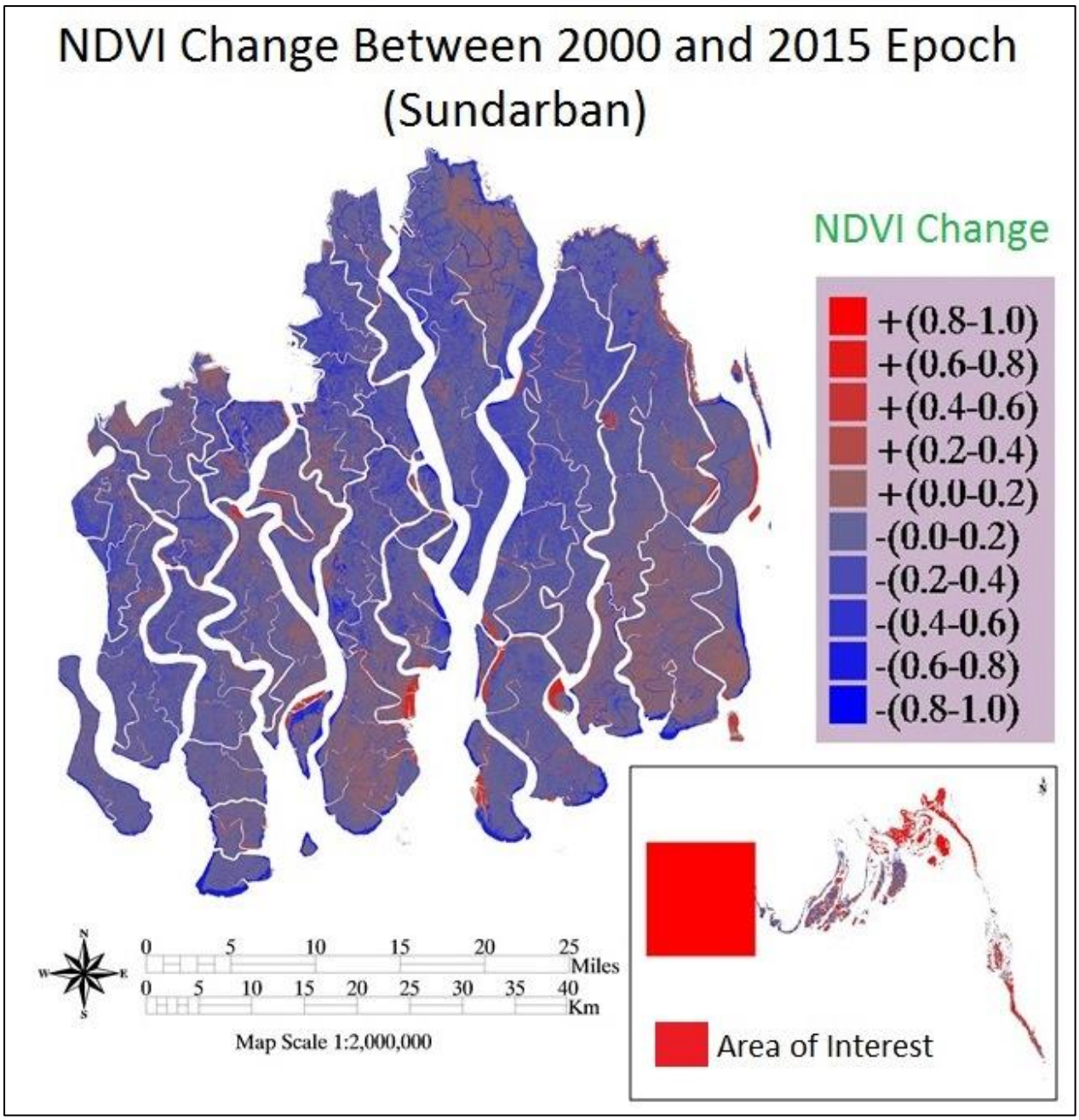

Figure.28: *NDVI Difference Map between 2000 and 2015 epoch*

Chapter Five-
Discussion

5.1 Sources of error and accuracy of the estimation

An accuracy assessment confirmed that it was possible to mangrove cover estimation within other classes in Bangladesh using satellite remote sensing techniques. The accuracy of the individual classes well taken how good maximum likelihood algorithm was to separate Mangroves and Non-mangrove vegetation and to differentiate mangroves from other LU/LC classes. Therefore, Landsat L8 OLI gave higher overall accuracy and kappa value than MSS, TM, and ETM+ images using this algorithm.

On the other hand, classification of satellite images for mangroves mapping is not free from uncertainty. For example, the absence of appropriate ground reference data, problems in class definitions, mixed pixel problems, tidal influence can lead to uncertainty in supervised classification (Rocchini *et. al.,* 2012; Saito *et. al.* 2003; Otero *et. al.,* 2016). Due to time limitation and funding, a field survey was not performed to collect training samples. Beside, High-resolution satellite images for large-scale time-series study would give higher accuracy but would also demand enormously more time and effort. In this study, Google Earth images were used to collect training samples (Kanniah *et al.,* 2015). Due to the unavailability of the reference data for the older images, using training data from present date imagery to interpret old-date images was the key solution to monitor ecosystem change dynamics (Paolini *et al.,* 2006). The study area boundary was carefully demarked and mainly limited to mangrove regions to reduce misclassification problem. Mangroves are compacted ecosystems. After visual analysis of classification, satellite image, and using Google Earth, a little mangrove misclassification was found in the Patuakhali-Bhola regions (Figure.29). Since there was some compacted non-mangrove vegetation, have spectrally behaved mangroves class *(Otero et. al., 2016).* In overall, mangroves areas were successfully quantified with Maximum likelihood classification, and with this method, Mangrove classification gave higher accuracy than other types of classes (Otero. *et. al.,* 2016; Rahman *et. al.,* 2013).

A small error has occurred for the shrimp & salt class (located outside upper part of the Sundarbans) classification in 1989, 2000 epochs. This error is due to the shrimp & salt field spectrally behaving similarly as a water body (generally shrimp and salt ground filled with water). This small error was verified in accuracy assessment report (Table. 6-7). However,

floating sediment in the open sea (deposited from upstream) is sensitive to NDVI. Floating sediment seems same like non-mangrove vegetation (such as agriculture land). NDVI error does not affect the mangrove estimation in this study. Because sedimentation effect has been reduced by normalization and a small error has been occurred in non-mangrove estimation (see Figure.S2 in Appendix). In this study, additionally, previous mangrove inventory reports were used to know causes behind mangrove extent and density variation in the study area.

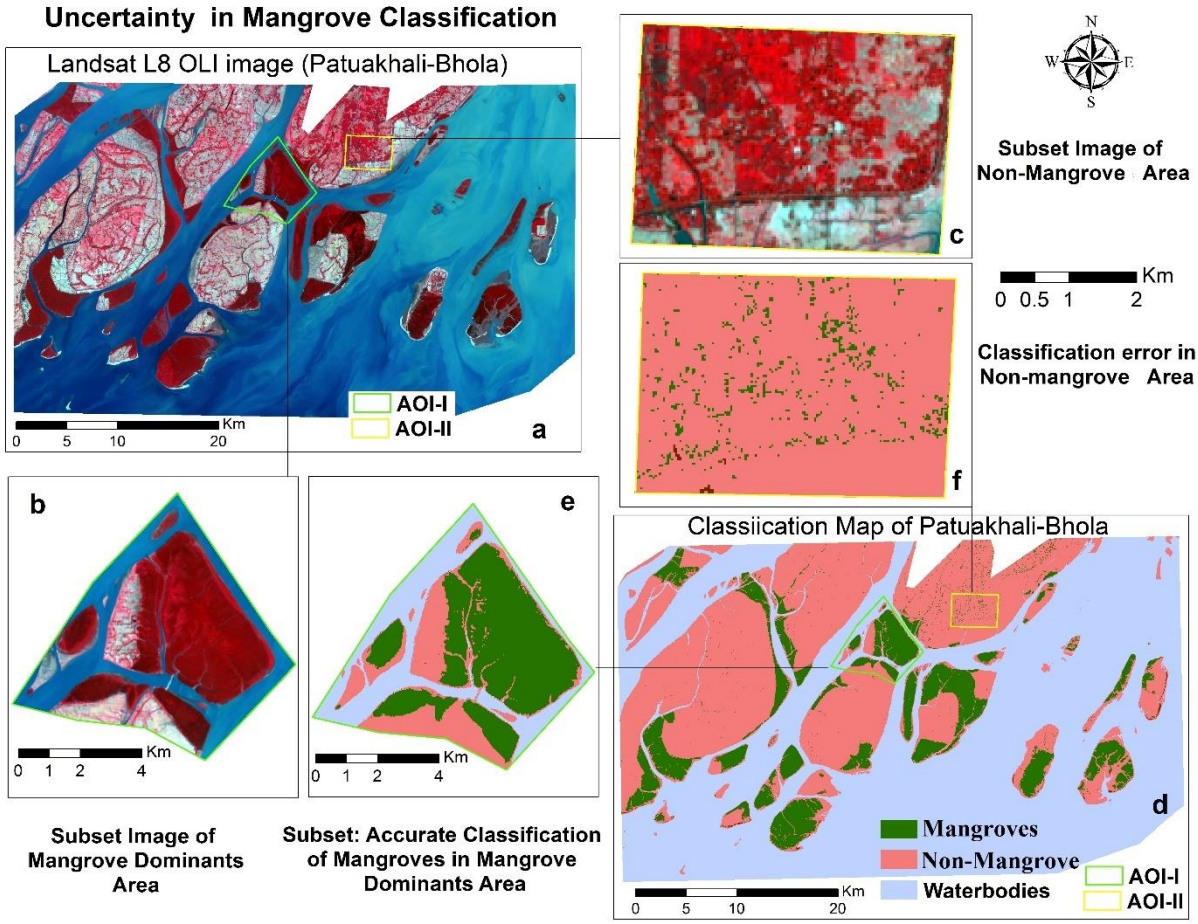

Figure.29: *Uncertainty in Mangrove cover classification. a) Landsat L8 OLI images composed of the Near-infrared, red, and green band with represents Area of Interest (AOI) in Patualhali-Bhola; b) subset image of L8OLI images represents Non-Mangrove vegetation area; c) subset of L8OLI images represents Mangroves dominants area; d) Classification map of Patuakhali -Bhola obtained from (a) with represents two AOI. Here, supervised classification accurately classified mangroves in mangroves dominant area (e) and mangrove classification error occurred in the non-mangrove area (f) where non-mangrove classified as mangroves (b).*

5.2 Estimation of mangrove extent and density variations/changes

The present study indicates positive changes of the mangrove extent in the study area during the last four epochs except negative changes found in Chakaria Sundarbans. Mangrove extension direction is found from landward to seaward in the study area. However, NDVI analysis suggests that density varies within the Sundarbans and outside the Sundarbans in the study area. Furthermore, it was possible to mangrove extent and density estimation in the study area using a large volume of satellite data.

Mangrove estimation in the Study Area:

Mangroves in Bangladesh are located in the coastal belt of the country (Figure.4). Former estimates of the mangrove cover in the study area differ among studies (Table 16). This variation is due to using different data source, methods, mangroves definitions, and boundary selection (Giri *et. al.,* 2007). This multi-temporal Landsat satellite data analysis revealed Bangladesh gained 3.10% mangroves area between 1976 epoch and 2015 epoch. While 1.79% mangroves were increased between 2000 and 2015 epoch. The area estimates found in the present study are smaller in 2000 than the reported values for the whole country by reliable estimation of FAO 2005. But values of current study estimation are almost nearer to FAO estimation. Based on literature, recent estimation of the mangrove forest in the country was not found. The most reliable estimate for the mangrove area obtained in this study was 494,757 ha which was calculated with the Maximum Likelihood algorithm for the 2015 epoch. However, this value overestimates the area because of land use/land cover map obtained in 2015 epoch shows mangroves at the of Patuakhali-Bhola where mangroves are not existing (Figure. 29).

Table.16: *Available Mangrove estimations in the Bangladesh.*

Study	**Mangroves Area**
National Level (whole country)	
FAO (2005)	476,000 ha in 2000
Present Study	461,170 ha in 2000; 494757 ha in 2015
Regional level (Sundarbans)	
Emch *et. al.* (2006)	347,853 ha in 2000
Giri *et. al.* (2007)	348,985 ha in 2000 (calculated from India-Bangladesh estimation)

FAO (2002)	411,233 ha in 2000
Present Study	415,910 ha in 2000; 408,912 ha in 2015
Local Level (Chakaria Sundarbans)	
Rahman *et. al.* (2011)	170 ha in 2012
Present Study	1761 ha in 2015

Mangrove Changes in Sundarbans

The study reveals that the mangrove forest area in Sundarbans remains almost unchanged and well-protected over the last forty years. These results are in agreement with other remote sensing studies such as Giri *et al.*, (2007); Emch *et al.*, (2006); Islam, M.T., (2014), FAO (2015); and Rahman *et al.*, (2013). Mangroves in the Sundarbans was increased 1.30% from 1976 epoch to 2015 epoch but decreased 1.03% between 2000 and 2015 epoch. Estimations of the extent of the mangrove forest in the Sundarbans is found to be higher in present studies than in the former. For example, In 2000, estimation of the current study is 20% more than from Giri *et. al.* 2007. Simplified image pre-processing steps and sample selection for classification could be the reason (like as Giri *et. al.* 2007 used only first order normalized image) for this variation. But present estimation is found closer to the FAO (2002) estimation in 2000 (Table 16).

The Sundarbans is the main mangrove forest region in Bangladesh. There, the Sundarbans lost about 467 ha of mangroves per year between 2000 and 2015 (Table.10). Here, Erosion and sedimentation play a vital role in mangrove changes in the Sundarbans. For example, Figure.23 shows how the mangrove forest moved to a depositional landform in the northern part of Kalir Char area from 1976 to 2015. This map also is shown, major mangrove was lost to bareland between 1976 and 1989, again mangrove gained between 1989 and 2000, finally fall into bareland again in between 2000 and 2015. The eastern part of the Kalir char has experienced by coastal erosion.

Although the edge of the Sundarbans has well protected by river channel, the North-western part of the Sundarbans has suffered deforestation between 1976 and 2015 (Figure.30). Mangroves were converted into a shrimp farm in this area.

Though, the NDVI study suggests that forest degradation occurred within the Sundarbans. For example, 95% of the area has decreased its density between 2000 and 2015, especially in the coast (Figure.28). The likely reason is that severe cyclone Sidr in 2007 (Figure.S1 in appendix-A) damaged Sundarbans mangrove forests in the study area. These results could be confirmed in Bhowmik *et al.*, (2013), Conforth *et al.*, (2013), Ishtiaque *et al.*, (2016).

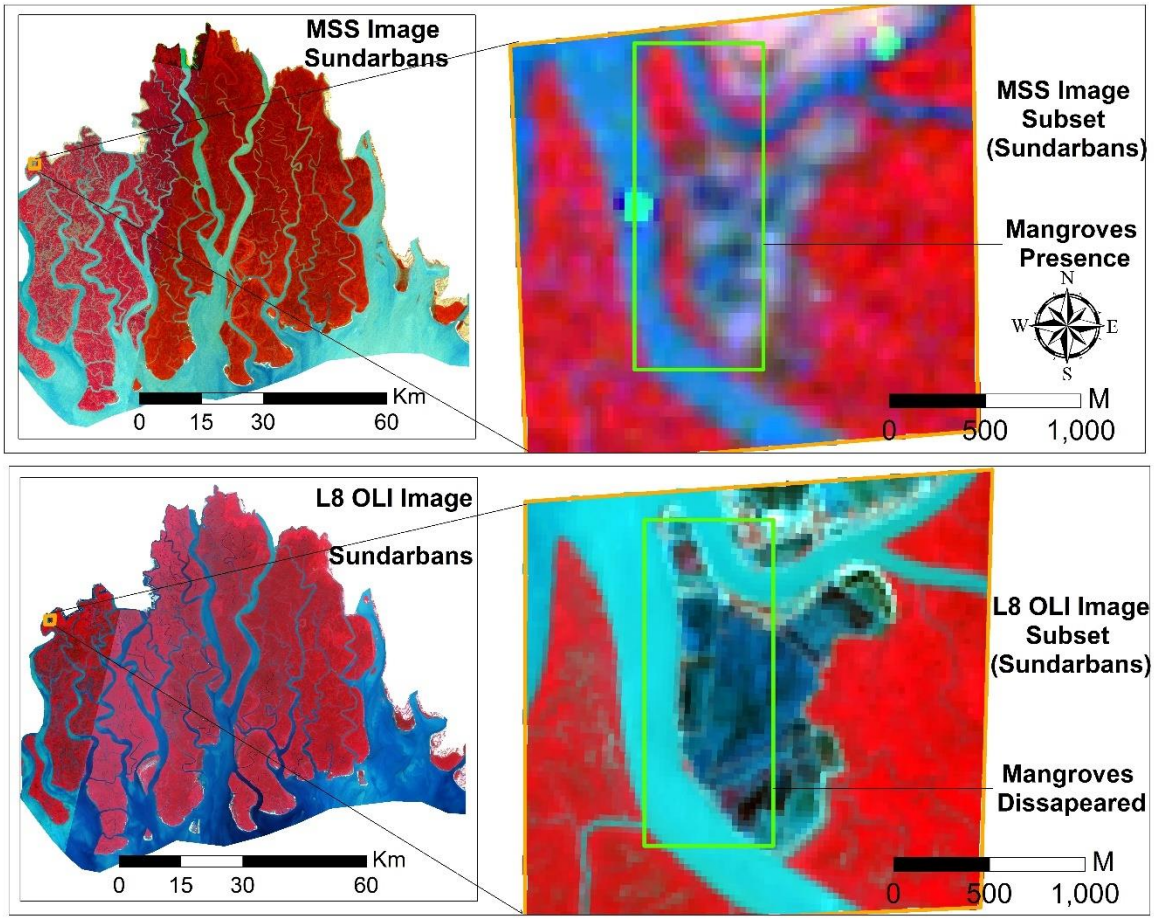

Figure.30: *Subset image of MSS shows mangroves presence (green rectangle) in North-west part of Sundarbans (yellow mark) in 1976, but a subset of L8 OLI images Mangroves has disappeared (green rectangle) in 2015. Mangroves were transformed into shrimp farm in this area after deforestation. Here, band combination is Near-infrared, red, and green.*

Mangrove Changes in Patuakhali-Bhola

There has been a continuous change of mangroves about 253 ha per year from 1976 to 1989, 298 ha from 1989 to 2000, and 251 ha from 2000 to 2015 (Table.11). Positive Mangrove forest changes were found in the part of Patuakhali-Bhola region after 1976. Due to sedimentation, waterbodies were firstly transformed to grassland (after a stable condition of newly-formed land), and then the mangroves migrated in those type of land from neighbors

land. Aggradation and degradation of landform are common in this area (Sarwar *et al.*, 2013). Mangrove plantation program also contributed to increase the mangroves area in this region. However, misclassification of mangroves was found here due to non-mangrove seemed as mangroves in the classification (Figure.29).

Mangrove Changes in Feni-Chittagong

The mangroves also increased in this coastal area from 1976 to 2015. The present study found that a rapid increase of mangrove forest was found in 1989 epoch than in 1976 epoch in Noakhali-Feni-Chittagong coastal region (For example Figure.24). Landsat images between 1976 and 1989 showed the sedimentation has increased in this area after construction of the dam (Figure.31). The Feni-river closure dam was built in 1985 (Stroeve 1993), after that huge amount of sediment deposited in the ocean about 4 km far from the closure dam. This study argued sedimentation is the main possible positive reason for mangrove extension in this area. Nevertheless, mangrove plantation program is also contributed to increase mangrove in this area (Uddin *et. al.* 2014).

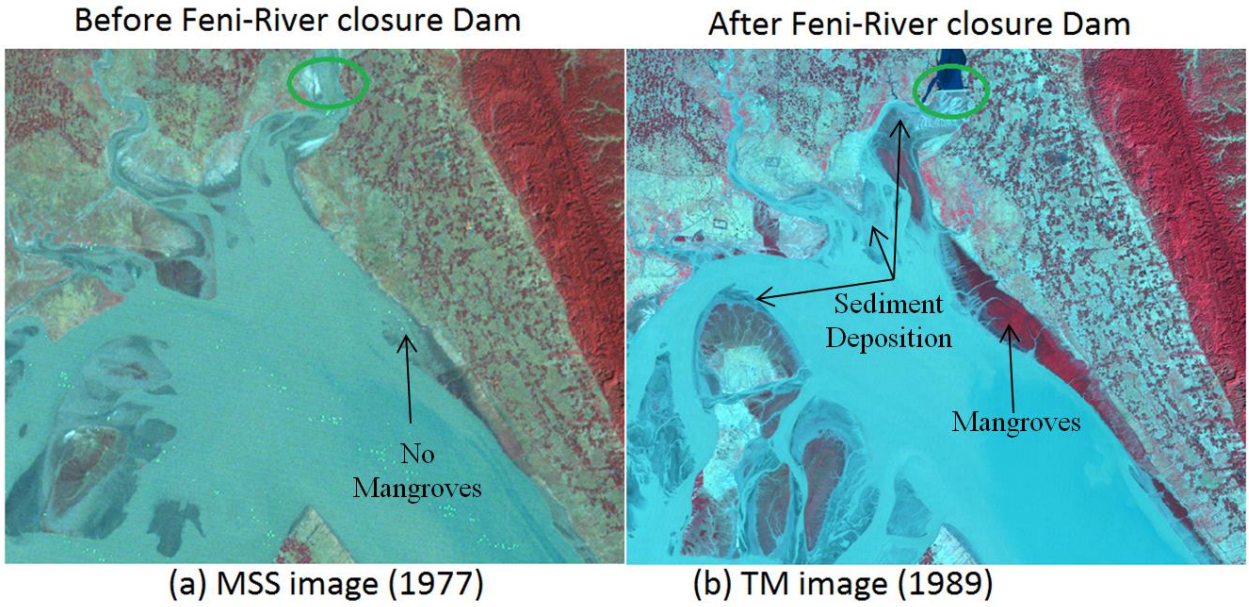

Figure. 31: *An example of deposition of sediment affected mangrove expansion after dam construction in Noakhali-Feni-Chittagong coastal zone between 1976 and 1989 epoch. Green circle represents approximate dam location. Note: Here, images from 1976-1977 considered as 1976 epoch (for details see Table.S1)*

Mangrove Changes in Chakaria Sundarbans

There was a gradual decrease of mangroves in Chakaria Sundarbans while the substantial increase of shrimp and salt farms occurred between 1976 and 2015 (Fig.15-18). The study found that expansion of shrimp & salt farm is the main reason for mangrove degradation in Chakaria Sundarbans. For example, Mangrove has been decreased from 60% to 20% while shrimp & salt farm has been increased from 0% to 100% between 1976 and 1989 (Table.12, Figure.15-18). This same reason is also confirmed by Hossain *et al.,* (2001) and Rahman *et al.,* (2015). World Bank and UNDP have had promoted to the government by financing to commercial shrimp farms in Chakaria Sundarbans (Ishtiaque *et al.* 2016). As an ultimate result, due to shrimp & salt farms (Figure.16-17), the oldest mangrove forest in Bangladesh became almost disappeared (Hussain *et al.,* 2001). However, a recent increase (see Figure.21-22) of the mangrove forests was recorded between 2000 and 2015 in the coast of chakaria, due to the mangrove plantation program (Alam *et al.,* 2014).

5.3 Comparison between the classification and NDVI analysis

The results of LU/LC classification analysis show that the area of mangrove forests in the Sundarbans remained almost constant between 1976 and 2015. However, mangrove degradation was clearly observed in the inside all over the Sundarbans from the NDVI maps. In the LU/LC classification, mangrove degradation is seen in areas such as Kalir char. These two classifications identified severely degraded forest areas such as Kalir Char. Thus, NDVI analysis could be used to monitor mangrove density (increasing or decreasing) in the study area while LU/LC classification could be used to know the extension of the mangroves. NDVI analysis suggests that dense mangroves have been observed between 1976 and 1989, a medium density between 1989 and 2000, very low density observed between 2000 and 2015. However, LU/LC classification analysis shows, Mangrove areas has been increased slightly from 1976 to 1989 and decreased slightly in 2015.

Outside the Sundarbans, where non-mangrove vegetation (grassland, agriculture, forest) is present beside the mangroves, LULC classification has easily identified the tiny areas of mangrove forest separately, while the NDVI analysis only shows the occurrence of vegetation mixed with non-mangroves NDVI values such as Feni-Chittagong coast (see Figure.15-18 and Figure.19-22). Hence, the classification is optimal for identifying the mangrove extension while an NDVI analysis is optimal for investigating the density of the forest. The LU/LC Classification gave the best results to trace the mangrove extension in the

whole study area (Figure.15-18). While NDVI analysis produced information of density variation of the mangrove forest in the study area (Figure.19-22).

Regarding the classifications, the 'true' change for each pixel was determined by visual inspection of the Landsat time series with high-resolution Google Earth imagery (due to the absence of field data). This method has also followed by Song *et al.* 2015. Mangrove changes have mainly found from water to mangrove and from mangrove to water (see Figure.23 and Figure.24). Changes found in the classification are reasonable for example changes of water to mangroves between 1976 and 1989 (Figure.24) has shown in Landsat scenes (Figure.31). However, Regarding NDVI (density), the largest density changes are found when compared with small differences in NDVI such as NDVI difference in Sundarbans between 1989 and 2000 epoch (Figure.27).

In spite of some pros and cons, the study suggests that both methods could be used to trace mangrove forest change dynamics in the study area. LU/LC classification method could be used to identify mangrove, then NDVI could be used to know vegetation status of the study area.

Chapter Six-
Conclusions

Monitoring mangrove forest dynamics using multi-temporal Landsat scenes in large scale areas needs large volumes of data and requires reliable measures of forest extent and density changes/variations. While previous studies have successfully mapped mangrove extent and density in the Sundarbans, these studies have used rather simplified pre-processing steps and not performed in regional scales like inside and outside the Sundarbans. The present study has focused this issue. The satellite images were processed using both absolute and relative radiometric correction method. The maximum-likelihood algorithm used in the study gave higher accuracy to detect mangroves forests than other land use/land cover classes. Results indicate that Bangladesh gained about 3.10% mangrove forest from 1976 to 2015, even if variations occurred within the area. About 1.79% mangroves area was increased between 2000 and 2015 due to deposition of sediment and mangrove plantation program. In the Sundarbans, for instance, the area seemed to have increased 1.30% from 1976 to 2015 but lost 1.03% between 2000 and 2015. This increase and the decrease were associated with cyclone, deforestation, erosion and deposition of landform. Outside the Sundarbans, there has a gradual increase of mangrove forests in Patuakhali-Bhola, Feni-Chittagong coastal region between 1976 and 2015 due to deposition of sediment and mangrove plantation. Chakaria Sundarbans, however, is the exception; about 30% mangrove forest has been exchanged into shrimp and salt farm during this time. On the other hand, NDVI analysis shows that the density varies back and forth during the study period, from a general decreased from 1976 to 1989, a recover from 1989 to 2000, and then a decrease again from 2000 to 2015. NDVI variation was found as a result of the coastal erosion and tropical cyclone.

Robust estimation of the mangroves was not possible in the study area. There is a variation of estimation due to the error in the classification of mangroves and non-mangrove, absence of a field and previous mangrove data source. In this study, High-resolution Google Earth images, previous published reports and articles as well as local knowledge of the author about the mangrove vegetation was helped to quantify true mangroves and to reduce the classification error in the study. However, Use of field data, high-resolution satellite data like as worldview or hyperspectral data could be useful to improvements in classification accuracy between mangroves and non-mangrove vegetation. In conclusion, the results of this research may assist in decision making to conservation and management planning of mangrove forests in Bangladesh.

References:

Akhter, M., 2006. Remote sensing for developing an operational monitoring scheme for the Sundarban Reserved Forest, Bangladesh (Doctoral dissertation, Department of World Forestry, University of Hamburg).

Alam, S., Hossain, M.L., Foysal, M.A. and Misbahuzzaman, K., 2014. Growth Performance of Mangrove Species in Chakaria Sundarban. *International Journal of Ecosystem*, *4*(5), pp.233-238.

Alphan, H., Doygun, H., and Unlukaplan, Y.I., 2009. Post-classification comparison of land cover using multitemporal Landsat and ASTER imagery: the case of Kahramanmaraş, Turkey. *Environmental monitoring and assessment*, *151*(1-4), pp.327-336

Alongi, D.M., 2002. Present state and future of the world's mangrove forests. *Environmental Conservation*, *29*(03), pp.331-349.

Aziz, A. and Paul, A.R., 2015. Bangladesh Sundarbans: Present Status of the Environment and Biota. *Diversity*, *7*(3), pp.242-269.

Awal, M.A., 2014. Analysis of Relationship between Salinity and Top-Dying Diseases of Sundri Trees in Sundarbans, Bangladesh. *Science Journal of Analytical Chemistry*, 2(4), p.29.

Baboo, S.S., and Devi, M.R., 2010. An analysis of different resampling methods in Coimbatore, District. *Global Journal of Computer Science and Technology*, *10*(15).

Banglapedia, 2014, National Encyclopedia of Bangladesh, available at http://en.banglapedia.org/index.php?title=Char

Banskota, A., Kayastha, N., Falkowski, M.J., Wulder, M.A., Froese, R.E. and White, J.C., 2014. Forest monitoring using Landsat time series data: A review. *Canadian Journal of Remote Sensing*, *40*(5), pp.362-384.

Baumann, P.R. 2010, Remote Sensing: Landsat Program, State University of New York, Oneonta, New York 13820, Accessed on July 15th, 2016, available at http://www.oneonta.edu/faculty/baumanpr/geosat2/RS%20Landsat/RS-Landsat.htm

Bhandari, S., Phinn, S. and Gill, T., 2012. Preparing Landsat Image Time Series (LITS) for monitoring changes in vegetation phenology in Queensland, Australia. *Remote Sensing*, *4*(6), pp.1856-1886.

Bhowmik, A.K., and Cabral, P., 2013. Cyclone Sidr Impacts on the Sundarbans Floristic Diversity. *Earth Science Research*, *2*(2), p.62.

Biswas, S.R., and Choudhury, J.K., 2007. Forests and forest management practices in Bangladesh: the question of sustainability. *International Forestry Review*, *9*(2), pp.627-640.

Bohonak, A.J., 2004. RMA: software for reduced major axis regression v. 1.17. *San Diego State University, San Diego, California., available at http://www.bio.sdsu.edu/pub/andy/RMAmanual.pdf*

Canty, M.J., Nielsen, A.A. and Schmidt, M., 2004. Automatic radiometric normalization of multitemporal satellite imagery. *Remote Sensing of Environment*, *91*(3), pp.441-451.

Campbell, J. B. 2002b. Image Classification. *Introduction to remote sensing.* 3rd ed. London: Taylor & Francis.

CEGIS, 2007, Effect of cyclone Sidr on the Sundarbans A Preliminary Assessment, *Center For Environmental and Geographic Information Services*, Dhaka, Bangladesh. Available at http://www.lcgbangladesh.org/derweb/cyclone/cyclone_assessment/effect%20of%20cyclone%20sidr%20on%20sundarbans_cegis.pdf

Chaffey, D.R., Miller, F.R., and Sandom, J.H., 1985. A forest inventory of the Sundarbans, Bangladesh (Main Report). *Land Resources Development Centre, England, KT6, 7DY.*

Chander, G., Markham, B.L. and Helder, D.L., 2009. Summary of current radiometric calibration coefficients for Landsat MSS, TM, ETM+, and EO-1 ALI sensors. *Remote sensing of Environment*, *113*(5), pp.893-903.

Chavez, P.S., 1996. Image-based atmospheric corrections-revisited and improved. *Photogrammetric engineering and remote sensing*, *62*(9), pp.1025-1035.

Chen, C.F., Son, N.T., Chang, N.B., Chen, C.R., Chang, L.Y., Valdez, M., Centeno, G., Thompson, C.A. and Aceituno, J.L., 2013. Multi-decadal mangrove forest change detection and prediction in Honduras, Central America, with Landsat imagery and a Markov chain model. *Remote Sensing*,*5*(12), pp.6408-6426.

Choudhury, J.K., and Hossain, M.A.A., 2011. Bangladesh forestry outlook study. *Asia-Pacific Forestry Sector Outlook Study II, FAO*.

Congalton, R.G., 1991. A review of assessing the accuracy of classifications of remotely sensed data. *Remote sensing of Environment*, *37*(1), pp.35-46.

Cornforth, W.A., Fatoyinbo, T.E., Freemantle, T.P. and Pettorelli, N., 2013. Advanced land observing satellite phased array type L-band SAR (ALOS PALSAR) to inform the conservation of mangroves: Sundarbans as a case study. *Remote Sensing*, *5*(1), pp.224-237.

Dittmar, T., Hertkorn, N., Kattner, G. and Lara, R.J., 2006. Mangroves, a major source of dissolved organic carbon to the oceans. *Global biogeochemical cycles*, *20*(1).

Diyan, M.A., 2011. *Multi-scale vegetation classification using earth observation data of the Sundarban mangrove forest, Bangladesh* (MSc. Dissertation in Geospatial technologies, Instituto Superior de Estatística e Gestão de Informação Universidade Nova de Lisboa Lisboa, Portugal).

Eckhardt, D.W., Verdin, J.P. and Lyford, G.R., 1990. Automated update of an irrigated lands GIS using SPOT HRV imagery. *Photogrammetric Engineering and Remote Sensing*, *56*(11), pp.1515-1522.

El-Hattab, M.M., 2016. Applying post classification change detection technique to monitor an Egyptian coastal zone (Abu Qir Bay). *The Egyptian Journal of Remote Sensing and Space Science*, *19*(1), pp.23-36

Emch, M. and Peterson, M., 2006. Mangrove forest cover change in the Bangladesh Sundarbans from 1989-2000: A remote sensing approach. *Geocarto International*, *21*(1), pp.5-12.

Erener, A. and Düzgün, H.S., 2009. A methodology for land use change detection of high-resolution pan images based on texture analysis. *Italian Journal of Remote Sensing*, *41*(2), pp.47-59.

ESA, 2015. Height of Bangladesh Mangrove, *European Space Agency*, Accessed on April 14th, 2016 available at http://www.esa.int/spaceinimages/Images/2015/01/Height_of_Bangladesh_mangrove

FAO, 2007. The world's mangroves 1980-2005. *FAO Forestry Paper*, 153, p.89.

FAO, 2005. Global Forest Resources Assessment 2005, Thematic study on Mangroves: Bangladesh Country Profile, Forest Department, FAO, Rome (Italy).

FAO, 2002. *FAO's database on mangrove area estimates*, (by M.L. Wilkie, S. Fortuna and & O. Souksavat). Forest Resources Assessment Working Paper No. 62. Rome.

Foster, J.R., 2013. Ecological segregation of the late jurassic stegosaurian and iguanodontian dinosaurs of the morrison formation in north america: pronounced or subtle?. *PalArch's Journal of Vertebrate Palaeontology*, *10*(3).

Forbes, K. and Broadhead, J., 2007. *The role of coastal forests in the mitigation of tsunami impacts*. FAO.

Gao, F., Masek, J. and Wolfe, R.E., 2009. Automated registration and orthorectification package for Landsat and Landsat-like data processing. *Journal of Applied Remote Sensing*, *3*(1), pp.033515-033515.

Giri, C., Long, J., Abbas, S., Murali, R.M., Qamer, F.M., Pengra, B. and Thau, D., 2015. Distribution and dynamics of mangrove forests of South Asia. *Journal of environmental management*, *148*, pp.101-111.

Giri, C., Zhu, Z., Tieszen, L.L., Singh, A., Gillette, S. and Kelmelis, J.A., 2008. Mangrove forest distributions and dynamics (1975–2005) of the tsunami-affected region of Asia. *Journal of Biogeography*, *35*(3), pp.519-528.

Giri, C. and Muhlhausen, J., 2008. Mangrove forest distributions and dynamics in Madagascar (1975–2005). *Sensors*, *8*(4), pp.2104-2117.

Giri, C., Pengra, B., Zhu, Z., Singh, A. and Tieszen, L.L., 2007. Monitoring mangrove forest dynamics of the Sundarbans in Bangladesh and India using multi-temporal satellite data from 1973 to 2000. *Estuarine, coastal and shelf science*, *73*(1), pp.91-100.

Giri, C., Ochieng, E., Tieszen, L.L., Zhu, Z., Singh, A., Loveland, T., Masek, J. and Duke, N., 2011. Status and distribution of mangrove forests of the world using earth observation satellite data. *Global Ecology and Biogeography*, *20*(1), pp.154-159.

Green, E., Mumby, P., Edwards, A. and Clark, C., 2000. *Remote Sensing: Handbook for Tropical Coastal Management*, United Nations Educational Scientific and Cultural Organization (UNESCO), Paris.

Harper, W.V., 2014. Reduced Major Axis Regression: Teaching Alternatives to Least Squares, available at http://digitalcommons.otterbein.edu/math_fac/24/

Helmer, E.H., and Ruefenacht, B., 2007. A comparison of radiometric normalization methods when filling cloud gaps in Landsat imagery. *Canadian Journal of Remote Sensing*, *33*(4), pp.325-340.

Hermosilla, T., Wulder, M.A., White, J.C., Coops, N.C. and Hobart, G.W., 2015. Regional detection, characterization, and attribution of annual forest change from 1984 to 2012 using Landsat-derived time-series metrics.*Remote Sensing of Environment*, *170*, pp.121-132.

Heumann, B.W., 2011. An object-based classification of mangroves using a hybrid decision tree—Support vector machine approach. *Remote Sensing*, *3*(11), pp.2440-2460.

Huang, C., Goward, S.N., Masek, J.G., Gao, F., Vermote, E.F., Thomas, N., Schleeweis, K., Kennedy, R.E., Zhu, Z., Eidenshink, J.C. and Townshend, J.R., 2009. Development of time series stacks of Landsat images for reconstructing forest disturbance history. *International Journal of Digital Earth*, *2*(3), pp.195-218.

Hasmadi, I.M., Pakhriazad, H.Z. and Norlida, K., 2011. Remote sensing for mapping RAMSAR heritage site at Sungai Pulai mangrove forest reserve, Johor, Malaysia. *Sains Malaysiana*, *40*(2), pp.83-88.

Harris geospatial solutions, 2016. Collect and edits tie points, Accessed on July 15th, 2016, available at http://www.harrisgeospatial.com/docs/CollectingEditingTiePoints.html

Iftekhar, M.S., and Islam, M.R., 2004. Degeneration of Bangladesh's Sundarbans mangroves: a management issue. *International Forestry Review*, *6*(2), pp.123-135.

Islam, M.S., 2001. *Sea-level changes in Bangladesh: the last ten thousand years*. Asiatic Society of Bangladesh.

Islam, M.T., 2014. Vegetation changes of Sundarbans based on Landsat Imagery analysis between 1975 and 2006. *Acta Geographica Debrecina. Landscape & Environment Series*, *8*(1), p.1.

Ishtiaque, A., Myint, S.W. and Wang, C., 2016. Examining the ecosystem health and sustainability of the world's largest mangrove forest using multi-temporal MODIS products. *Science of The Total Environment*, *569*, pp.1241-1254.

Jones, T.G., Glass, L., Gandhi, S., Ravaoarinorotsihoarana, L., Carro, A., Benson, L., Ratsimba, H.R., Giri, C., Randriamanatena, D. and Cripps, G., 2016. Madagascar's mangroves: quantifying nation-wide and ecosystem specific dynamics, and detailed contemporary mapping of distinct ecosystems. *Remote Sensing*, *8*(2), p.106.

Kanniah, K.D., Sheikhi, A., Cracknell, A.P., Goh, H.C., Tan, K.P., Ho, C.S. and Rasli, F.N., 2015. Satellite images for monitoring mangrove cover changes in a fast growing economic region in southern Peninsular Malaysia.*Remote Sensing*, *7*(11), pp.14360-14385.

Kathiresan, K. and Bingham, B.L., 2001. Biology of mangroves and mangrove ecosystems. *Advances in marine biology*, *40*, pp.81-251.

Kauffman, J.B., and Donato, D., 2012. *Protocols for the measurement, monitoring, and reporting of structure, biomass and carbon stocks in mangrove forests* (No. CIFOR Working Paper no. 86, p. 40p). Center for International Forestry Research (CIFOR), Bogor, Indonesia.

Kuenzer, C., Bluemel, A., Gebhardt, S., Quoc, T.V. and Dech, S., 2011. Remote sensing of mangrove ecosystems: A review. *Remote Sensing*, *3*(5), pp.878-928.

Lanly, J.P., 1981. Tropical forest resources assessment project (GEMS): tropical Africa, tropical Asia, tropical America, 4 Vols. *UN Food and Agriculture Organization/UN Environment Programme, Rome*.

LDEO, 1998. Remote Sensing Glossary, Lamont-Doherty Earth Observatory, Earth Institute, Columbia University, Newyork, Accessed on July 15th, 2016, available at http://www.ldeo.columbia.edu/res/fac/rsvlab/glossary.html

Lehmann, E.A., Wallace, J.F., Caccetta, P.A., Furby, S.L. and Zdunic, K., 2013. Forest cover trends from time series Landsat data for the Australian continent. *International Journal of Applied Earth Observation and Geoinformation*, *21*, pp.453-462.

Li, M.S., Mao, L.J., Shen, W.J., Liu, S.Q. and Wei, A.S., 2013. Change and fragmentation trends of Zhanjiang Mangrove forests in southern China using multi-temporal Landsat imagery (1977–2010). *Estuarine, Coastal and Shelf Science*, *130*, pp.111-120.

Liang, S., Fang, H. and Chen, M., 2001. Atmospheric correction of Landsat ETM+ land surface imagery. I. Methods. *IEEE Transactions on Geoscience and Remote Sensing*, *39*(11), pp.2490-2498.

Long, J.B. and Giri, C., 2011. Mapping the Philippines' mangrove forests using Landsat imagery. *Sensors*, *11*(3), pp.2972-2981.

Lu, D., Mausel, P., Brondizio, E. and Moran, E., 2004. Change detection techniques. *International journal of remote sensing*, *25*(12), pp.2365-2401.

Mas, J.F., 1999. Monitoring land-cover changes a comparison of change detection techniques. *International journal of remote sensing*, *20*(1), pp.139-152

Masek, J.G., Honzak, M., Goward, S.N., Liu, P. and Pak, E., 2001. Landsat-7 ETM+ as an observatory for land cover: Initial radiometric and geometric comparisons with Landsat-5 Thematic Mapper. *Remote Sensing of Environment*, *78*(1), pp.118-130.

MoEF, 2011. *Collaborative redd+ifm Sundarbans project (crisp),* Ministry of Environment and Forests Forest Department, Government of Bangladesh

Mohammed, N.Z. and Eisa Eiman, A.E., 2013. The Effect of Polynomial Order on Georeferencing Remote Sensing Images. *Int. J. Eng. Innov. Technol*, *2*, pp.5-8

Moran, M.S., Jackson, R.D., Slater, P.N. and Teillet, P.M., 1992. Evaluation of simplified procedures for retrieval of land surface reflectance factors from satellite sensor output. *Remote Sensing of Environment*, *41*(2), pp.169-184.

Murshed, S. and Rahman, S.,2011. Spatial Changes of Land Use/Land Cover of Moheshkhali Island, Bangladesh: A Fact Finding Approach by Remote Sensing Analysis, Dhaka University Journal of Earth and Environmental Sciences, 2,pp.43-54

Nitta, I. and Ohsawa, M., 1997. Leaf dynamics and shoot phenology of eleven warm-temperate evergreen broad-leaved trees near their northern limit in central Japan. *Plant Ecology*, *130*(1), pp.71-88

Paolini, L., Grings, F., Sobrino, J.A., Jiménez Muñoz, J.C. and Karszenbaum, H., 2006. Radiometric correction effects in Landsat multi-date/multi-sensor change detection studies. *International Journal of Remote Sensing*, *27*(4), pp.685-704.

Payo, A., Mukhopadhyay, A., Hazra, S., Ghosh, T., Ghosh, S., Brown, S., Nicholls, R.J., Bricheno, L., Wolf, J., Kay, S. and Lázár, A.N., 2016. Projected changes in area of the Sundarban mangrove forest in Bangladesh due to SLR by 2100. *Climatic Change*, *139*(2), pp.279-291.

Pham, T.D. and Yoshino, K., 2015. Mangrove Mapping and Change Detection Using Multi-temporal Landsat imagery in Hai Phong City, Vietnam. *The International Symposium on Cartography in Internet and Ubiquitos Environments, Tokyo*, available at http://ubimap.csis.utokyo.ac.jp/ciu2015/Proceedings/Full_Paper/G2_Mangrove%20Mapping%20and%20Change%20Detection%20Using%20Multitemporal%20Landsat%20imagery%20in%20Hai%20Phong%20city,%20Vietnam.pdf

Pflugmacher, D., Cohen, W.B., Kennedy, R.E. and Yang, Z., 2014. Using Landsat-derived disturbance and recovery history and lidar to map forest biomass dynamics. *Remote Sensing of Environment*, *151*, pp.124-137.

Pflugmacher, D., Cohen, W.B. and Kennedy, R.E., 2012. Using Landsat-derived disturbance history (1972–2010) to predict current forest structure. *Remote Sensing of Environment*, *122*, pp.146-165.

Rahman, M.R. and Hossain, M.B., 2015. Changes in land use pattern at Chakaria Sundarbans mangrove forest in Bangladesh. *Bangladesh Research Publications Journal*, ISSN: 1998-2003, 11(1), pp.13-20.

Rahman, M., Ullah, R., Lan, M., Sri Sumantyo, J.T., Kuze, H. and Tateishi, R., 2013. Comparison of Landsat image classification methods for detecting mangrove forests in Sundarbans. *International journal of remote sensing*,*34*(4), pp.1041-1056.

Rahman, M.M., 2012. Time-Series Analysis of Coastal Erosion in the Sundarbans Mangrove. *ISPRS-International Archives of the Photogrammetry, Remote Sensing, and Spatial Information Sciences*, *1*, pp.425-429.

Rahman, A.F., Dragoni, D. and El-Masri, B., 2011. Response of the Sundarbans coastline to sea level rise and decreased sediment flow: A remote sensing assessment. *Remote Sensing of Environment*, *115*(12), pp.3121-3128.

Rahman, M.A., 1996. Top dying of sundri (Heritiera fomes) and its impact on the regeneration and management in the mangrove forests of Sunderbans in Bangladesh. *Impact of diseases and insect pests in tropical forests*, pp.117-133.

Rosati, I. et al., 2010. 10 World Atlas of Mangroves, *Food and Agricultural Organization*, Rome, Italy.

Roy, D.P., Wulder, M.A., Loveland, T.R., Woodcock, C.E., Allen, R.G., Anderson, M.C., Helder, D., Irons, J.R., Johnson, D.M., Kennedy, R. and Scambos, T.A., 2014. Landsat-8: Science and product vision for terrestrial global change research. *Remote Sensing of Environment*, *145*, pp.154-172.

Roy TK, Hossain ST., 2015. Role of Sundarbans in Protecting Climate Vulnerable Coastal People of Bangladesh. *Climate Change*, 1(1), pp.40-44, Discovery Publications Ltd., Kanyakumari District, Tamilnadu, India.

Sajjaduzzaman, M., Muhammed, N. and Koike, M.A.S.A.O., 2005. Mangrove plantation destruction in Noakhali coastal forests of Bangladesh: a case study on causes, consequences, and model prescription to halt deforestation. *Int J Agric Biol*, *7*.

Salam, M.A., Ross, L.G. and Beveridge, C.M.C., 2003. The use of GIS and remote sensing techniques to classify the Sundarbans Mangrove vegetation.

Sarker, S.K., Reeve, R., Thompson, J., Paul, N.K., and Matthiopoulos, J., 2016. Are we failing to protect threatened mangroves in the Sundarbans world heritage ecosystem?. *Scientific reports*, *6*.

Schott, J.R., Salvaggio, C. and Volchok, W.J., 1988. Radiometric scene normalization using pseudo invariant features. *Remote Sensing of Environment*, *26*(1), pp.1IN115-1416.

Schroeder, T.A., Cohen, W.B., Song, C., Canty, M.J. and Yang, Z., 2006. Radiometric correction of multi-temporal Landsat data for characterization of early successional forest patterns in western Oregon. *Remote sensing of Environment*, *103*(1), pp.16-26.

Shapiro, A.C., Trettin, C.C., Küchly, H., Alavinapanah, S. and Bandeira, S., 2015. The Mangroves of the Zambezi Delta: Increase in Extent Observed via Satellite from 1994 to 2013. *Remote Sensing*, *7*(12), pp.16504-16518.

Son, N.T., Chen, C.F., Chang, N.B., Chen, C.R., Chang, L.Y. and Thanh, B.X., 2015. Mangrove mapping and change detection in Ca Mau Peninsula, Vietnam, using Landsat data and object-based image analysis. *IEEE Journal of Selected Topics in Applied Earth Observations and Remote Sensing*, *8*(2), pp.503-510.

Song, D.X., Huang, C., Sexton, J.O., Channan, S., Feng, M. and Townshend, J.R., 2015. Use of Landsat and Corona data for mapping forest cover change from the mid-1960s to 2000s: Case studies from the Eastern United States and Central Brazil. *ISPRS Journal of Photogrammetry and Remote Sensing*, *103*, pp.81-92.

Spalding, M., 2010. *World atlas of mangroves*. Routledge.

Spalding, M.D., Blasco, F. & Field, C.D. (eds) (1997) World mangrove atlas. *The International Society for Mangrove Ecosystems*, Okinawa

Sremongkontip, S., Hussin, Y.A., Groenindijk, L. and Detection, C., 2000. Detecting changes in the mangrove forests of Southern Thailand using remotely sensed data and GIS. *International Archives of Photogrammetry and Remote Sensing*, *33*(1), pp.567-574.

Stroeve, F.M., 1993. *The Feni-river closure dam reviewed* (Doctoral dissertation, TU Delft, Delft University of Technology).

Sulaiman, N.A., Ruslan, F.A., Tarmizi, N.M., Hashim, K.A. and Samad, A.M., 2013, August. Mangrove forest changes analysis along Klang coastal using remote sensing technique. In *System Engineering and Technology (ICSET), 2013 IEEE 3rd International Conference on* (pp. 307-312). IEEE.

Syed, M.A., Hussin, Y.A. and Weir, M., 2001, November. Detecting fragmented mangroves in the Sundarbans, Bangladesh using optical and radar satellite images. In *Paper presented at the 22nd Asian Conference on Remote Sensing* (Vol. 5, p. 9).

Tucker, C.J., Grant, D.M. and Dykstra, J.D., 2004. NASA's global orthorectified Landsat data set. *Photogrammetric Engineering & Remote Sensing*, *70*(3), pp.313-322.

Uddin, M.M., Rahman, M.S., Hossain, M.K. and Akter, S., 2014. Growth density and regeneration of afforested mangroves at Mirersarai forest range in Bangladesh. *Forest Science and Technology*, *10*(3), pp.120-124.

Uddin, M.S., van Steveninck, E.D.R., Stuip, M. and Shah, M.A.R., 2013. Economic valuation of provisioning and cultural services of a protected mangrove ecosystem: a case study on Sundarbans Reserve Forest, Bangladesh. *Ecosystem Services*, *5*, pp.88-93.

USGS, 2016a. Landsat Scene, Accessed on 14th April 2016, available at https://earthexplorer.usgs.gov/

USGS, 2016b. Landsat 8 (L8) Data Users Handbook, Accessed on 14th April 2016, Available athttps://landsat.usgs.gov/sites/default/files/documents/Landsat8DataUsersHandbook.pdf

USGS 2016c, Landsat Quality Assessment Band, *United States Geological Survey*; Accessed on April 14th 2016, available at http://landsat.usgs.gov/qualityband.php

Verbesselt, J., Hyndman, R., Newnham, G., and Culvenor, D., 2010. Detecting trend and seasonal changes in satellite image time series. *Remote Sensing of Environment*, *114*(1), pp.106-115.

Vogelmann, J.E., Xian, G., Homer, C. and Tolk, B., 2012. Monitoring gradual ecosystem change using Landsat time series analyses: Case studies in selected forest and rangeland ecosystems. *Remote Sensing of Environment*,*122*, pp.92-105.

Wulder, M.A., Masek, J.G., Cohen, W.B., Loveland, T.R. and Woodcock, C.E., 2012. Opening the archive: How free data has enabled the science and monitoring promise of Landsat. *Remote Sensing of Environment*, *122*, pp.2-10.

Wulder, M.A., Hall, R.J., Coops, N.C. and Franklin, S.E., 2004. High spatial resolution remotely sensed data for ecosystem characterization. *BioScience*,*54*(6), pp.511-521.

Worldbank, 2016. Average Monthly Rainfall of Bangladesh from 1900 to 2012, Accessed on July 15th, 2016, Available at http://sdwebx.worldbank.org/climateportal/index.cfm?page=country_historical_climate&ThisRegion=Asia&ThisCCode=BGD

Xie, Y., Sha, Z. and Yu, M., 2008. Remote sensing imagery in vegetation mapping: a review. *Journal of plant ecology*, *1*(1), pp.9-23.

Zhong, C., Xu, Q. and Li, B., 2016. Relative Radiometric Normalization for Multitemporal Remote Sensing Images by Hierarchical Regression. *IEEE Geoscience and Remote Sensing Letters*, *13*(2), pp.217-221.

Appendix-A

Table.S1: *Landsat image characteristics of collected images*

S.N.	Path/Row	Acquisition Time	Landsat Spacecraft	Cloud Cover	Pixel Size	UTM	Epoch
1	P135 R046	1976-03-01	MSS 2	0.0%	60m	46N	1976
2	P136 R044	1977-01-02	MSS 2	0.0%	60m	46N	
3	P136 R045	1977-01-02	MSS 2	0.0%	60m	46N	
4	P137 R044	1977-02-08	MSS 2	0.0%	60m	46N	
5	P137 R045	1977-02-08	MSS 2	0.0%	60m	46N	
6	P138 R044	1977-02-09	MSS 2	0.0%	60m	45N	
7	P148 R045	1977-01-22	MSS 2	0.0%	60m	45N	
8	P136 R045	1989-01-21	TM 4	0.0%	30m	46N	1989
9	P135 R046	1989-02-23	TM 4	0.0%	30m	46N	
10	P136 R044	1989-01-13	TM 4	0.0%	30m	46N	
11	P137 R044	1989-11-20	TM 4	0.0%	30m	46N	
12	P137 R045	1989-02-05	TM 4	0.0%	30m	46N	
13	P138 R044	1989-01-11	TM 4	0.0%	30m	45N	
14	P138 R045	1989-01-27	TM 4	0.0%	30m	45N	
15	P135 R046	2000-02-14	ETM+ 7	0.0%	30m	46N	2000
16	P136 R044	2001-02-07	ETM+ 7	0.0%	30m	46N	
17	P136 R045	2001-02-07	ETM+ 7	0.0%	30m	46N	
18	P137 R044	2001-01-29	ETM+ 7	0.0%	30m	46N	
19	P137 R045	2000-11-26	ETM+ 7	0.0%	30m	46N	
20	P138 R044	2000-11-17	ETM+ 7	0.0%	30m	45N	
21	P138 R045	2000-11-17	ETM+ 7	0.0%	30m	45N	
22	P135 R046	2015-11-30	L8 OLI	0.15%	30m	46N	2015
23	P136 R044	2014-02-19	L8 OLI	0.04%	30m	46N	
24	P136 R045	2014-03-30	L8 OLI	0.09%	30m	46N	
25	P137 R044	2014-03-30	L8 OLI	0.07%	30m	46N	
26	P137 R045	2015-03-17	L8 OLI	0.10%	30m	46N	
27	P138 R044	2014-03-05	L8 OLI	0.08%	30m	45N	
28	P148 R045	2015-03-08	L8 OLI	0.12%	30m	45N	

Table.S2: *Landsat Band Designations*

Bands	Landsat MSS		Landsat MSS		Landsat MSS		Landsat MSS	
	WL(**µm)**	Band	WL(**µm)**	Band	WL(**µm)**	Band	WL(**µm)**	Band
Coastal Aerosol	-	-	-	-	-	-	0.43-0.45	1
Blue	-	-	0.45-0.52	1	0.45-0.52	1	0.45-0.51	2
Green	0.5-0.6	1	0.52-0.60	2	0.52-0.60	2	0.45-0.51	3
Red	0.6-0.7	2	0.63-0.69	3	0.63-0.69	3	0.64-0.67	4
Near Infrared	0.7-0.8	3	0.76-0.90	4	0.76-0.90	4	0.85-0.88	5
Near Infrared2	0.8-1.1	4	-	-	-	-	-	-
SWIR1	-	-	1.55-1.75	5	1.55-1.75	5	1.57-1.65	6
SWIR2	-	-	-	-	-	-	2.11-2.29	7

Here, WL-Wavelength, For MSS 1-4 band originally named band 6-7 but band name are same like TM, ETM+, L8OLI.

Table.S3: *Co-registration and Average RMSE*

Sl.No.	Base Image (Landsat 7)	Warp Image	Path/Row	Tie-Point	Average RMSE (half of the resolution of pixel size)——
1	ETM+P135 R046	Landsat 2 (MSS)	P145 R046	33	0.25
		Landsat TM	P135 R046	56	0.01
		Landsat 8 OLI	P135 R046	45	0.0043
2	ETM+P135 R044	Landsat 2 (MSS)	P146 R044	42	0.30

		Landsat TM	P136 R044	87	0.0005
		Landsat 8 OLI	P136 R044	76	0.0051
3	ETM+P136 R045	Landsat 2 (MSS)	P146 R045	27	0.29
		Landsat TM	P136 R045	30	0.30
		Landsat 8 OLI	P136 R045	25	0.30
4	ETM+P137 R044	Landsat 2 (MSS)	P147 R044	38	0.31
		Landsat TM	P137 R044	85	0.0002
		Landsat 8 OLI	P137 R044	27	0.01
5	ETM+P137 R045	Landsat 2 (MSS)	P147 R045	26	0.62
		Landsat TM	P137 R045	26	0.49
		Landsat 8 OLI	P137 R045	25	0.18
6	ETM+P138 R044	Landsat 2 (MSS)	P148 R044	25	0.234
		Landsat TM	P138 R044	41	0.0060
		Landsat 8 OLI	P138 R044	36	0.0047
7	ETM+P138 R045	Landsat 2 (MSS)	P148 R045	29	0.30
		Landsat TM	P138 R045	35	0.0040
		Landsat 8 OLI	P138 R045	27	0.0028

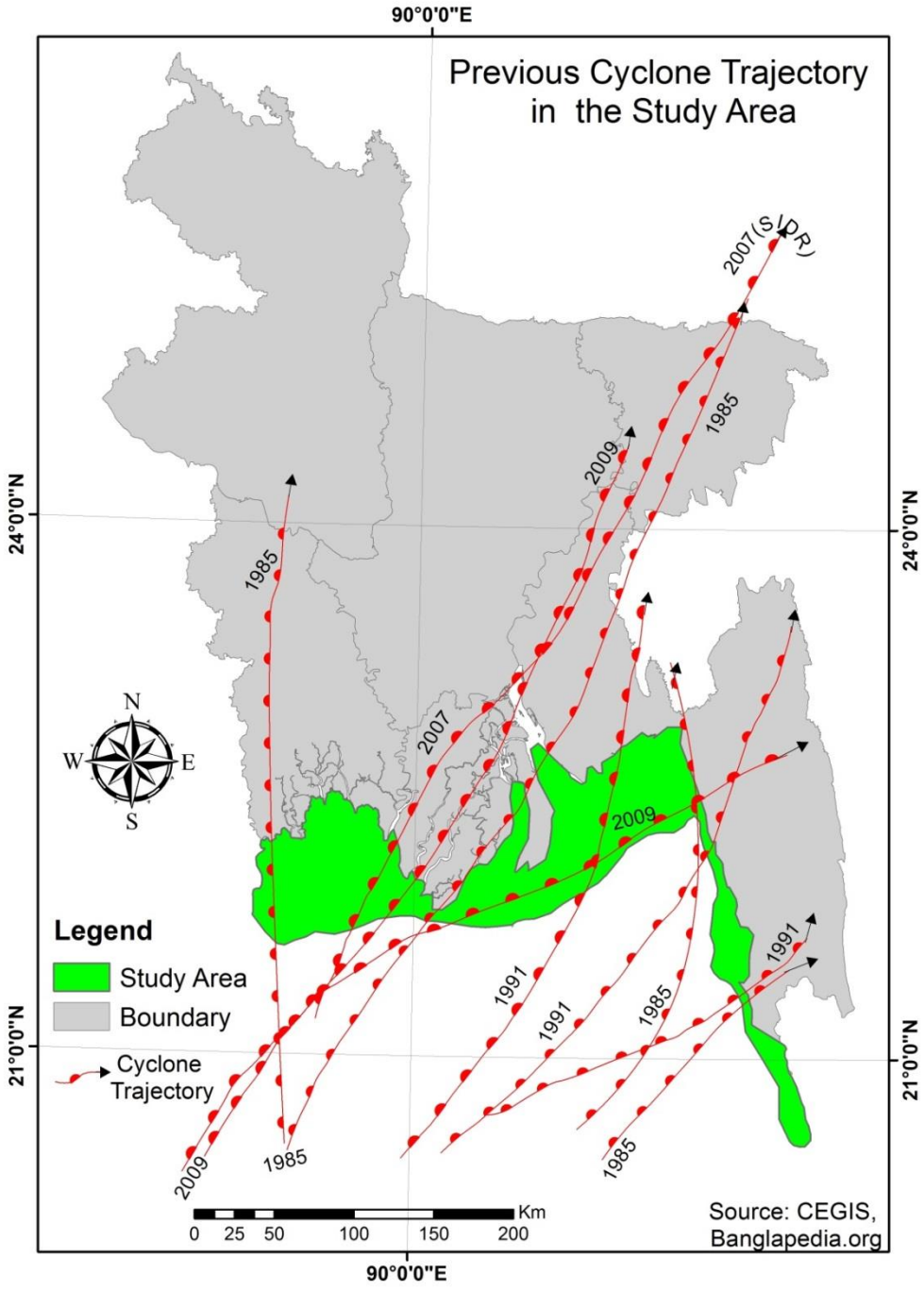

Figure.S1: *Previous major Cyclone trajectory in the study area. This cyclone also damaged mangrove forest and affected NDVI values. The data obtained from banglapedia.org as .jpg format and digitized in ArcGIS. These data can be used for research and education purpose.*

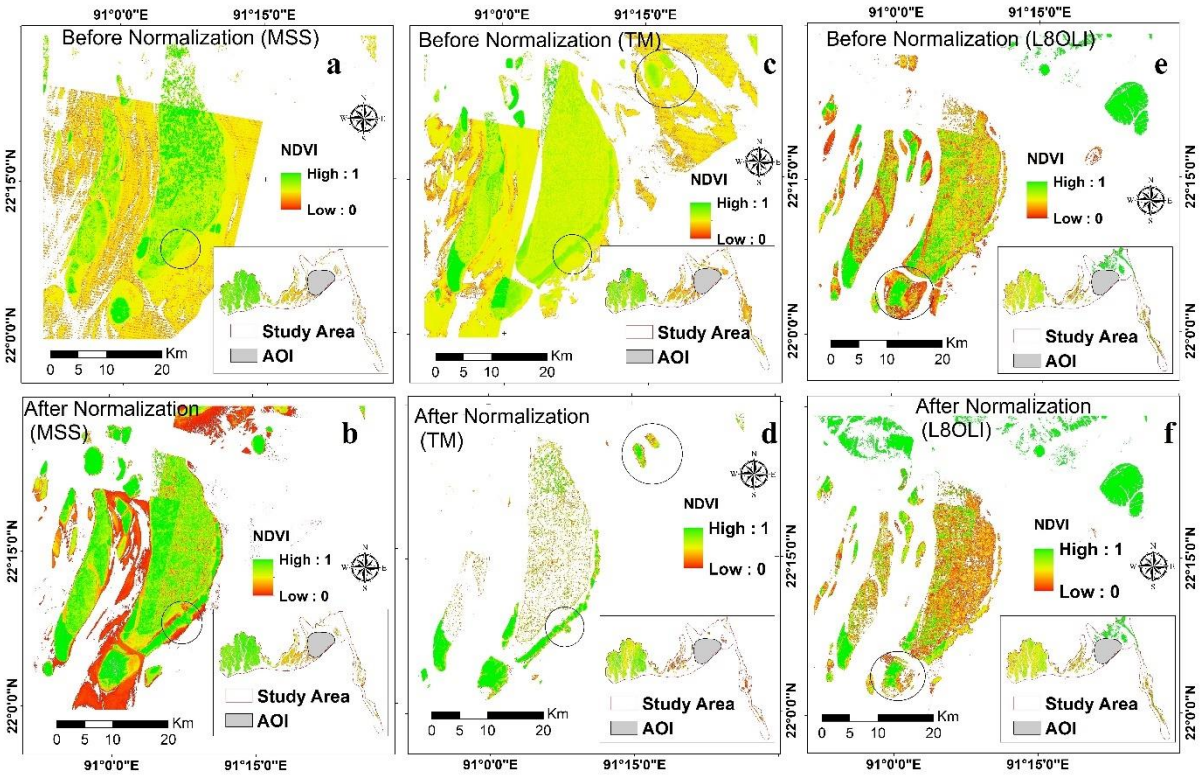

Figure.S2: *NDVI values of (a,b) MSS, (c,d) TM, and (e,f) L8 OLI images in Bhola-hatia Regions before and after normalization. A black circle indicates normalization has been overcome the sedimentation effects (floating sediment in the ocean). Non-vegetated (Floating sediment areas in water bodies (red color in 29b) areas have zero NDVI values reduced from NDVI value 0.4 (29a). Mangrove areas recaptured from sedimentation effects (29c-d and 29 e-f).*

Institutionen för naturgeografi och ekosystemvetenskap, Lunds Universitet.

Student examensarbete (Seminarieuppsatser). Uppsatserna finns tillgängliga på institutionens geobibliotek, Sölvegatan 12, 223 62 LUND. Serien startade 1985. Hela listan och själva uppsatserna är även tillgängliga på LUP student papers (https://lup.lub.lu.se/student-papers/search/) och via Geobiblioteket (www.geobib.lu.se)

The student thesis reports are available at the Geo-Library, Department of Physical Geography and Ecosystem Science, University of Lund, Sölvegatan 12, S-223 62 Lund, Sweden. Report series started 1985. The complete list and electronic versions are also electronic available at the LUP student papers (https://lup.lub.lu.se/student-papers/search/) and through the Geo-library (www.geobib.lu.se)

372 Andreas Dahlbom (2016) The impact of permafrost degradation on methane fluxes - a field study in Abisko

373 Hanna Modin (2016) Higher temperatures increase nutrient availability in the High Arctic, causing elevated competitive pressure and a decline in *Papaver radicatum*

374 Elsa Lindevall (2016) Assessment of the relationship between the Photochemical Reflectance Index and Light Use Efficiency: A study of its seasonal and diurnal variation in a sub-arctic birch forest, Abisko, Sweden

375 Henrik Hagelin and Matthieu Cluzel (2016) Applying FARSITE and Prometheus on the Västmanland Fire, Sweden (2014): Fire Growth Simulation as a Measure Against Forest Fire Spread – A Model Suitability Study –

376 Pontus Cederholm (2016) Californian Drought: The Processes and Factors Controlling the 2011-2016 Drought and Winter Precipitation in California

377 Johannes Loer (2016) Modelling nitrogen balance in two Southern Swedish spruce plantations

378 Hanna Angel (2016) Water and carbon footprints of mining and producing Cu, Mg and Zn: A comparative study of primary and secondary sources

379 Gusten Brodin (2016) Organic farming's role in adaptation to and mitigation of climate change - an overview of ecological resilience and a model case study

380 Veránika Trollblad (2016) Odling av *Cucumis Sativus* L. med aska från träd som näringstillägg i ett urinbaserat hydroponiskt system

381 Susanne De Bourg (2016) Tillväxteffekter för andra generationens granskog efter tidigare genomförd kalkning

382 Katarina Crafoord (2016) Placering av energiskog i Sverige - en GIS analys

383 Simon Nåfält (2016) Assessing avalanche risk by terrain analysis An experimental GIS-approach to The Avalanche Terrain Exposure Scale (ATES)

384 Vide Hellgren (2016) Asteroid Mining - A Review of Methods and Aspects

385 Tina Truedsson (2016) Hur påverkar snömängd och vindförhållande vattentrycksmätningar vintertid i en sjö på västra Grönland?

386 Chloe Näslund (2016) Prompt Pediatric Care Pediatric patients' estimated travel times to surgically-equipped hospitals in Sweden's Scania County

387 Yufei Wei (2016) Developing a web-based system to visualize vegetation trends by a nonlinear regression algorithm

388 Greta Wistrand (2016) Investigating the potential of object-based image analysis to identify tree avenues in high resolution aerial imagery and lidar data

389 Jessica Ahlgren (2016) Development of a Web Mapping Application for grazing resource information in Kordofan, Sudan, by downloading MODIS data automatically via Python

390 Hanna Axén (2016) Methane flux measurements with low-cost solid state sensors in Kobbefjord, West Greenland

391 Ludvig Forslund (2016) Development of methods for flood analysis and response in a Web-GIS for disaster management

392 Shuzhi Dong (2016) Comparisons between different multi-criteria decision analysis techniques for disease susceptibility mapping

393 Thirze Hermans (2016) Modelling grain surplus/deficit in Cameroon for 2030

394 Stefanos Georganos (2016) Exploring the spatial relationship between NDVI and rainfall in the semi-arid Sahel using geographically weighted regression

395 Julia Kelly (2016) Physiological responses to drought in healthy and stressed trees: a comparison of four species in Oregon, USA

396 Antonín Kusbach (2016) Analysis of Arctic peak-season carbon flux estimations based on four MODIS vegetation products

397 Luana Andreea Simion (2016) Conservation assessments of Văcărești urban wetland in Bucharest (Romania): Land cover and climate changes from 2000 to 2015

398 Elsa Nordén (2016) Comparison between three landscape analysis tools to aid conservation efforts

399 Tudor Buhalău (2016) Detecting clear-cut deforestation using Landsat data: A time series analysis of remote sensing data in Covasna County, Romania between 2005 and 2015

400 Sofia Sjögren (2016) Effective methods for prediction and visualization of contaminated soil volumes in 3D with GIS

401 Jayan Wijesingha (2016) Geometric quality assessment of multi-rotor unmanned aerial vehicle-borne remote sensing products for precision agriculture

402 Jenny Ahlstrand (2016) Effects of altered precipitation regimes on bryophyte carbon dynamics in a Peruvian tropical montane cloud forest

403 Peter Markus (2016) Design and development of a prototype mobile geographical information system for real-time collection and storage of traffic accident data

404 Christos Bountzouklis (2016) Monitoring of Santorini (Greece) volcano during post-unrest period (2014-2016) with interferometric time series of Sentinel-1A

405 Gea Hallen (2016) Porous asphalt as a method for reducing urban storm water runoff in Lund, Sweden

406 Marcus Rudolf (2016) Spatiotemporal reconstructions of black carbon, organic matter and heavy metals in coastal records of south-west Sweden

407 Sophie Rudbäck (2016) The spatial growth pattern and directional properties of *Dryas octopetala* on Spitsbergen, Svalbard

408 Julia Schütt (2017) Assessment of forcing mechanisms on net community production and dissolved inorganic carbon dynamics in the Southern Ocean using glider data

409 Abdalla Eltayeb A. Mohamed (2016) Mapping tree canopy cover in the semi-arid Sahel using satellite remote sensing and Google Earth imagery

410 Ying Zhou (2016) The link between secondary organic aerosol and monoterpenes at a boreal forest site

411 Matthew Corney (2016) Preparation and analysis of crowdsourced GPS bicycling data: a study of Skåne, Sweden

412 Louise Hannon Bradshaw (2017) Sweden, forests & wind storms: Developing a model to predict storm damage to forests in Kronoberg county

413 Joel D. White (2017) Shifts within the carbon cycle in response to the absence of keystone herbivore *Ovibos moschatus* in a high arctic mire

414 Kristofer Karlsson (2017) Greenhouse gas flux at a temperate peatland: a comparison of the eddy covariance method and the flux-gradient method

415 Md. Monirul Islam (2017) Tracing mangrove forest dynamics of Bangladesh using historical Landsat data